MiR-145 plays a role in oligodendrocyte differentiation by regulating cytoskeleton- and myelin-related gene expression

Samantha F. Kornfeld

This thesis is submitted as a partial fulfillment of the M.Sc. program in Cellular and Molecular Medicine.

Department of Cellular and Molecular Medicine
Faculty of Medicine
University of Ottawa
Ottawa, Canada

Abstract

A key problem in multiple sclerosis (MS) is the diminished capacity for myelin repair. Although oligodendrocyte (OL) precursors can be seen at the lesion site, their ability to differentiate appears inhibited. MicroRNAs are key regulators of OL differentiation, and have been observed to be misregulated in MS lesions compared to healthy white matter. Thus, aberrant microRNA expression in MS lesions may disrupt the ability of incoming oligodendrocyte progenitor cells (OPCs) to differentiate. Specifically, a microRNA known as miR-145 is downregulated as OPCs progress to OLs, but is found at unusually high levelsin MS lesions. In this study, we investigated how misregulation of miR-145 affects OL differentiation *in vitro*. Bioinformatic analysis revealed that putative targets of miR-145 are significantly enriched for factors which promote actin cytoskeleton organization and myelination.An immortalized OL cell line was transduced with an inducible lentivirus to create stable lines that overexpress miR-145. These stable lines were characterized while proliferating, early in differentiation and late in differentiation. Immunofluorescence was used to quantify changes in proliferation rate, apoptosis, branching ability and myelin gene expression. qPCR arrays were used to quantify changes in microRNA target expression levels between induced and uninduced cells. Two stable lines were created: ON-145-1 and ON-145-2, which upon induction, over-express miR-145 ~33-fold and ~11-fold, respectively. When proliferating, no significant morphological differences nor target expression differences could be detected between induced and uninduced cells. Proliferation was significantly decreased in ON-145-1 induced cells, but not in ON-145-2. No changes in apoptosis frequency were detected. In contrast, during early and late differentiation, both induced cell lines showed significant morphological defects characterized by a reduction in both

primary and secondary branching. Further, significant differences in branching ability were observed between induced cells of ON-145-1 and ON-145-2, suggesting a dose-dependent response to miR-145 overexpression. Expression of MAG, a myelin marker, was also significantly lowered in induced cells of both cell lines. Finally, we found that multiple miR-145 targets involved in promoting cytoskeletal organization and myelination were significantly decreased both early and late in differentiation.These results suggest that overexpression of miR-145 during OL differentiation may disrupt actin organization and myelin gene expression required for successful process extension and subsequent myelinating ability. Thus, the increase in miR-145 in MS lesions may be a significant contributing factor to the loss of myelin repair in MS lesions.

Table of Contents

List of Tables

List of Figures

Abbreviations

Ach - acetylcholine
CIS – clinically isolated syndrome
CNP – 2’3’-cyclic nucleotide-3’-phosphodiesterase
CNS – central nervous system
CSF – cerebrospinal fluid
dNTP – deoxynucleotide triphosphate
DAVID – database for annotation, visualization and integrated discovery
DD3 – differentiation day 3
DD6 – differentiation day 6
dbcAMP – dibutyryl cyclic adenosine monophosphate
EAE – experimental autoimmune encephalitis
EASE – expression analysis systematic explorer
ELOVL7 – elongation of very long chain fatty acids protein 7
FAC – functional annotation tools
F-actin – filamentous actin
FAK – focal adhesion kinase
FGF – fibroblast growth factor
GFP – green fluorescent protein
GO- gene ontology
Hes5 – hair and enhancer split 5
ILK – integrin-linked kinase
MAG – myelin associated glycoprotein
Mash1 – mammalin achaete scute homolog 1
MBP – myelin basic protein
miRISC – microRNA induced silencing complex
miRNA – microRNA
Mobp – myelin oligodendrocyte basic protein
MOG – myelin oligoendrocyte glycoprotein
MRF – myelin regulatory factor
MS – multiple sclerosis
MyT1 – myelin transcription factor 1
N-WASP – Wiscott-Aldrich syndrome protein
OL – oligodendrocyte
OPC – oligodendrocyte progenitor cell
P - proliferating
PBMC – peripheral blood mononuclear cells
PDGF – platelet-derived growth factor
PLP – proteolipid protein
PMP22 – peripheral myelin protein 22

PNS – peripheral nervous system
PPMS – primary progressive multiple sclerosis
Pri-miRNA – primary miRNA
PSA-NCAM – polysialylated neural cell adhesion molecule
qRT-PCR – quantitative reverse transcription-polymerase chain reaction
RIS – radiologically isolated syndrome
RISC – RNA-induced silencing complex
RRMS – relapsing remitting multiple sclerosis
RNA – ribonucleic acid
RNA Pol II – RNA polymerase II
RT-PCR – reverse transcription- polymerase chain reaction
Sox – sex determining region Y box
SPMS – secondary progressive multiple sclerosis
TPPP – tubulin polymerization protein
UTR – untranslated region
WAVE1 – WASP family verprolin homologous 1

Acknowledgements

I would first like to recognize my supervisor Dr. Rashmi Kothary for his support of this project. His willingness to allow me to pursue my own research path is very much appreciated. I would like to thank Dr. Lyndsay Murray, for invaluable discussions – about science and many other things – and for being a truly excellent friend since I joined the lab. I would also like to thank the members of the Kothary lab for their helpful insights and suggestions during the course of this study.

Thanks to my mum for her unfailing interest in my research, and to my dad for providing the perfect escape from failed experiments. The biggest debt of gratitude is owed to my husband, who has at times tolerated, encouraged, supported, congratulated and consoled me, and without whom I would likely take life far too seriously.

Introduction

Multiple Sclerosis

Multiple Sclerosis (MS) is an inflammatory demyelinating disease of the central nervous system (CNS). It is typified by areas of inflammation and demyelination in CNS white matter, followed by eventual axonal and neuronal degeneration. Areas of demyelination, or plaques, may be found anywhere in the CNS; however, they occur most frequently in the brain stem, optic nerve, spinal cord and periventricular regions (Noseworthy *et al*., 2000). Loss of myelin in the CNS is manifested as both physical and cognitive disabilities in patients. Early in the disease, remyelination can occur, leading to an apparent recovery. But MS is a progressive disease, and these symptoms return and become more debilitating with disease chronicity. MS most commonly presents in young adulthood, with diagnosis occurring typically between the ages of 20-40, and affects approximately 2.5 million people globally (Antel *et al*., 2012). It affects women more often than men, at a ratio which in recent years appears to be increasing (D'hooghe *et al*., 2013).

There are various subtypes of MS, which include relapsing-remitting MS (RRMS), primary progressive MS (PPMS), and secondary progressive MS (SPMS). As the name suggests, RRMS is characterized by periods of disability or relapse, interrupted by periods of recovery or remission. These periods of relief from symptoms can be attributed to remyelination in plaques, leading to partial or full return of neuron communication in the damaged area. Newly formed myelin in plaques is not as thick however, and appears to be more susceptible to subsequent attack (Franklin & Ffrench-Constant, 2008).In most patients, RRMS will eventually deteriorate to SPMS, in which

there are no longer periods of remission and symptoms persist and consistently worsen (Antel *et al*., 2012). PPMS is progressive from disease onset.

Currently, diagnosis requires both dissemination in space by visualization of plaques on magnetic resonance imagining (MRI) and dissemination in time requiring clinical progression for at least one year. Diagnosis is sometimes accompanied by cerebrospinal fluid (CSF) analysis. Two conditions may or may not develop into MS; these are radiologically isolated syndrome (RIS) in which one or more plaques are detected by MRI but without symptoms, and clinically isolated syndrome (CIS) in which a patient has presented with a single attack of symptoms and one or more plaques visualized by MRI (Granberg *et al*., 2013; Miller *et al*, 2005).

The etiology of MS remains poorly understood. It is widely considered to be a T-cell-dependent autoimmune disease (McFarland & Martin, 2007). Support for this is found in the fact that risk alleles associate with MS are almost entirely immune-related genes. However, while active demyelination in lesions is usually characterized by the presence of activated T-cells and severe inflammation, it has been suggested that the disease is in fact an oligodendendriopathy in which inflammation is merely a byproduct. There is also support for this hypothesis, as autopsy of MS lesions has sometimes shown severe oligodendrocyte apoptosis without the presence of inflammatory cells (Barnet & Prineas, 2004). Additional roles for B-cells, environmental factors and viral infection also have a basis in scientific evidence (Hernandez-Pedro *et al*., 2013; Simpson *et al*., 2011; Pakpoor *et al*., 2013). What is clear is that there is no single cause of MS, and the mechanisms of its origin are likely heterogeneous.

The difficulty of elucidating the etiology of MS has consequently lead to difficulties in treating it. There is currently no cure for the disease, and most therapies are immunomodulatory, aimed at preventing myelin damage. The fact that the disease progresses in the majority of cases indicates that these treatments lack efficacy. Further, they are only effective in patients with RRMS; at present there are no treatment strategies for patients suffering from progressive MS. It is therefore critical that research is done to discover treatment strategies that focus on the regeneration of the myelin sheath once it has been damaged.

Oligodendrocytes and CNS myelination

Oligodendrocytes (OLs) are the myelinating cells of the CNS. Mature OLs contact axons via long processes which wrap themselves in concentric circles around the axon. The plasma membrane which spirals around the axon is transformed into a fatty, compact membrane containing myelin-specific proteins. In addition to its compacted form, myelin is characterized by several proteins unique to its composition, such as proteolipid protein (PLP), myelin-associated glycoprotein (MAG), 2′:3′-cyclic nucleotide-3′-phosphodiesterase (CNP), myelin basic protein (MBP) and myelin oligodendrocyte protein (MOG).

The myelinated areas of the axon, or internodes, are arranged discontiguously along the axon. A single OL can myelinate up to fifty axons, and a single axon is myelinated by many OLs (Pfeiffer *et al*., 1993). The insulating properties of myelin both increase resistance and reduce capacitance of the axon (Pfeiffer *et* al., 1993;Bakiri*et al*., 2011), making it the critical factor in determining the speed and efficiency of action

potentials as they can only occur at the unmyelinated areas of the axon, or Nodes of Ranvier. This saltatory nerve conduction, or “jumping” of the current, only occurs in myelinated axons and is required for proper function of the CNS. Additionally, myelin confers protection on axons from oxidative and inflammatory insults. Thus, the importance of myelin is paramount, as is made evident by its loss in a demyelinating disease such as MS.

Developmentally, OLs originate from neuroepithelial stem cells that give rise to oligodendrocyte progenitor cells (OPCs). During embryonic development, OPCs arise from ventral ventricular zones of the neural tube and later from dorsal telencephalic ventricular and sub-ventricular zones (Yu *et al*., 1993; Richardson *et al*., 2006). The developmental stages between OPC and mature, myelinating OL are marked by both morphological and gene expression changes; notably, these sequential gene expression changes have allowed for characterization of the different stages of OL maturation (Pfeiffer *et al*., 1993). Maintenance of proliferating OPCs and the transition to differentiating OL is orchestrated by a complex array of cross-talk between external cues, intrinsic inhibitors of differentiation and intrinsic promoters of differentiation. In order to differentiate, OPCs must cease proliferation, exit the cell cycle, express a host of appropriate OL-specific genes, extend processes, contact and wrap axons, and finally produce myelin.Upon interaction with appropriate environmental signals and the expression of a host of necessary genes, OPCs will terminally differentiate to post-mitotic myelinating cells (Baumann & Pham-Dinh, 2001; Emery, 2010).

OPCs are both motile and mitotic and can be found throughout the CNS. They typically display a bipolar morphology. Two growth factors with a well-characterized role

in promoting OPC proliferation are platelet-derived growth factor (PDGF) and fibroblast growth factor 2 (FGF2) (Bansal *et al*., 1996; Fortin *et al*., 2005; Cui *et al*., 2010; Huang *et al*., 2013). Additional factors known to promote proliferation are FGF8, FGF17, FGF18 and acetylcholine (ACh) (Fortin *et* al., 2005; de Angelis *et al.,* 2011). Responsiveness of OPCs to these factors is dependent on tight control of the expression of appropriate cell-surface receptors. In fact, the receptors PDGF receptor α (PDGFRα), FGF receptor 1 (FGFR1), FGFR3, and muscarinic receptors M1, M2 and M3, which bind PDGF, FGF2, FGF8/17/18 and ACh respectively, have all been found to be highly upregulated in OPCs compared to differentiated OLs (Bansal *et al*., 1996; Fortin *et al*., 2005; Cui *et al*., 2010; Huang *et al*., 2013, de Angelis *et al.,* 2011). The GD3 ganglioside A2B5 and the chondroitin sulfide proteoglycan (CSPG) NG2 are also highly expressed in OPCs, and are commonly used as markers of OPC identity (Pfeiffer *et al*., 1993). Transcription factors involved in the regulation of OPC genes at this stage include Olig1, Olig2, myelin transcription factor 1 (MyT1), mammalian achaete scute homolog 1 (Mash1), hair and enhancer of split 5 (Hes5), and sex determine region Y box 5 and 6 (Sox5 and Sox6; Huang *et* al., 2013; Watanabe*et al*., 2004; Fancy *et al*., 2004; Sim *et al*., 2002; Emery, 2010). Of these, Olig2 is the only factor required for specification of OPCs to the OL lineage; in this context, the remainder function to maintain their proliferative capacity and to inhibit differentiation (Ligon *et al*., 2006; Emery, 2010). A schematic illustrating some important gene expression changes is provided in Figure 1.

The transition from OPC to differentiating OL is also highly influenced by extrinsic factors, such as ciliary neurotrophic factor (CNTF), brain-derived neurotrophic factor

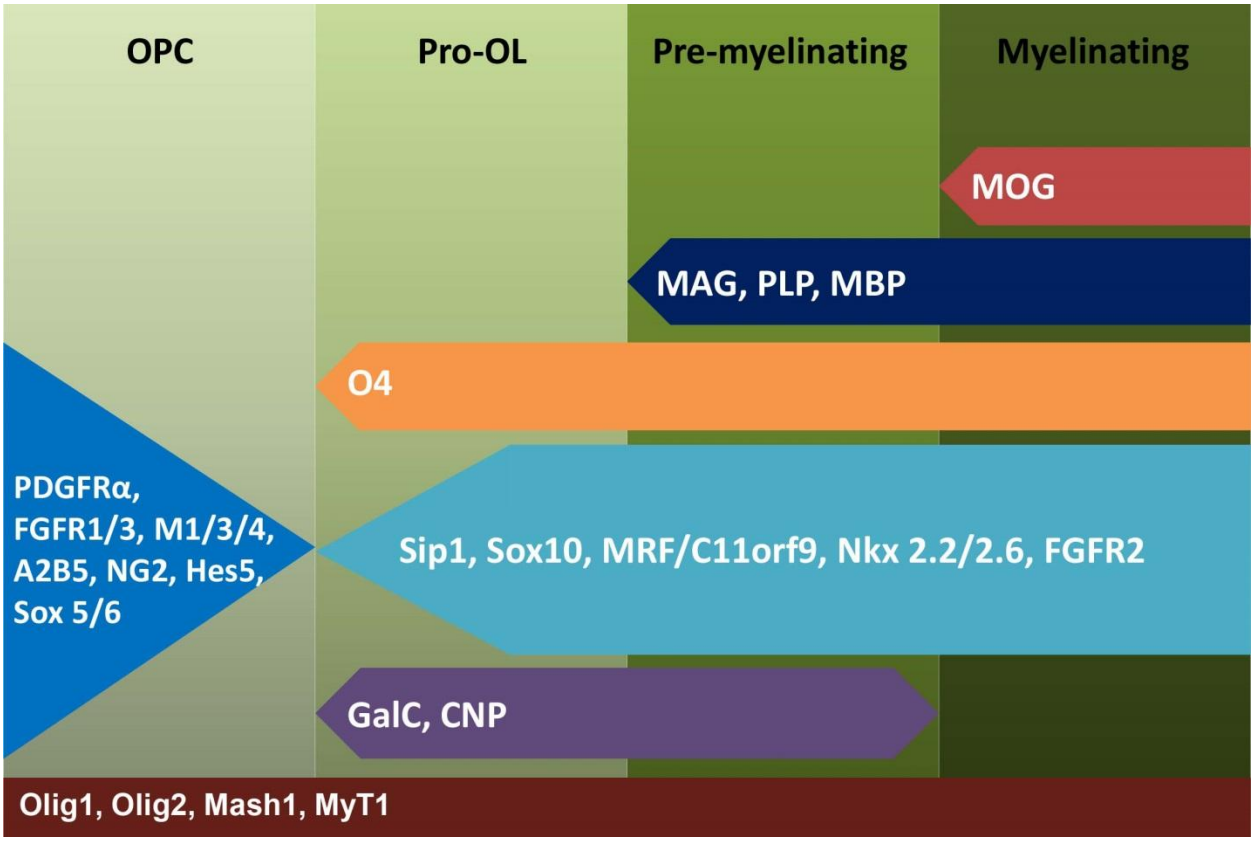

Figure 1. Expression patterns of differentially regulated genes as OPCs progress through the stages of differentiation to become myelinating OLs. Differentiation and myelination require multi-faceted coordination of the precisely times downregulation of factors which promote proliferation and inhibit differentiation and the upregulation of factors that promote differentiation and myelination.

(BDNF), insulin-like growth factor-1 (IGF-1), and the thyroid hormone triiodothyronine (T3) (Van't Veer *et al*., 2008; Huang *et al*., 2013; Miron *et al*., 2011). Of these, T3 has been the most widely investigated, with studies showing that application of T3 to OPCs in culture is sufficient to induce differentiation even in the presence of PDGF (Barres *et al*., 1994; Jones *et al*., 2003). Transcription factors Smad-interacting protein 1 (Sip1), Sox10 and myelin gene regulatory factor (MRF; human homolog C11orf9) are all requirements for OL differentiation and myelination, as indicated by the lack of myelination observed in various knockout models generated for each protein (Figure 1; Weng *et al*., 2012; Stolt *et al*., 2002; Emery *et al*., 2009).

Additional transcription factors have been found to be important in differentiation; however, their role is likely involved in the still poorly understood "internal clock" possessed by OPCs. This timing of oligodendrocyte differentiation was first observed by Temple and Raff (1986), in which the authors found that OPCs cultured on a monolayer of astrocytes would divide a maximum of eight times before terminally differentiating, without any additional experimental stimulation. This led to a hypothesis that OPCs somehow counted the number of cell divisions they underwent and would spontaneously differentiate once they had reached a division limit. This was amended by a study which showed that OPCs taken from the same source cultured in the presence of mitogens at either 33^{o}C or 37^{o}C underwent different numbers of cell divisions in each group but differentiated at approximately the same time, suggesting that some instrinsic OPC mechanism measured time and not cell divisions (Gao *et al*., 1997). Gao *et al*. further noted the intrinsic timing of differentiation could be overridden by exogenous application of differentiation-promoting factors *in vitro.*While this internal

clock is still not fully understood, multiple positive regulators of differentiation are believed to be involved in the timing of differentiation. These include transcription factors homeobox proteins Nkx2.2 and Nkx2.6, as well as transcription factors previously implicated in proliferating OPCs, MyT1, Mash1, Olig1 and Olig2 (Huang *et al*, 2013). It has been suggested that those factors also expressed in proliferating OPCs likely take on different roles as cells differentiate; for example, Mash1 has been shown to collaborate with Nkx2.2 to promote OPC differentiation, and Olig1 works with Sox10 to promote myelin gene expression and was found to relocate from the nucleus to the cytoplasm as cells differentiate (Ligon *et al*., 2006; Li *et al*., 2007; Niu *et al,* 2006). As cells move through the different stages of differentiation, a canonical set of markers are commonly used to identify them (Baumann & Pham-Dinh, 2001; Huang *et al*., 2013; Miron *et al*., 2011; Jackman *et al*., 2010). Pro-oligodendrocytes (pro-OLs) express 2’3’-cyclic nucleotide 3’-phosphodiesterase (CNP), galactosylceramidase (GalC), and a sulfatide recognized by the antibody O4,. Premyelinating OLs continue expression of O4, CNP and GalC, but also begin to express myelin associated glycoprotein (MAG), proteolipid protein (PLP) and myelin basic protein (MBP). Finally, mature myelinating OLs express the same host of markers as premyelinating OLs with the addition of myelin oligodendrocyte protein (Figure 1; MOG).

In addition to the extrinsic and intrinsic factors required for proper OL development, organization of the cytoskeleton is also a requirement for successful differentiation. Contact with axons and the wrapping of membrane and subsequent compaction require that cells have the ability to extend many elaborate processes from the cell body. Process extension is mediated by both actin microfilaments and

microtubules. Initial membrane protrusions are created by localized actin polymerization and branching of single microfilaments to form filopodia, which are then expanded into microfilament-rich lamellipodia (Bauer *et al*., 2009). Microtubules then follow the path of microfilaments into lamellipodia, and together continue to extend the process. The primary branches which extend from the cell body will branch further into secondary, tertiary and quaternary branches through a process similar to that of the primary branch extension. Actin and tubulin organization is orchestrated by a host of cytoskeleton associated proteins. Actin-associated proteins are many and have diverse roles, but share the mutual characteristic of binding to microfilaments. Intracellular signalling mechanisms involved in actin organization have been elucidated that highlight roles for Src family kinase (SRK) Fyn, focal adhesion kinase (FAK), Wiscott-Aldrich syndrome protein (N-WASP), and WASP family verprolin homologous 1 (WAVE1). In fact, knockdown or knockout of any of these factors results in reduced myelination *in vivo* and a reduction in process extension in differentiating oligodendrocytes *in vitro* (Kim *et al*., 2006; Goto *et al* 2004; Bacon *et al.,* 2007; Forrest *et al*. 2009). Tubulin organization is equally critical to OL differentiation, as evidenced by a total inhibition of differentiation in oligodendrocytes in which tubulin polymerization promoting protein (TPPP/p25) is knocked down (Lehotzky *et al*., 2010). Clearly, the course of OL development is governed by a multitude of factors, both extracellular and intracellular, which act collectively to set the stage for successful differentiation and myelination.

Oligodendrocytes and remyelination in MS

In healthy white matter, myelination continues to take place throughout adulthood. Much of this is done to replace myelin lost in the course of oligodendrocyte death (Young *et al*., 2013). Mature oligodendrocytes do not appear to be involved in this process.Instead, a demyelinating event is followed by the recruitment of OPCs distributed throughout the CNS to the demyelinated area; these cells then differentiate and remyelinate denuded axons (Blakemore & Keirstead, 1999; Franklin, 2002). While newly established internodes tend to be shorter, thinner and more numerous in comparison to myelin sheaths created during development, they appear to be equally efficient in allowing conduction of saltatory nerve impulses (Franklin & Ffrench-Constant, 2008; Young *et al*., 2013).

Remyelination can also occur in MS but this capacity is severely reduced and disappears over time until there is complete remyelination failure. Further, patients who present with PPMS exhibit little to no remyelination. Reasons for this may be multi-faceted. Recruitment of OPCs to the area may be impaired due to a loss of chemoattractants such as Semaphorin A (Williams *et al*., 2007; Boyd *et al*, 2013). Many lesions, however, are replete with OPCs that never differentiate, indicating that lack of OPCs is not the cause for loss of remyelination (Wolswijk, 1998; Kuhlmann *et al*., 2008). This inhibition of differentiation is like due to the inhospitable microenvironment of the lesion; multiple factors have been found to be upregulated in lesion tissue which are negative regulators of OL differentiation. These factors include polysialylated neural cell adhesion molecule (PSA-NCAM), the glycosaminoglycan hyaluronan, jagged-1 via Notch1 signalling, and multiple factors via Wnt signaling (Kotter *et al*., 2011; Fancy *et*

al., 2010; Franklin & Ffrench-Constant, 2008). Myelin debris resulting from demylination is itself an inhibitor of remyelination.

Currently, there are no approved treatments available for MS aimed at enhancing myelin regeneration. The fact that disease continues to progress even with treatment by immunomodulatory therapies indicates that such strategies require ongoing rigorous research. This could benefit not only patients with RRMS through combination of therapeutics to both relieve immune-mediate attack on myelinand enhance remyelination, but also SPMS and PPMS patients for whom there are currently no effective strategies to slow disease progression.

MicroRNA

MicroRNAs (miRNAs)are short, non-coding RNAs capable of regulating protein expression within a cell. These 18-25 nucleotide transcripts are able to bind with full or partial complementarity usually to the 3' untranslated region (UTR)of mRNA targets, resulting in the inhibition of translation or degradation of that target (Leung & Sharp, 2010; Grimson *et al*., 2007; Schier & Giraldez, 2006). It is estimated that at least 60% and up to 90% of all mammalian mRNAs may be targeted by miRNAs (Friedman *et al*., 2009a; Perron & Provost, 2008), and at this time over 1000 miRNAs have been identified in the human genome (http://www.mirbase.org). A single miRNA may target multiple mRNAs, and a single mRNA may have multiple miRNA binding sites (Lewis *et al*., 2003; Bartel, 2004). Obviously, simply due to their sequence diversity and the fact that they are predicted to target the majority of mRNAs in mammals, this regulatory pathway is of great importance. In fact, through a myriad of comparative expression analyses and gain- and loss-of function experiments, miRNAs have been shown to be

critically involved in biological development, cell differentiation, apoptosis, cell-cycle control, stress response and disease pathogenesis (Shi & Jin, 2009; Chan *et al*., 2005; Leung & Sharp, 2010; Ivey & Srivastava, 2010).

Three miRNA structures exist over the course of maturation: the primary miRNA (pri-miRNA), the precursor miRNA (pre-miRNA) and the mature miRNA, each containing fewer nucleotides and a less complex secondary structure than the last (Krol *et al*., 2004; Hausser *et al*., 2009). A specialized pathway exists to progress the pri-miRNA to the mature miRNA in eukaryotes, which includes both RNase and nuclear transport proteins, as well as a variable host of proteins which associate with the mature miRNA to facilitate target binding and subsequent translational control(Figure 2). Processing occurs in both the nuclear and cytoplasmic compartments (Krol *et* al., 2010; Zeng *et* al., 2005; Perron & Provost, 2010). The canonical processing pathway involves the nuclear RNase III enzyme Drosha, followed by the cytoplasmic RNase III enzyme Dicer1 (Lee *et al.,* 2003; Zeng *et al*., 2005; Krol *et al.*, 2010; Perron & Provost, 2010). Recently, alternative processing machinery has also been discovered in which either Drosha or Dicer1 is substituted by a different cleavage enzyme (Yang & Lai, 2011; Yang *et al*., 2012); however only a small proportion of microRNAs are likely to be processed by either Drosha- or Dicer1-independent means as it appears that miRNAs fitting into this category also have non-canonical pri- or pre-miRNA structures.

Many levels of control exist in the miRNA processing pathway that lead to highly monitored regulation of both miRNAs and their associated proteins within the cell. The sequences of both pre-miRNA and miRNA appear to be highly conserved in mammals and the protein components of miRNA-mediated pathways may have been present as

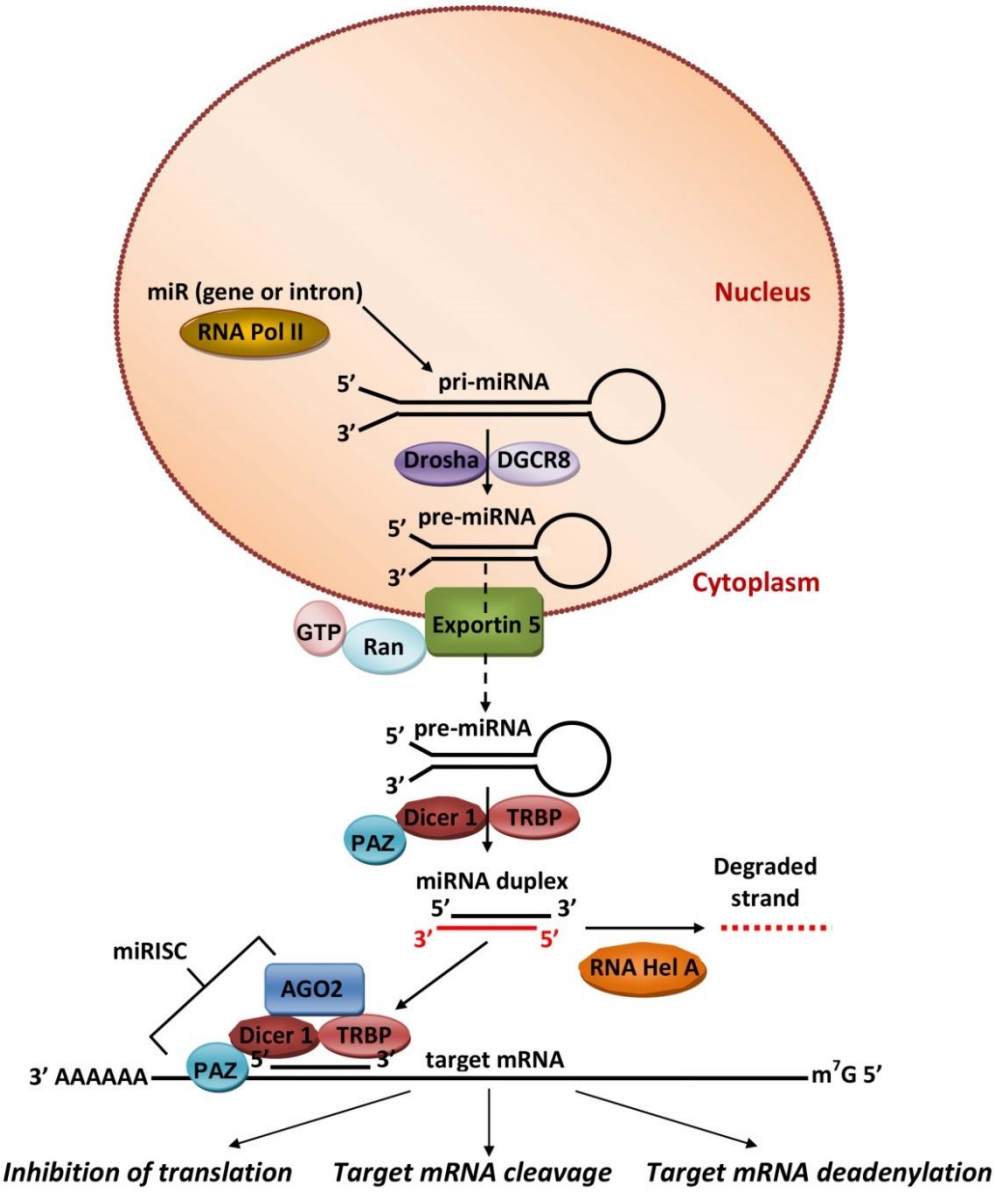

Figure 2.Schematic representation of canonical microRNA processing. Primary microRNA (pri-miRNA) is first transcribed and then processed to pre-miRNA. This is exported from the nucleus, and is then processed to the miRNA duplex. Normally, one strand of the duplex is degraded, while the other is incorporated into miRISC. This complex binds to a complementary region in the 3' UTR of a mRNA target, which subsequently undergoes degradation or translational inhibition.

far back in evolution as the last eukaryotic common ancestor (LECA) (Shabalina & Koonin, 2009). This theory is based on the presence of the same or homologous proteins in both plants and animals which are major players in miRNA biogenesis, indicating that these miRNA-processing factors evolved before divergence of the two major eukaryotic lineages (Shabalina & Koonin, 2009).

MiRISC is the effector complex that mediates binding and inhibition of translation or degradation of target mRNAs. This complex includes Dicer1, TRBP and the Paz domain, as well as Argonaute (Ago) proteins of which there are four (Krol *et al*., 2010; Ikeda *et al*., 2006). The degree of complementarity between miRNA and mRNA will determine the mode of mRNA degradation or if its translation will be inhibited without degradation (Friedman *et al*, 2009b; Weston *et al,* 2006). Full complementarity promotes endonucleolytic activity of miRISC-associated proteins such as Ago2 (Ikeda e*t al*., 2006; Krol *et al*., 2010). If pairing is only partially complementary, translational repression or degradation through deadenylation and mRNA uncapping will occur (Krol *et al*., 2010; Nishiara *et al*., 2013). Ago proteins have been shown to interact with a class of proteins called GW182, which appears to function in repression of mRNA translation through an as-yet uncharacterized mechanism (Pauley *et al*., 2006). Proteins from this class as well as miRISC:mRNA complexes have been found to aggregate into units called processing bodies (P-bodies), in which miRNA-repressed mRNAs build up and are eventually either degraded or rescued for translation (Pauley *et al*., 2006). The degradation of mRNAs in this context is by shortening of the poly-A tail; this leads to recruitment of uncapping proteins, which leaves the mRNA susceptible to the cytoplastic exonuclease XRN1 (Nishihara *et al*., 2013).

The first 6-8 nucleotides of the 5' ends of miRNA are known as the 'seed,' and are responsible for specifying complementarity with target mRNAs. Four types of seed mRNA complementarity patterns with varying binding/modification efficacy have been elucidated based on the positions of complementary nucleotides between miRNA and mRNA (Lewis *et* al., 2005; Friedman*et al,* 2009b). Matching sequences in mRNA are generally found in 3' UTRs (though not always), and binding sites found outside the path of the ribosome have been found to have greater efficacy of miRNA regulation (Weston *et al*, 2006; Friedman *et al*, 2009b). While seed region binding is generally recognized as the most important factor in miRNA target site recognition, the following factors also come into play: the location of the site in the 3'UTR of the mRNA, the sequence composition in the immediate vicinity of the target site, the accessibility of the target site with respect to the stop codon, any base pairing that may occur between the 3' end of the miRNA and the target site, and the positions of multiple miRNA target sites with respect to each other (Hausser *et* al., 2009; Grimson *et al*., 2007).

MicroRNAs are required for oligodendrocyte differentiation

In addition to the complicated landscape of factors required for OL development discussed above, microRNAs add an extra layer to the complexity of differentiation and myelination. MicroRNAs have been shown to be critical to OLsboth in the developing and adult CNS. In mice, conditional embryonic knockout of *Dicer1* in uncommitted neuronal precursors was shown to lower numbers of both OPCs and mature OLs in that compartment (Kawase-Koga *et al*., 2009), likely due to a decrease in OPC production rather than a reduction in OPC expansion (Dugas & Notterpek, 2010).Failure to

differentiate was also shown in two independent Cre-mediated conditional OPC *Dicer1* knockout mice. Distinct mouse models using Olig2-, CNP- and Olig1-driven deletion of Dicer1 by Cre recombinase showed defects in CNS myelination and OL differentiation *in vivo* (Dugas *et al*., 2010; Zhao *et* al., 2010). Interestingly, despite the loss of Dicer1, OPCs were able to proliferate in an apparently normal manner. Postnatal conditional knockout of *Dicer1* specifically in mature OLs in P30 mice using PLP-driven Cre expression was found to reduce myelin protein levels and mature OL numbers in the white matter of the cerebellum and corpus callosum, suggesting that loss of Dicer1 resulted in demyelination in these areasdue to deficits at both the molecular and cellular levels (Shin *et al*., 2010).

Several specific microRNA species and their respective targets have been elucidated as particularly important for OL differentiation(Figure 3).In proliferating OPCs, miRs 9, 214, 199a-5p and 145 are expressed at higher levels than in differentiating or mature OLs. Both miR-199a-5p and miR-145 have predicted but unconfirmed target sites in the 3' UTR of *C11orf9,* the putative human homolog of mouse myelin regulatory factor (*MRF*).Loss of this transcription factor in mice leads to a severe reduction in myelin genes such as PLP, MBP, MOG and MAG (Emery *et* al., 2009; Koenning*et al*., 2012). MiR-214 is also predicted to target a myelin-associated gene, myelin-associated oligodendrocyte basic protein (*Mobp),* involved in organizing proper compact myelin structure (Yoshikawa, 2001). Thus, stronger expressionof these miRNAs in OPCs may block myelin gene expression during the proliferative stage, and their downregulation during differentiation may release this block. The transcript for peripheral myelin protein (*Pmp22*) has been confirmed as a target of miR-9; Pmp22 is

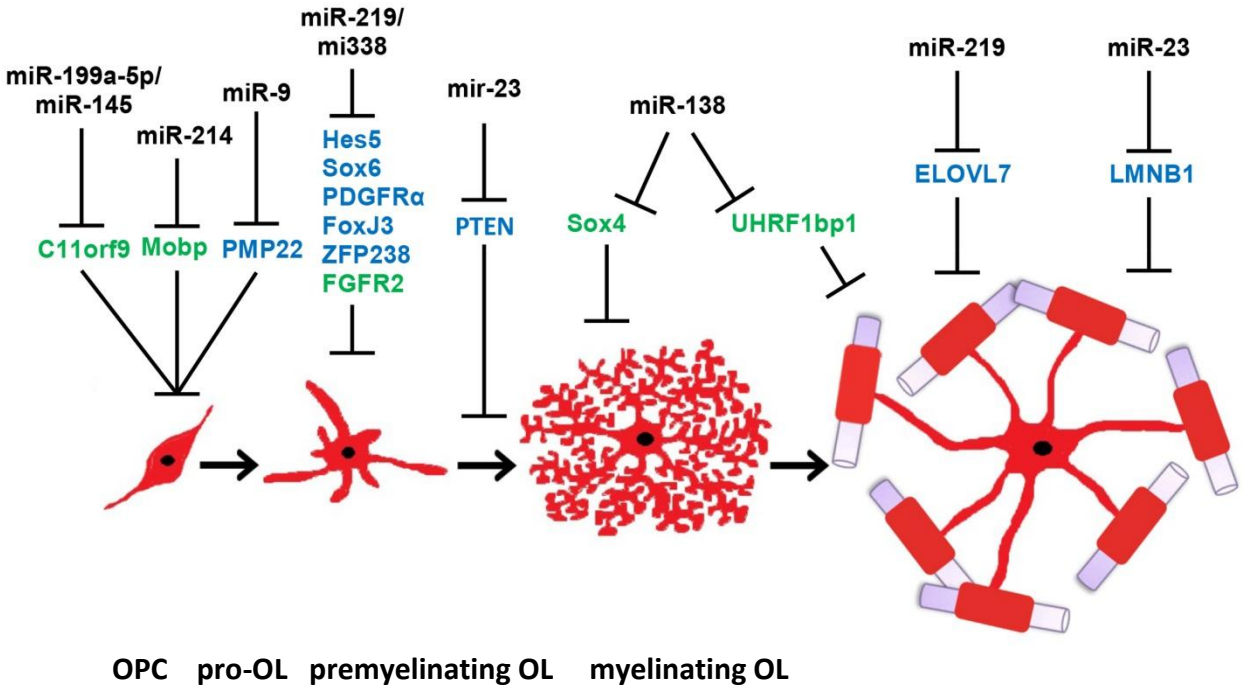

Figure 3.Schematic representation of the possible roles of several microRNAs known to be differentially regulated at different timepoints as OPCs progress to myelinating OLs. MiRNAs shown are upregulated at their respective timepoints during OL lineage progression. Confirmed miR targets are in blue, suspected targets are in green.OPC – oligodendrocyte progenitor cell; pro-OL – pro-oligodendrocyte.

important in Schwann cell myelination in the peripheral nervous system (PNS), but is found only at the mRNA level and never at the protein level in OPCs and OLs (Lau *et al*., 2008).

MiRs -219 and -338 and -138 have all been shown to be strongly upregulated in differentiated OLs compared to OPCs (Lau *et al*., 2008; Dugas *et* al., 2010; Zhao *et al*., 2010). Using the Olig2- and CNP-drivenCre-mediated conditional *Dicer1* knockout modelsmentioned above, Dugas *et al*. (2010) were able to illustrate that OL-specific miR-219 was not only required but sufficient to induce OL differentiation in vitro, and was further able to partially rescue the loss of differentiation in OPCs in which endogenous miRNA production was ablated. Using the Olig2-driven conditional *Dicer1* knockout, a separate group recapitulated these results and additionally showed that miR-338 was also able to induce differentiation in proliferating OPCs as well as partially rescue *Dicer1* knockout OPCs from differentiation defects(Zhao *et al*., 2010). They further found that application of both of these microRNAs simultaneously produced a slightly synergistic rescue effect (Zhao *et al*., 2010). Knockdown of these two miRNAs in cultured OPCs as well as in zebrafish leads to a reduction in OL differentiation (Zhao *et al*., 2010). Mir-219 and miR-338 have been found to jointly target multiple factors - including *PDGFRα, Hes5, FoxJ3, Sox6, ZFP238* and *FGFR2* - that normally maintain OPCs in an undifferentiated and proliferative state (Figure 3; Dugas *et al*., 2010; Zhao *et al*., 2010).Additionally, miR-219 is known to target the fatty acid elongase named elongation of very long chain fatty acids protein 7 (*ELOVL7*). While very long chain fatty acids (VLCFAs) are integrated into PLP and are thus an important constituent of the myelin sheath, their accumulation produces an increase in oxidative damage and leads

to demyelination (Shin *et al*., 2009; Dugas, 2010). In this case, miR-219 regulation of *ELOVL7* likely serves to tightly control active protein levels within a functional but not detrimental range. The role of miR-138 in OL differentiation is somewhat paradoxical. Purified OPCs can be induced to differentiate with transfection of miR-138 but only as far along the lineage as CNP^+/MBP^+ cells. However, miR-138 expression strongly represses expression of MOG required in late differentiation (Dugas *et al*., 2010). Interestingly, once OLs are MOG^+ they no longer retain the capacity to contact new axons and produce new myelin sheaths (Watkins *et al*., 2008). Regulation of genes by miR-138 might therefore allow an extension of the period during which OLs are able to reach and initiate myelination of additional axons. Potential target candidates for this miRNA include SRY-box 4(*Sox4)*, which is an early differentiation inhibitor, and ubiquitin-like containing PHD and RING finger domains 1 binding protein 1 (*UHRF1bp1*), which is an indirect promoter of late differentiation (Figure 3; Dugas *et al*., 2006).An additional miRNA upregulated during differentiation is miR-23. Specifically overexpressing miR-23 *in vivo* was shown to increase OPC differentiation and to lead to hypermyelination of the CNS (Lin *et al*., 2013). This miRNA species was shown to directly target both lamin B1 (LMNB1), which negatively regulates PLP, along with phosphatase and tensin homolog (PTEN), which negatively regulates OL differentiation via the PI3K/Akt/mTor pathway (Figure 3; Lin & Fu, 2009; Lin *et al*., 2013).Taken together, these studies show that mature microRNAs are required for the generation of OPCs and mature OLs, as well as the development and maintenance of the myelin sheath.

MicroRNAs are misregulated in MS

In recent years, several studies have been done which highlight potential roles for miRNAs in the pathogenesis of MS. Profiling done on whole blood samples and peripheral blood mononuclear cells (PBMCs) has revealed some interesting findings. One group found that after microarray analysis of miRNA profiles in whole blood taken from MS patients and healthy controls, they were able to reliably differentiate between the two groups based solely on differential miRNA expression (Keller *et al*., 2009). Another group found that they could distinguish RRMS patients in relapse from healthy controls based on differential expression of miRNAs in PBMCs (Otaegui *et al*., 2009). These and similar studies have highlighted the potential of circulating miRNAs as biomarkers for MS diagnosis, a valuable prospect as current diagnosis criteria involve long-term monitoring and considerable uncertainty for patients.

A study investigating miRNA profiling in active and chronic MS plaquesby microarray has also yielded interesting results. This study identified many miRNAs that exhibited altered expression levels in MS lesions compared to healthy white matter (Junker *et al*., 2009). They further investigated one of these miRNAs, miR-155, which was upregulated in lesions. These authors found that miR-155 was expressed by astrocytes, and was predicted to target a gene called *CD47* expressed by brain resident cells which functions as a self-marker to preventimmune reaction. They further found that *CD47*transcript was downregulated in lesion tissue compared to healthy white matter, and were able to show that miR-155 is able to directly bind the 3’ UTR of *CD47 in vitro*. Interestingly, another study profiling miRNA expression in PBMCs found that miR-155 was the most upregulated miRNA in MS patient samples compared to healthy

controls (Paraboschi *et al*., 2011). Additional study of this miRNA revealed that it plays a significant role in mediating inflammatory responses by enhancing the development of inflammatory T-cells, and that mice deficient in miR-155 showed strong resistance to experimental autoimmune encephalitis (EAE), an animal model of MS (O'Connell *et al*., 2012). While it is crucial to better understand the molecular mechanisms of miRNAs in MS, these results suggest that they are likely to be advantageous as lines of investigation for therapeutic potential.

Rationale and Hypothesis

It has been established that miRNAs are necessary for OL differentiation, and that the expression of many miR species are precisely timed as OPCs progress toward myelinating OLs. In MS, OPCs are known to migrate to the lesion site, but appear to become progressively less able to differentiate with disease chronicity. A likely reason for this is that the microenvironment of the lesion is rife with factors that inhibit differentiation. Further, microarray data from human lesion tissue has shown that miRNAs are misregulated within the lesion site as compared to healthy white matter. Based on these, we hypothesized that OPC differentiation may be negatively impacted by misregulation of miRNAs, leading to a loss of differentiating and myelinating ability. The objective of this project was to investigate the soundness of this hypothesis through characterization of the effects of misregulation of a miRNA, found to be both differentially expressed during OL differentiation and misregulated in MS lesions, on the differentiating ability of OPCs *in vitro*.

The following aims were formed to address our objectives:

1. ***Identify relevant candidate microRNA***

   A subset of possible candidates was isolated through comparison of available miRNA microarrayexpression data from important timepoints in OL differentiation and from MS active and chronic lesion tissue. Chosen candidates exhibit expression levels in lesions that might negatively impact OL differentiation. Lists of putative targets for these candidates were generated using an available algorithm-based database. The putative target list for each candidate was subjected to bioinformatic analysis by gene ontology clustering and KEGG pathway analysis to determine the most relevant single candidate. Since an immortalized mouse oligodendrocyte cell line – *Oli-neu* – was used for our experiments, expression of the candidate microRNA was verified and differential expression was quantified during proliferation and differentiation.

2. ***Establish stable inducible cell line that expresses the candidate miRNA in a manner similar to expression levels found in MS lesions***

   Oli-neu cells were transduced with an inducible lentivirus to produce

   stable lines. These cells were characterized in non-inducing and inducing conditions at three timepoints: proliferation, early differentiation (day 3; DD3) and late differentiation (day 6; DD6). Changes in proliferation rates and the frequency of apoptosis were assessed. Changes in morphology were investigated through quantification of both primary and secondary branching ability. Progression

through lineage development was measured by myelin-associated gene expression. Finally, expression of relevant putative targets of our candidate miRNA as identified by bioinformatic analysis was measured at each timepoint.

Materials and Methods

Generation of putative miR target lists and bioinformatics analysis

Putative target lists were generated using TargetScanMouse version 6.1 (www.targetscan.org; Lewis *et al*., 2005; Grimson *et al*., 2007; Friedman *et al.*, 2009b), using an algorithm based on seed region:3' UTR complementarity and thermodynamic stability of target binding. Functional clustering and pathway analyses of complete putative target lists was done using the Database for Annotation, Visualization and Integrated Discovery (DAVID) Functional Annotation Tools (FAC). High stringency EASE score parameters were used to indicate confident enrichment scores (http://david.abcc.ncifcrf.gov/; Huang *et al*., 2009a; Huang *et al*., 2009b). Heat map analyses were conducted using DAVID based on the clustering results to show the correlation between each gene ontology term and each gene in the cluster. A positive correlation is indicated in green; a negative or unconfirmed correlation is indicated in black. For miR-145, KEGG pathway analysis was also done through DAVID to visualize pathway enrichment from the complete putative target list.

Oli-neu cell culture

Oli-neu cells were incubated in SATO medium with 1% horse serum in Dulbecco's Modified Eagle's Medium (Wisent) at 37.5^{o}C and 10% CO_2 (Jung *et al*., 1995). Medium was replaced every 2-3 days. Cells were plated on poly-L-lysine coated plates or coverslips (poly-L-lysine; Sigma). To differentiate cells, 1mM dbcAMP (Sigma) was added to the medium. To passage cells, plates were incubated for 1 min with 0.05% trypsin (Invitrogen) at 37.5^{o}C, followed by trypsin deactivation with 10% horse serum in

D-MEM. Detached cells were spun at 1200 rpm for 3 min and then replated in SATO medium as above. For all experiments, n=1 was considered to be cells from differentpassages.

Lentiviral transduction of Oli-Neu cells

Oli-neu cells were plated as above and allowed to proliferate to ~40% confluency. Cells were infected with Lenti-GFP-miR Pre-made Virus (ABMGood) specific for miR-145 at MOI 80-100 in proliferation medium with 5 µg/mL polybrene (Sigma). This construct represents a tetracycline-inducible system, in which tetracycline treatment results in expression of both miR-145 and GFP. After 24 hrs, virus-containing medium was replaced with selection medium (proliferation medium with 1 µg/mL puromycin). Transduced cells were differentiated and passaged as above, and medium was consistently supplemented with 1 µg/mL puromycin. To induce overexpression of miR-145, cells were treated with 1ng/mL tetracycline every 24 hrs. For proliferating cells, cells were lysed for RNA isolation or fixed for immunofluorescence on day 6 after initiating of tetracycline treatment. For differentiation, cells were treated with tetracycline for 4 days followed by 1mM dbcAMP treatment + tetracycline every 24 hrs until lysed or fixed, as appropriate. For early differentiation, cells were evaluated on day 3 after initiation of differentiation, and for late differentiation cells were evaluated on day 6 after initiation of differentiation.

RNA isolation

Total RNA was extracted from approximately 10^6 cells per sample. Medium was removed from cells followed by washing in ice cold 1x PBS. The PBS was aspirated and cells were then lysed using 1 mL Trizol® reagent (Qiagen). After 5 min incubation at room temperature, 250 µL chloroform was added to the Trizol®/cell lysate mixture and the sample was centrifuged at 10,000 rpm for 5 min. The aqueous phase was extracted, and RNA was precipitated with the addition of isopropanol followed by 10 min incubation at 4^oC. Samples were centrifuged at 14,000 rpm at 4^oC for 30 min. The resultant RNA pellet was washed in 1mL of 75% ethanol in RNase-free water (Qiagen), centrifuged at 9500 rpm for 5 min and finally resuspended in RNase-free water (Qiagen). RNA concentration was measured using a NanoDrop ####. RNA quality was assessed by measuring $OD_{260/280}$; only samples with $OD_{260/280}$>1.8 were used in further analysis. RNA quality was additionally ensured by running total RNA on a 1% agarose gel by electrophoresis to visualize clear bands for 18S and 28S rRNA. Samples were stored at -80^oC until use.

microRNA reverse transcription

Reverse transcription of miR-145 and snU6 was done according to Biggar *et al*. (2011) to produce specific DNA for each small RNA species. In short, 1 µg total RNA was incubated with 5 µL 250 nM stem-loop primer in a total volume of 10 µL. This annealing reaction was carried out at 95^oC for 5 min, followed by 60^oC for 5 min. Samples were immediately centrifuged and held on ice for at least 1 min. Reverse transcription was done using 1 µL M-MLV Reverse Transcriptase (Invitrogen), 4 µL 5x First Strand Buffer

(Invitrogen), 2 µL 100 mM dithiothreitol (Invitrogen) and 1 µL premixed dNTPs (final concentration 25 µM each). Each reaction was brought to a 25 µL total volume using RNase-free water (Qiagen). The following protocol was used for reverse transcription: 16^{o}C for 30 min, 60 cycles of 20^{o}C for 30 s, 42^{o}C for 30 s and 50^{o}C for 1 s, followed by 85^{o}C for 5 min, using an Eppendorf Mastercycler. Stemloop primer used for miR-145 was 5'-CTCACAGTACGTTGGTATCCTTGTGATGTTCGATGCCATATTGTACTGTGAGAGGGATTC-3' and for snU6 was 5'-CTCACAGTACGTTGGTATCCTTGTGATGTTCGATGCCATATTGTACTGTGAGAAAAATATGGAACGCTT-3'. Primers were obtained from AlphaDNA.

microRNA qRT-PCR

Amplification of miR-145 and snU6 cDNA was done using specific forward primers and a universal reverse primer complementary to the stemloop portion of the cDNA. The primer sequences are as follows: miR-145 5'-ACACTCCAGCTGGGGTCCAGTTTTCCCAGG-3'; snU6 5'-ACACTCCAGCTGGGGTGCTCGCTTCGGCAGCACATA-3'; universal 5'-CTCACAGTACGTTGGTATCCTTGTG-3', obtained from AlphaDNA. Each qRT-PCR reaction contained 12.5µL 2x SsoFast EvaGreen Supermix (Bio-Rad), 0.8 µL each of 25 µM forward and universal primer, and 5 µL cDNA, filled to 25 µL total with RNase-free water (Qiagen). Samples were amplified using the following protocol: 95^{o}C for 10 min followed by 40 cycles of 95^{o}C for 15 s and 60^{o}C for 1 min, using a Bio-Rad CFX Connect. All samples were run using n=4 in technical triplicate. Primer validation was

done by standard curve efficiency analysis, melt curve analysis, and electrophoresis of qPCR products on a 5% agarose gel to verify proper product size.

Total mRNA reverse transcription

cDNA was constructed for total mRNA using the RT2 First Strand Kit (Qiagen) as per manufacturer's protocol. Briefly, 2 µL Buffer GE (Qiagen) was used to eliminate genomic DNA from 1 µg total RNA in RNase-free water in a total volume of 10 µL per sample. Samples were incubated at 42^{o}C for 5 min and then held on ice for at least 1 min. Reverse transcription was carried out by adding 4 µL 5x Buffer BC3 (Qiagen), 1 µL Control P2 (Qiagen), 2 µL RE3 Reverse Transcriptase Mix (Qiagen) and 3 µL RNase-free water (Qiagen), followed by incubation at 42^{o}C for 15 min and 95^{o}C for 5 min. Samples were diluted with 91 µL RNase-free water (Qiagen) and stored at -20^{o}C until use.

qRT-PCR arrays

Custom RT^{2} Profiler^{TM} PCR arrays were acquired from SuperArray Bioscience (SABioscience). Each 96-well plate contained 2 wells of pre-optimized lyophilized primer for each of 42 target genes, 3 reference genes and 3 controls, listed in Table 1. Reference genes used for normalization included *RN18S, Gusb* and *Actb*. Controls included RT control (NRT), control for genomic contamination (MGDC) and a positive control (PPC). Quality control of each array amplification was based on pre-determined parameters for the NRT, PCC and MGDC controls defined by SABiosciences to measure array reproducibility, genomic DNA control and RT efficiency; only array data

Table 1. List of genes included in custom RT^2 Profiler^{TM} PCR Array

Gene Symbols		
2900073G15Rik	Gabarapl1	Qk
Add3	MRF/Gm98	Rock1
Arhgap24	Gmfb	Serinc5
Arhgap26	Grlf1	Ssh2
Arpc5	Igf1r	Stk38l
Ccnd2	Kifap3	Tln2
Cfl2	Lasp1	Tmod1
Coro2b	Myo5a	Tmod3
Crkl	Nras	Tpm4
Cspg4	Pak4	Tppp3
Ctnnd1	Phactr1	Trim2
Epb4.1l5	Pmp22	Ywhag
Fgf10	Ppia	Actb
Flnb	Ppp1r9a	Gusb
Fscn1	Pxn	RN18S

that received a “pass” score for each was used for analysis. Amplification of cDNA was conducted as per the manufacturer’s protocol. Briefly, each reaction contained 1 µL of reverse transcription products, 12.5 µL 2x RT^2 SYBR Green Mastermix (Qiagen) and 11.5 µL RNase-free water (Qiagen). Amplification was carried out at 95^{o}C for 10 min followed by 40 cycles of 95^{o}C for 15 s and 60^{o}C for 1 min using a Bio-Rad CFX Connect. In addition to the intrinsic quality control measures, melt curve analysis was also done to ensure a single peak for each primer pair.

qRT-PCR analysis

For *Oli-neu* cells, miR-145 at P, DD3 and DD6 expression was analysed by the ΔCt method. For ON-145-1 and ON-145-2, both miR-145 and gene array expression data were analysed by the ΔΔCt method. For all miR-145 expression data, levels were normalized to snU6 expression, and analysis was conducted using the CFX Manager™ Software provided with the Bio-Rad CFX Connect system. Array genes were normalized to multiple reference genes and analysis was conducted using the web-based RT^2 Profiler® PCR Array Data Analysis provided by SABiosciences (Qiagen).

Immunofluorescence

Cells were fixed in 3% PFA for 15 min followed by permeabilization in 1% Triton-X100 in PBS for 5 min. After washing 3 x with PBS cells were incubated in blocking medium (10% goat serum in PBS) for ~1 hr. Incubation with primary antibody was done overnight at 4^{o}C, followed by 3 x washes with 1x PBS and 2-3 hrs incubation with secondary antibody at 4^{o}C. Actin staining was done using rhodamine-conjugated

phalloidin (Invitrogen) 1:200 in blocking serum for ~2 hrs. Nuclear staining was done using Hoescht 1:1000 in PBS for ~5 min. Primary antibodies were diluted in blocking serum at the following concentrations: green fluorescent protein (GFP; rabbit, Invitrogen) 1:500; MAG (mouse,Millipore) 1:100; alpha-tubulin (mouse, Millipore) 1:1000; cleaved caspase-3 (mouse, 1:400. Appropriate secondary antibodies were used at a dilution of 1:200 in PBS at 4^{o}C (AlexaFluor, Invitrogen). Coverslips were mounted on slidesusing Dako Fluorescent Mounting Medium. ***Proliferation Assay***

Quantification of proliferation of transduced *Oli-Neu* cells was done using the Click-iT® AlexaFluor 555 Imaging Kit (Invitrogen) as per the manufacturer's instructions. Induced cells were treated with 1 ng/mL tetracycline every 24 hrs for 6 days, while uninduced cells were allowed to grow in normal proliferation medium. Cells were incubated with EdU for the final 48 hrs of tetracycline treatment followed by fixation with 3% PFA and permeabilization with 1% Triton-X in PBS. Coverslips were first stained for GFP as above, followed by 30 min incubation with 0.5 mL Click-iT® Reaction Cocktail, made as per the manufacturer's protocol,at room temperature. Coverslips were then washed once with PBS, followed by Hoescht nuclear staining and mounting as above.

Microscopy and image acquisition

Phase contrast images were taken using Zeiss AxioVision software using the Zeiss Axiovert 200 inverted microscope. Fluorescent images were taken using Zeiss Zen 2008 software using the Zeiss LSM 510 confocal microscope.

Morphological analysis

Primary and secondary branch numbers were counted using Zeiss Zen 2008 software. Cells were differentiated for either 3 days or 6 days on poly-L-lysine-coated coverslips in the presence or absence of tetracycline. An extension was considered a “branch” if it was positive for both f-actin and α-tubulin staining. Branches were ordered based on their distance from the cell body, ie: a primary branch extends directly from the cell body, a secondary branch extends from a primary branch. Projections from the cell body that were fanned at the edge and not organized into a branch-like structure were not considered to be primary branches. For primary branch counting, a minimum of 30 cells per n were analysed (n=3). For secondary branch counting, a minimum of 30 primary branches were analysed (n=3).

Statistical analysis

Three way comparisons were done using one-way analysis of variance (ANOVA) followed by Tukey’s honestly significant difference (HSD) *post-hoc* test using n=3-4. Pair-wise comparisons were done by Student’s t-test using n=3-4. Results were deemed significant if $p<0.05$. All error bars represent ±SEM.

Results

miR-145 putative targets are enriched for actin cytoskeleton- and myelin-related genes

Using TargetScanMouse (www.targetscan.org; Lewis *et al*., 2005; Grimson *et al*., 2007; Friedman *et al.*, 2009b) a list of putative mRNA targets was generated for several miRNAs, including miR-145. These microRNAs were chosen for initial investigation because they share the mutual characteristics of being differentially regulated during OL differentiation and showing evidence of misregulation in the environment of the human MS brain lesion. MiR-145 has been shown to be expressed at relatively high levels in proliferating OPCs, but is strongly downregulated in differentiating and mature OLs (Letzen *et al.,* 2010). Further, it was found to be upregulated by ~3-fold in MS lesion tissue compared to white matter from healthy controls (Junker *et* al., 2009). To assess the value of our chosen candidates for further investigation, DAVID functional annotation tools were used to group the genes in each list into functional categories based on gene ontology (GO). Of the miRNAs examined, only miR-145 showed enrichment for genes involved both in cytoskeleton organization and myelination, indicating it was the most relevant candidate for study in OL differentiation and myelination. For miR-145, a total of 12 clusters were found to be significantly enriched based on an Expression Analysis Systematic Explorer (EASE) score greater than 1.3 (one-tailed Fisher's exact probability test, equivalent to non-log $p<0.05$). Of these clusters, four were deemed particularly relevant to OL differentiation and/or myelination (Table 2). These clusters were generally categorized as genes relating to the actin cytoskeleton (EASE score 2.54), focal adhesions (EASE score 2.42), adherens junctions (EASE score 2.35) and myelination (EASE score 1.58).The genes isolated in

Table 2.DAVID Functional Annotation Cluster (FAC) analysis of putative targets of miR-145. Twelve significant clusters (enrichment/EASE score >1.3; $p<0.05$) were revealed by FAC analysis of 456 targets predicted by TargetScan. Four clusters relevant to oligodendrocyte differentiation and myelination are indicated along with their respective enrichment scores and the number of genes implicated in each cluster.

GO Cluster	Enrichment	Genes
Actin cytoskeleton	2.54	20
Focal adhesion	2.42	15
Adherens junction	2.35	6
Myelination	1.58	4

these relevant clusters are shown in Figure 4 by heat map analysis indicating correlation with the related GO categories for each cluster. Additional significant clusters included genes generally categorized under the following headings: GTPase activation, angiogenesis, regulation of transcription, respiratory development, serine/threonine kinase activity, pleckstrin homology, sh3 domain and tube development. KEGG pathway analysis was also performed using DAVID. Of eight significantly enriched pathways ($p<0.05$), three were relevant to OL differentiation and related to previously identified significantly enriched clusters. These three pathways include regulation of actin cytoskeleton, focal adhesions and adherens junctions. KEGG pathways are displayed in Figure 5with putative miR-145 targets circled in red, and potentially affected downstream processes boxed in blue.

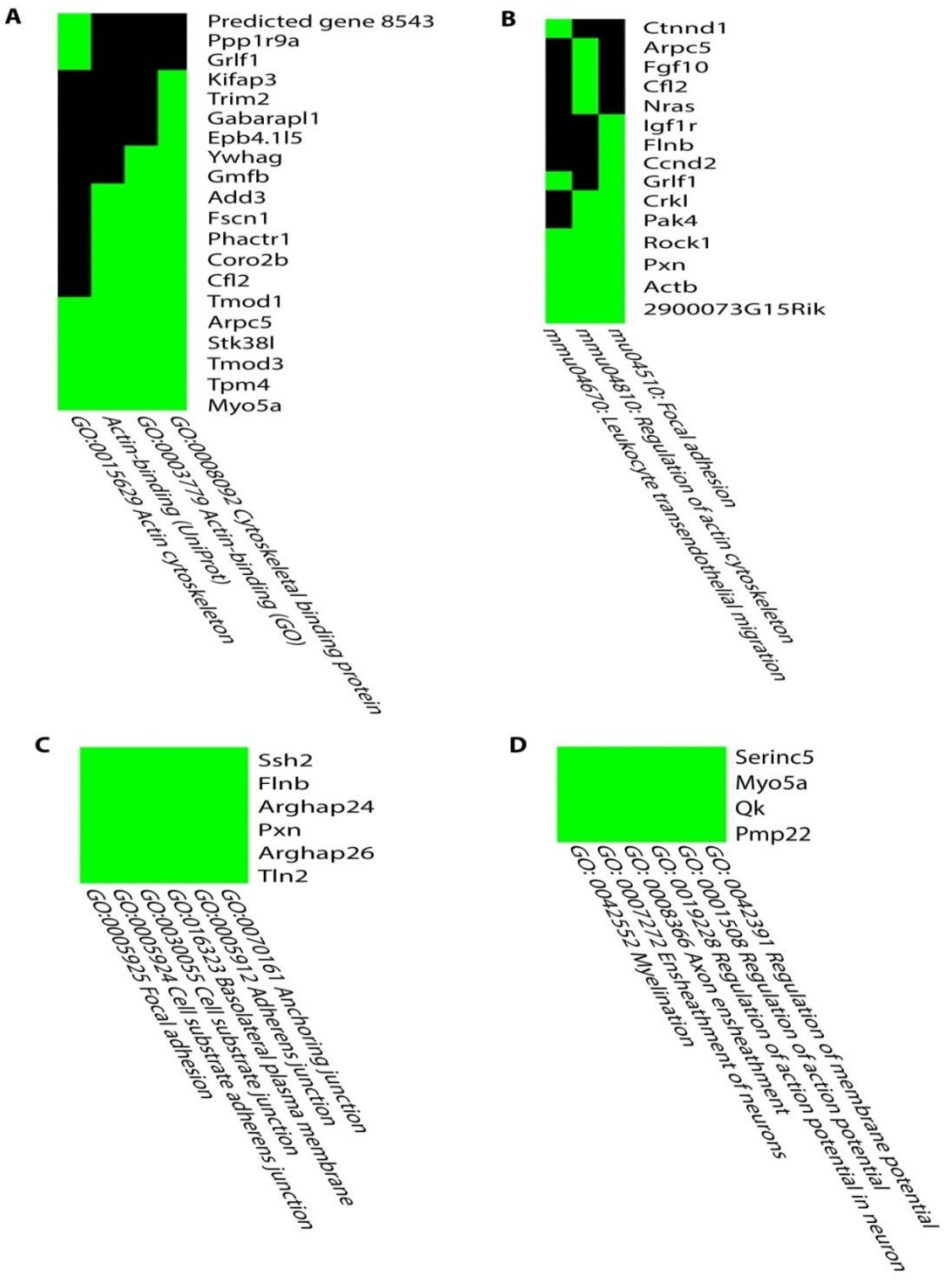

Figure 4.DAVID heat map analysis of significantly enriched gene clusters from putative miR-145 targets with possible relevance for oligodendrocyte differentiation. A. Actin cytoskeleton B. Focal adhesion C. Adherens junction D. Myelination. Positive and unconfirmed correlation of GO terms and *Mus musculus* genes are shown in green and black, respectively.

A

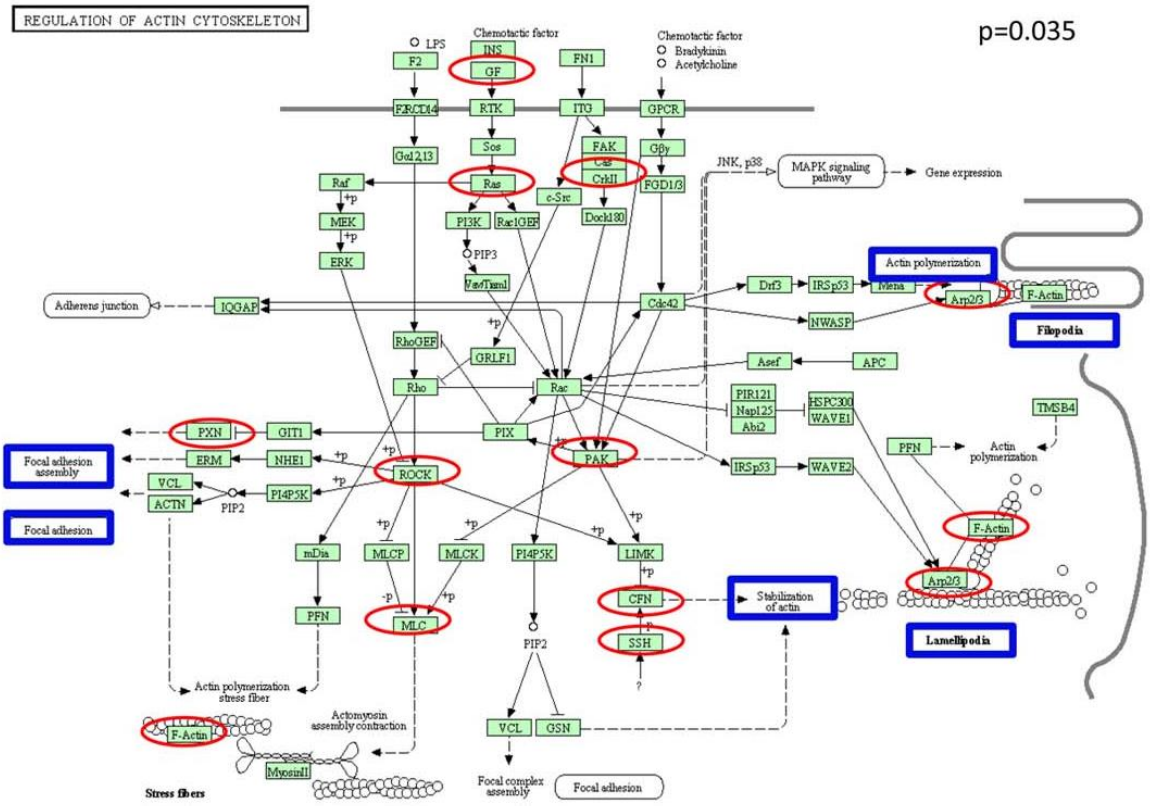
REGULATION OF ACTIN CYTOSKELETON
p=0.035
LPS
Chemotactic factor
Chemotactic factor
Bradykinin
Acetylcholine
JNK, p38
MAPK signaling pathway
Gene expression
Actin polymerization
Filopodia
Lamellipodia
Adherens junction
Focal adhesion assembly
Focal adhesion
Actin polymerization stress fiber
Actomyosin assembly contraction
Stress fibers
Focal complex assembly
Focal adhesion
Stabilization of actin

B

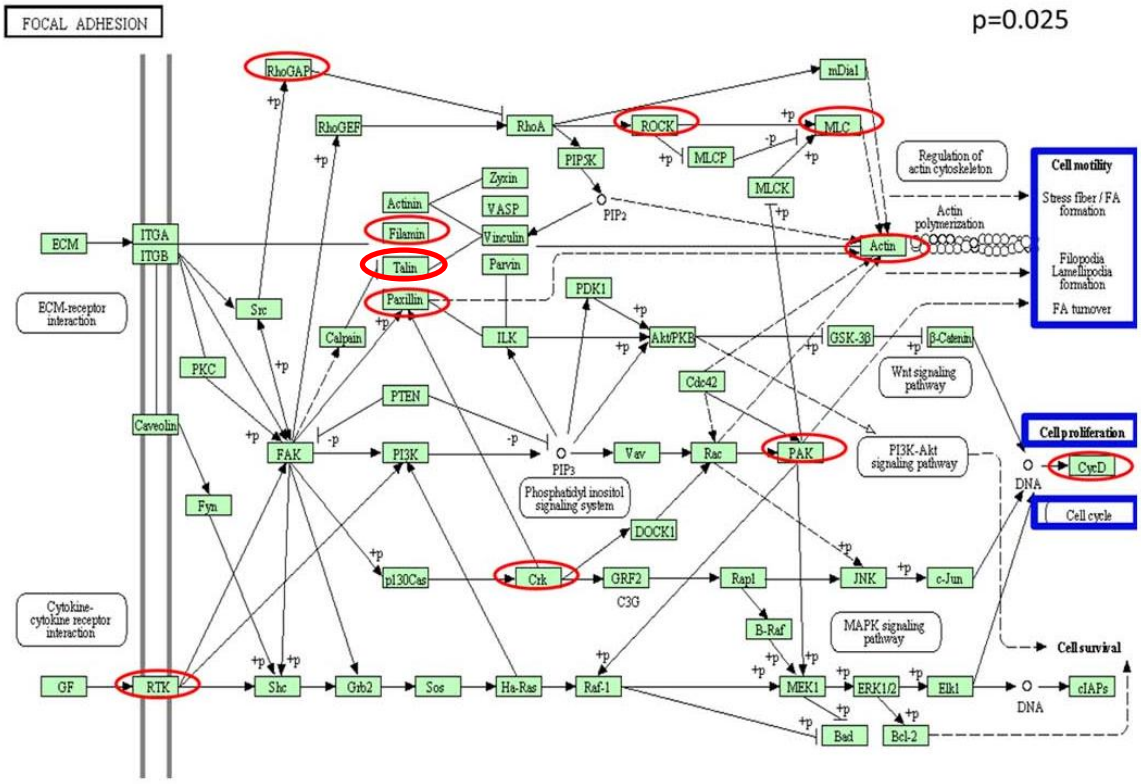
FOCAL ADHESION
p=0.025
ECM
ECM-receptor interaction
Cytokine-cytokine receptor interaction
Caveolin
Fyn
Src
PKC
Calpain
Actinin
Filamin
Talin
Paxillin
Zyxin
VASP
Vinculin
Parvin
PIP2
PIP3
Phosphatidyl inositol signaling system
Regulation of actin cytoskeleton
Actin polymerization
Cell motility
Stress fiber / FA formation
Filopodia Lamellipodia formation
FA turnover
Cell proliferation
CycD
DNA
Cell cycle
Cell survival
Wnt signaling pathway
PI3K-Akt signaling pathway
MAPK signaling pathway
C3G
DNA

C

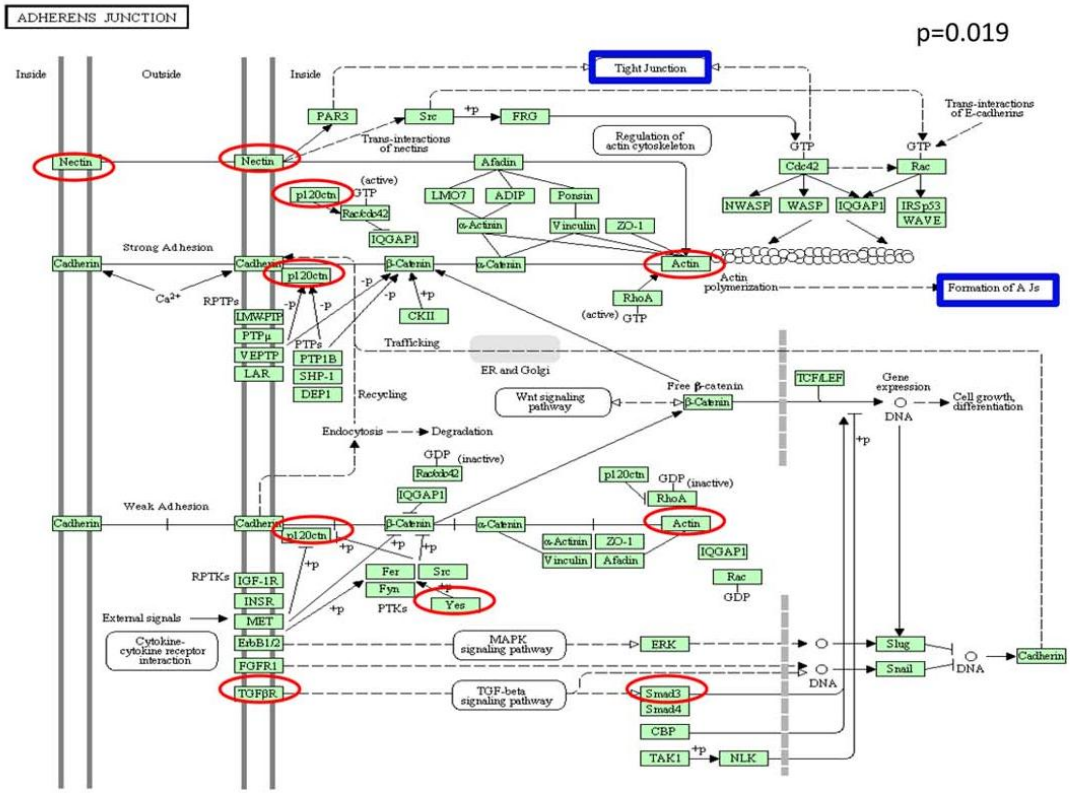

Figure 5.KEGG pathway analysis of putative miR-145 targets.A. Regulation of actin cytoskeleton. B. Focal adhesions. C. Adherens junctions. Red circles indicate genes predicted to be targeted by miR-145, with respective downstream biological processes boxed in blue. Significant p-values are shown in upper right corner of each pathway.

miR-145 is differentially expressed as Oli-neu cells differentiate

Oli-neu cells represent an immortalized mouse oligodendrocyte progenitor cell line stably transfected with the oncogene*t-neu* tyrosine kinase oncogene which maintains their proliferative state (Jung *et al*., 1995). These cells can be differentiated with application of dbcAMP, and when in co-culture with neurons will progress as far along the lineage pathway as to contact but not wrap axons.To examine the validity of *Oli-neu* cells as a model for exploring the role of miR-145, we needed to discover if differential expression of miR-145 in the *Oli-neu* cell lineage progression was similar to that of non-immortalized cells, i.e. with a relatively high expression level in a proliferative state and a strong downregulation in differentiating cells.The endogenous expression patterns of miR-145 were investigated by qRT-PCR in proliferating (P), and early (DD3) and late (DD6) differentiating *Oli-neu* cells. These cells maintain a generally bipolar morphology under growth conditions, but their branching becomes more complex as differentiation progresses (panel A, Figure 6). Relative expression was analysed by the ΔCt method, and miR-145 expression was normalized to snU6. In *Oli-neu* cells, the expression levels of miR-145 were found to be relatively high at timepoint P, with a significant downregulation of ~80% in cells early in differentiation on DD3 that was maintained into late differentiation on DD6 (panel B, Figure 6; $p<0.05$). No significant difference was found for expression levels between DD3 and DD6. For each timepoint, RNA was isolated from cells from different passages for n=4.

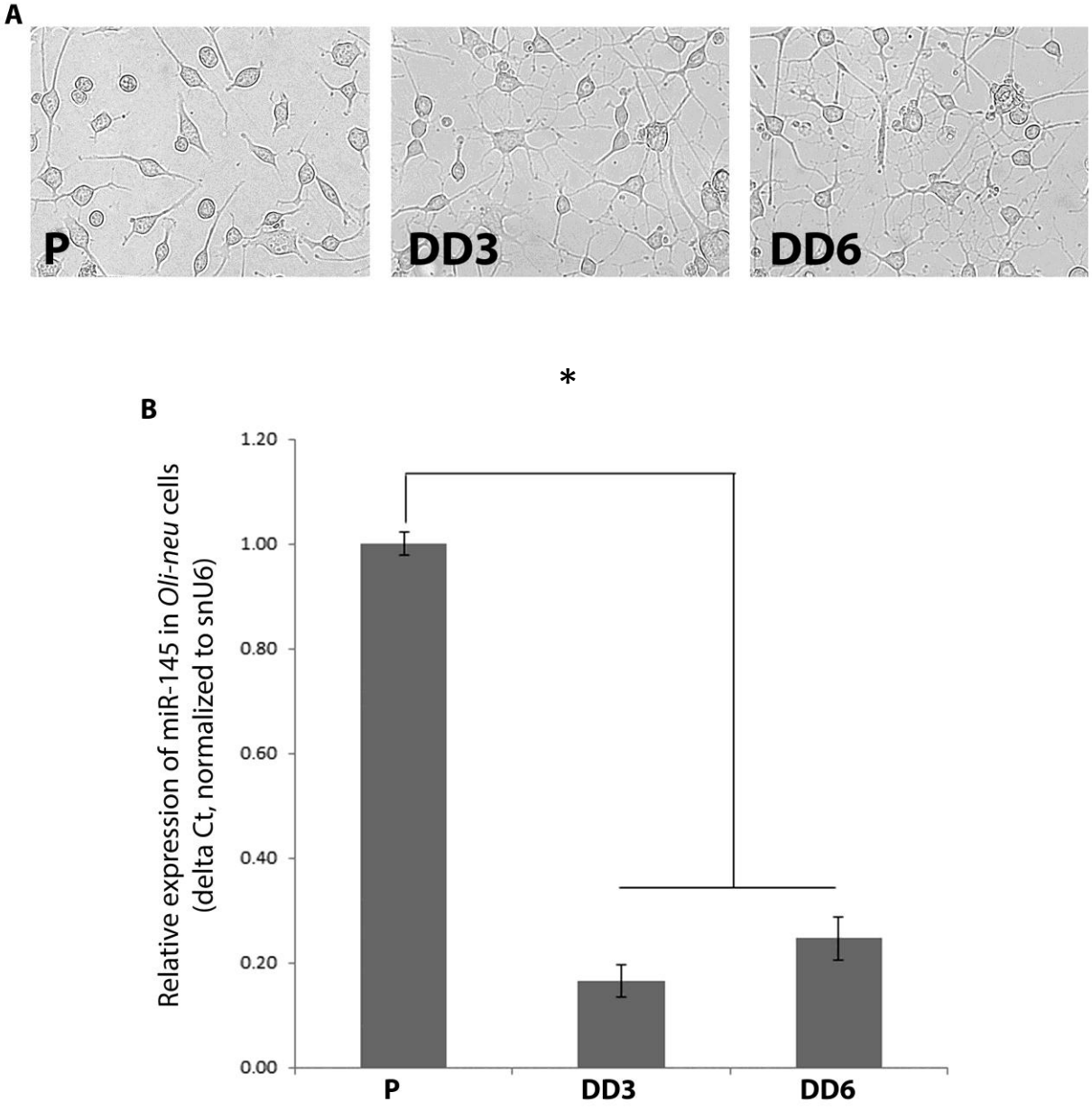

Figure 6.miR-145 is differentially expressed as *Oli-neu* cells progress from progenitor cells to differentiated cells. A. Phase contrast images of *Oli-neu* cells while proliferating (P), on differentiation day 3 (DD3) and differentiation day 6 (DD6). B. Quantification of relative miR-145 expression by qRT-PCR at timepoints P, DD3 and DD6. * indicates $p<0.05$ (One-way ANOVA; Tukey's HSD), n=4.

Generation of stable Oli-neu cell lines that inducibly overexpress miR-145

Oli-neu cells were infected with lentiviral particles in which pre-miR-145 was encoded under the control of a tetracycline response element (TET R.E.) Vector components can be seen in the schematic in panel A, Figure 7. Infection conditions were carefully optimized as these cells proved highly sensitive to chemical alterations to their normal growth conditions (Figure A1). Optimal selection conditions were established by determining the lowestconcentration of puromycin required to kill 100% of cells within 72 hrs (Figure A2).After infection, cells which survived in selection medium longer than 72 hrs were expanded and tested for GFP expression upon tetracycline induction (panel B, Figure 7). Conditions for ideal induction were determined by tetracycline treatment at varying dose amounts and timing (Figure A3. The treatment protocol we chose to follow was induction of miR-145 overexpression by 1 ng/mL tetracycline treatment every 24 hrs for 4 days, as this was the lowest dosage that showed 100% induction efficiency in the least amount of time (Figure A3). Two stable lines were successfully established, which we named ON-145-1 and ON-145-2. After sufficient expansion and passages, miR-145 expression levels were investigated in each cell line by qRT-PCR. ON-145-1 was found to overexpress miR-145 by ~ 33-fold in induced cells versus uninduced cells, while ON-145-2 was found to overexpress miR-145 by ~11-fold in induced versus uninduced cells ($p<0.05$, $\Delta\Delta Ct$ method, $n=4$; panel C, Figure 7).

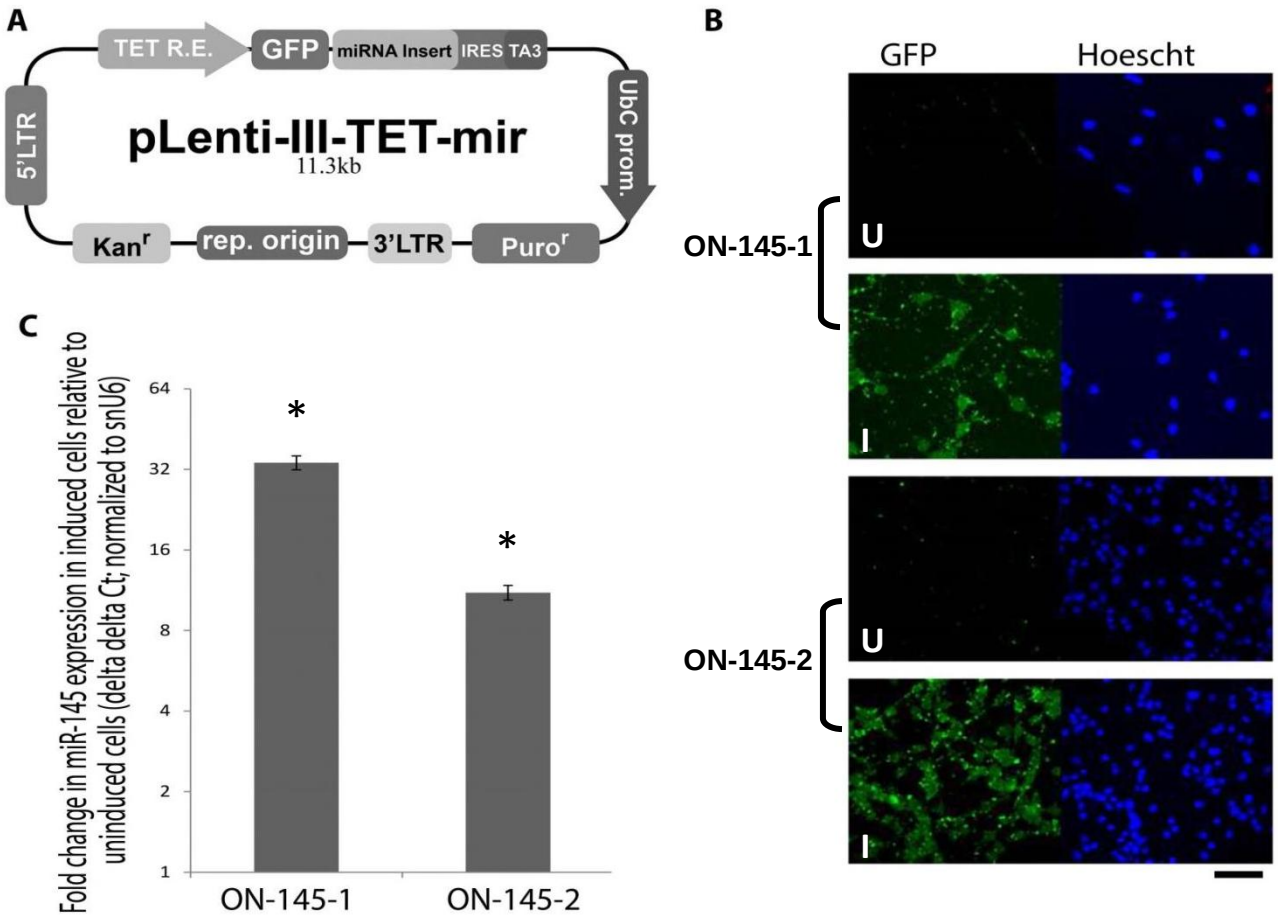

Figure 7. ON-145-1 and ON-145-2 cells inducibly overexpress miR-145. *Oli-neu* cells were transduced to create stable lines which overexpress miR-145 upon induction with tetracycline. A. Graphic representation of the tetracycline-inducible lentivirus vector used to transduce *Oli-neu* cells. B. Transduced ON-145-1 and ON-145-2 cell lines show GFP expression only upon induction with tetracycline treatment. U indicates uninduced cells, I indicates induced cells. Induced cells were treated with 1 ng/mL tetracycline in growth medium every 24 hrs for 4 days. Scale bar = 50 µm. C. Quantification of miR-145 expression in induced cells relative to uninduced cells. Fold change calculated using the ΔΔCt method, normalized to snU6 expression. * indicates $p<0.05$ (Student's two-tailed t-test), n=4.

Overexpression of miR-145 shows little effect on proliferating Oli-neu cells

To observe any differences in morphological characteristics in induced cells compared to uninduced cells, cells were treated with tetracycline or not, and allowed to proliferate in normal growth medium for 6 days. Immunofluorescent staining for filamentous actin (F-actin) and α-tubulin revealed no clear alteration in cytoskeletal morphology (Figure 8). Both uninduced and induced cells exhibited a similar range of cell shapes for proliferating *Oli-neu* cells including round, bipolar and tri-branched cells.

We next assessed whether there was any change in proliferation rate in miR-145 overexpressing cells. Cells were again treated with tetracycline or allowed to proliferate in normal proliferation medium for 6 days, but were additionally treated with EdU for the final 48 hrs. Quantification was done by counting the number of EdU+ cells as a mean percentage of total cells per sample. While no significant difference could be detected between induced and uninduced ON-145-2 cells, induced ON-145-1 cells showed a significant decrease at ~44% EdU+ cells per field of view compared to ~59% of uninduced cells ($p<0.05$, $n=3$; Figure 9).

Further evaluation was done to investigate any change in the frequency of apoptosis by staining for cleaved caspase-3. Cells were treated as they were for immunofluorescent staining above, and quantification of cleaved caspase-3+ cells was evaluated as a mean percentage of total cells per sample. There was no significant difference in induced ON-145-1 or ON-145-2 cells compared to their uninduced counterparts (Figure 10).

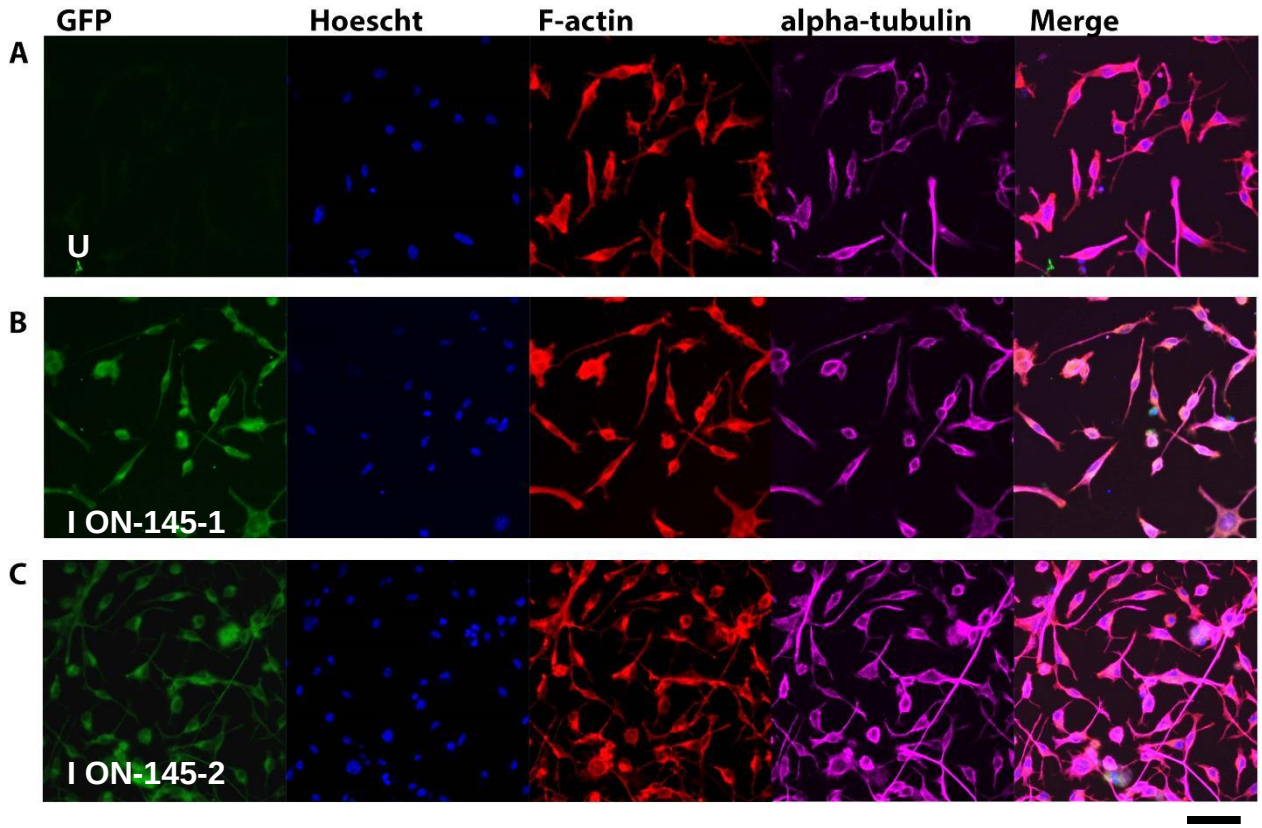

Figure 8. Proliferating cells overexpressing miR-145 appear morphologically normal. Confocal micrographs of proliferating ON-145-1 and ON-145-2 cells.A.Representative uninduced cells (ON-145-1). B. Induced ON-145-1 cells. C. Induced ON-145-2 cells. Induced cells were treated with 1 ng/mL tetracycline every 24 hrs for 6 days. I indicates induced cells, U indicates uninduced cells. Scale bar = 50 µm.

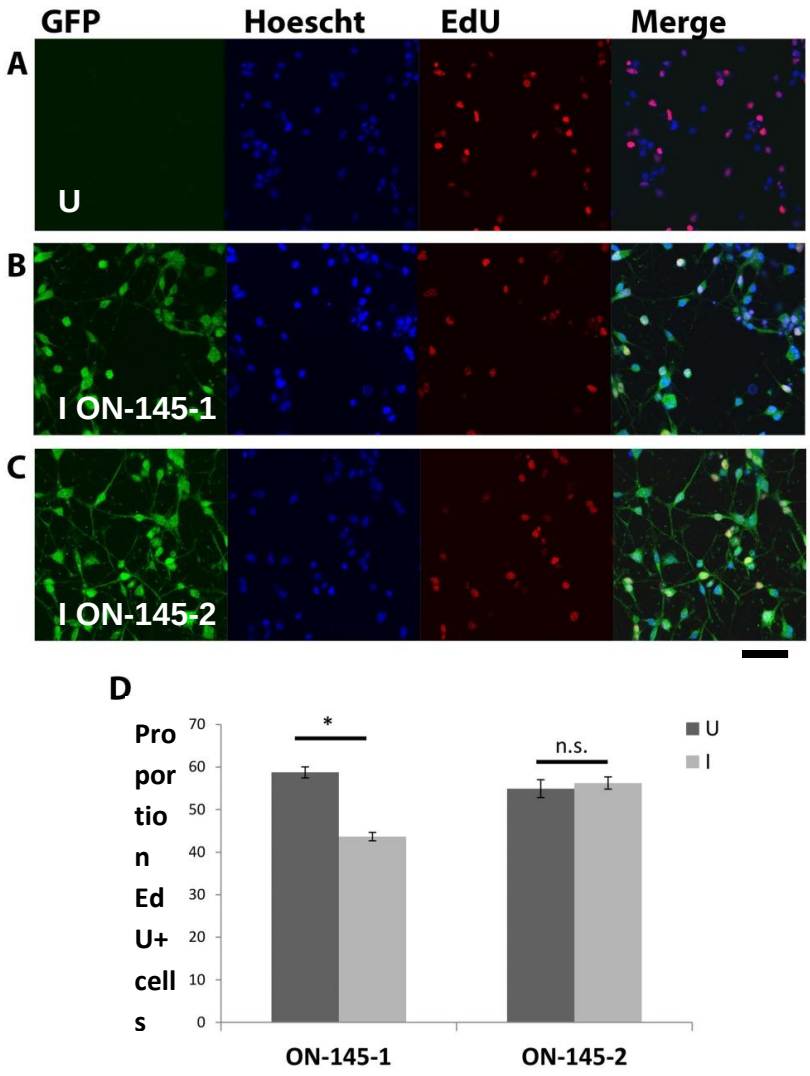

Figure 9.Only ON-145-1 cells show a change in proliferation rate when miR-145 is overexpressed. Confocal micrographs of uninduced and induced proliferating cells. Cells were allowed to proliferate for 6 days; induced cells were treated with 1 ng/mL tetracycline every 24 hrs, and both induced and uninduced cells were incubated with EdU for the final 48 hrs.A-C.Uninduced and induced cells from ON-145-1 and ON-145-2.Scale bar = 50 µm. D. Quantification of EdU+ cells expressed as a mean percent (± SEM). I indicates induced cells, U indicates uninduced cells. * indicates $p<0.05$, n.s. not significant, n=3.

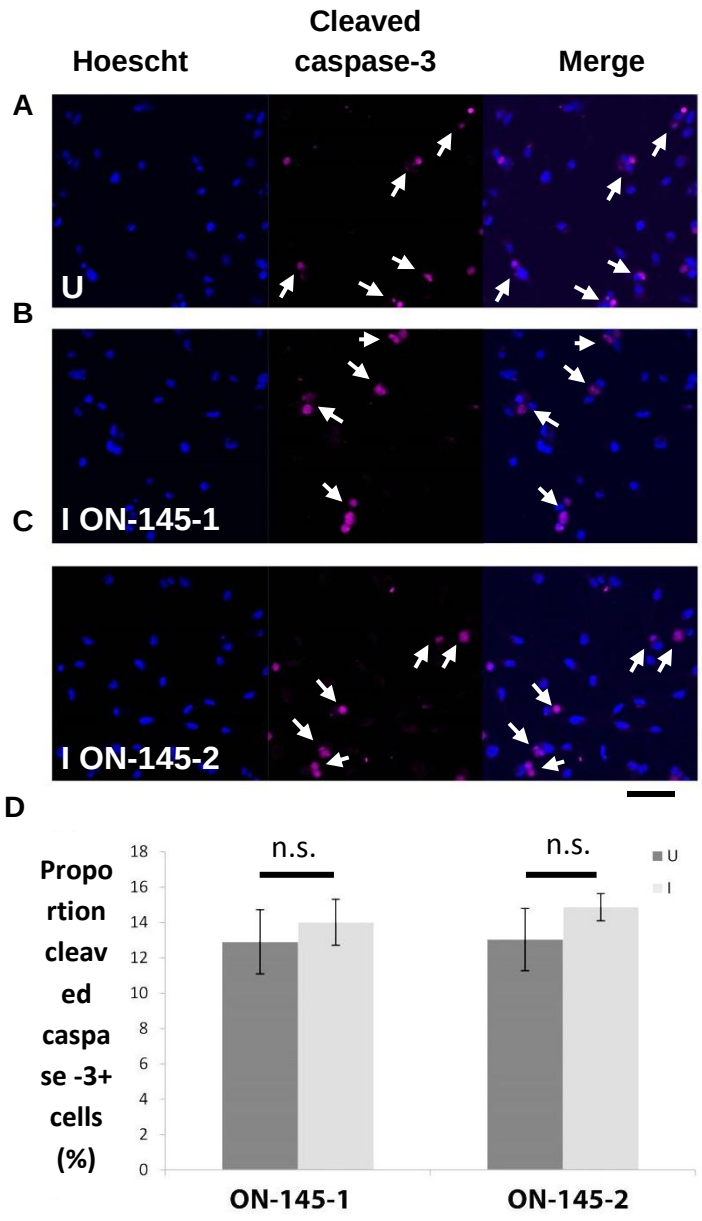

Figure 10.miR-145 overexpressing cells show no difference in the amount of cleaved caspase-3 mediated cell death. Confocal micrographs of uninduced and induced proliferating cells. Induced cells were treated with 1 ng/mL tetracycline every 24 hrs for 6 days. A. Representative uninduced (U) cells (ON-145-2). B. Induced (I) ON-145-1 cells. C. I ON-145-2 cells. White arrows indicate cleaved caspase-3+ cells. Scale bar = 50 µm. D. Quantification of cleaved caspase-3+ cells expressed as mean percent (± SEM). n.s. not significant, n=3.

miR-145 overexpression leads to a reduction in primary and secondary branching early in differentiation

Since overexpression of miR-145 appeared to have little effect on the morphology, proliferation and survival of OPCs, we next sought to address whether it might affect their ability to differentiate. Cells were either treated with tetracycline for 3 days to induced miR-145 overexpression, or allowed to proliferate in normal growth medium. On day 4, all cells were differentiated, and induced cells were continuously treated with tetracycline. To assess any changes in early differentiation, both induced and uninduced cells were analysed on day 3 after initiation of differentiation (DD3).

In contrast to our observations of proliferating cells, both ON-145-1 and ON-145-2 cells exhibited altered morphology when induced to overexpress miR-145 compared to when uninduced on DD3 (panels A, B, C, Figure 11).This effect was not observed when non-transduced *Oli-neu* cells were differentiated in the presence of tetracycline, suggesting that the altered morphology was not due to tetracycline exposure (Figure B1). In miR-145 overexpressing cells, their altered morphology was characterized by a clear reduction in branching complexity. Not all cells were uniform in their branching ability; this was true in both induced and uninduced cells of both cell lines, but with differing branching frequency distributions (Figure 12). For ON-145-1 cells, the majority of induced cells had 0 branches (52.7%), while those that did extend primary branches became progressively fewer as the branch number increased, with 22.2% with 1 branch, 11.1% with two branches, 8.3% with 3 branches and 5.6% with 4 branches. In uninduced cells, a frequency distribution was observed with the majority of cells extending 5 primary branches per cell (25.0%). Many cells were able to extend 3, 4, 6 or 7 branches at 13.9%, 16.8%, 19.4% and 16.7% respectively. Few cells extended only 1

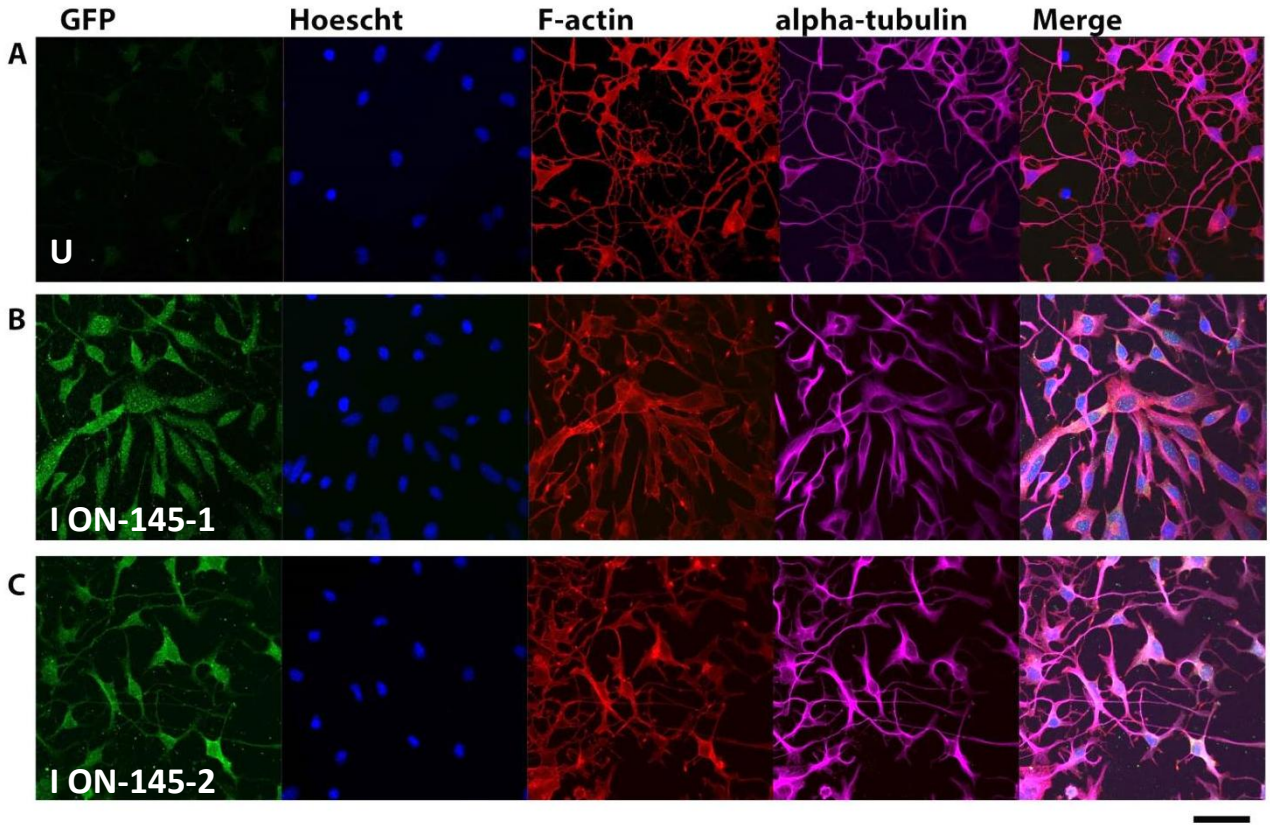

Figure 11.**On differentiation day 3 (DD3), cells overexpressing miR-145 display altered morphology.**Confocal micrographs showing ON-145-1 and ON-145-2 cells on DD3.A. Representative uninduced cells (ON-145-1). B. Induced ON-145-1 cells. C. Induced ON-145-2 cells. Uninduced cells were treated with 1mM dbcAMP every 24 hrs for 3 days. Induced cells were treated with 1 ng/mL tetracycline every 24 hrs for 3 days, followed by treatment with 1 ng/mL tetracycline + 1 mM dbcAMP for 3 days. Scale bar = 50 µm.

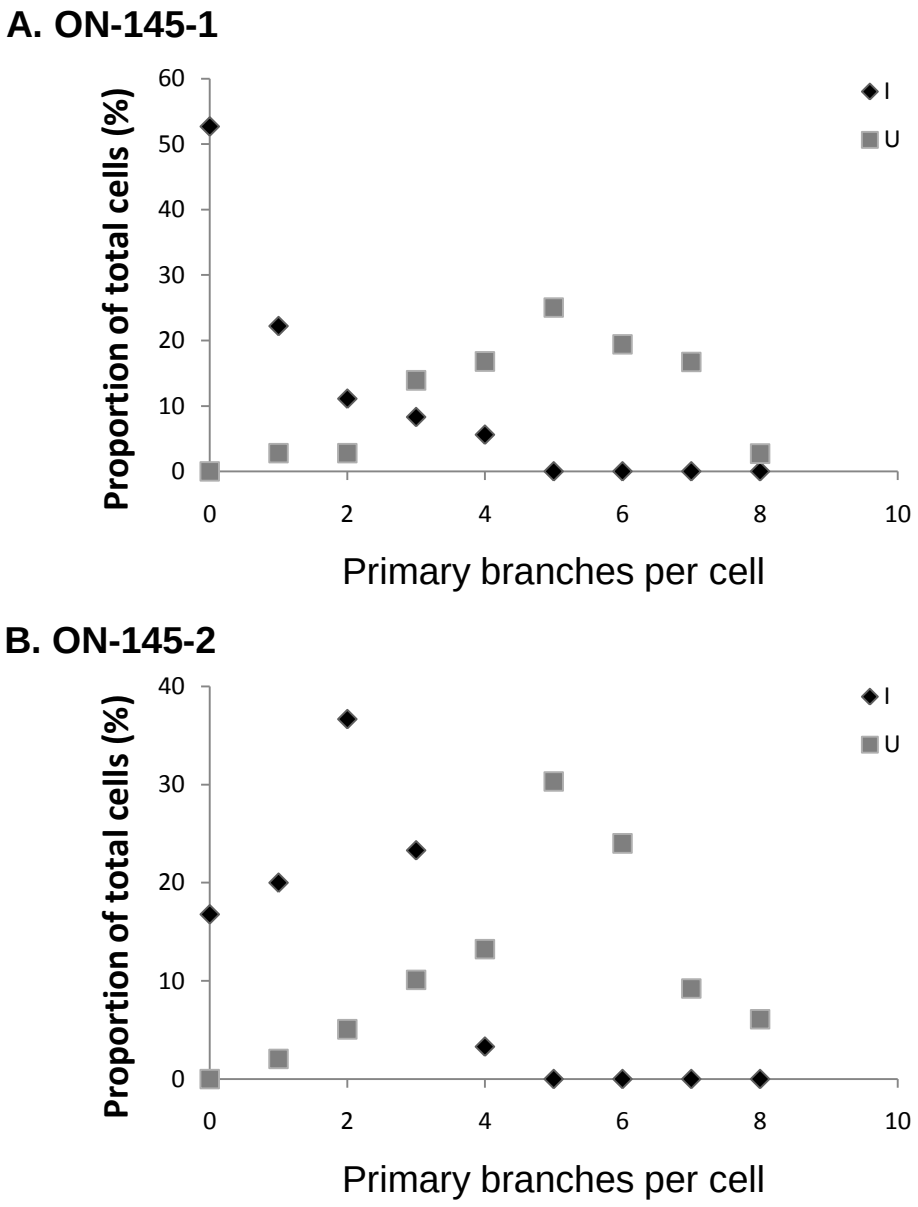

Figure 12. On differentiation day 3, the primary branching profile is altered between induced and uninduced cells. Uninduced cells were treated with 1mM dbcAMP every 24 hrs for 3 days. Induced cells were treated with 1 ng/mL tetracycline every 24 hrs for 3 days, followed by treatment with 1 ng/mL tetracycline + 1 mM dbcAMP for 3 days. A. ON-145-1 cells on DD3. B. ON-145-2 cells on DD3. Each condition includes pooled results from n=3. I indicates induced cells, U indicates uninduced cells.

or 2 primary branches (2.8% for each) or as many as 8 primary branches (2.6%). For uninduced cells, none were observed without primary branches. Cells from line ON-145-2 exhibited similar trends in uninduced cells, where 2.1% had 1 branch, 5.1% had 2, 10.1% had 3, 13.2% had four, 30.3% had 5, 23.9% had 6, 9.2% had 7 and 6.1% had 8. Again, no uninduced cells could be found without primary branching. The primary branching profile for induced ON-145-2 cells showed a different distribution not only from uninduced cells but also from ON-145-1 induced cells. In this case, the majority of cells extended 2 primary branches (36.7%). The proportion of induced ON-145-2 cells with 0 branches was 16.8%, with 1 branch was 20.0%, with 3 branches was 23.3% and with 4 branches was 3.3%.

In order to compare global branching ability for each condition, an average of primary branches per cell was taken for each condition. For ON-145-1 cells, mean primary branch number was significantly reduced from ~5 to ~1 per cell, while in ON-145-2 cells was significantly reduced from ~5 to between 2-3 per cell ($p<0.05$, $n=3$; panel A, Figure 13). While uninduced cells of both cell lines maintained a similar primary branching ability, induced ON-145-1 cells appeared more severely affected than ON-145-2 cells (Figure 11). This was confirmed by comparing the ratio of the mean number of branches in induced cells to uninduced cells between the two cell lines. ON-145-1 cells produced significantly fewer primary branches per cell relative to their uninduced counterparts than did ON-145-2 cells ($p<0.05$, $n=3$; panel B, Figure 13).

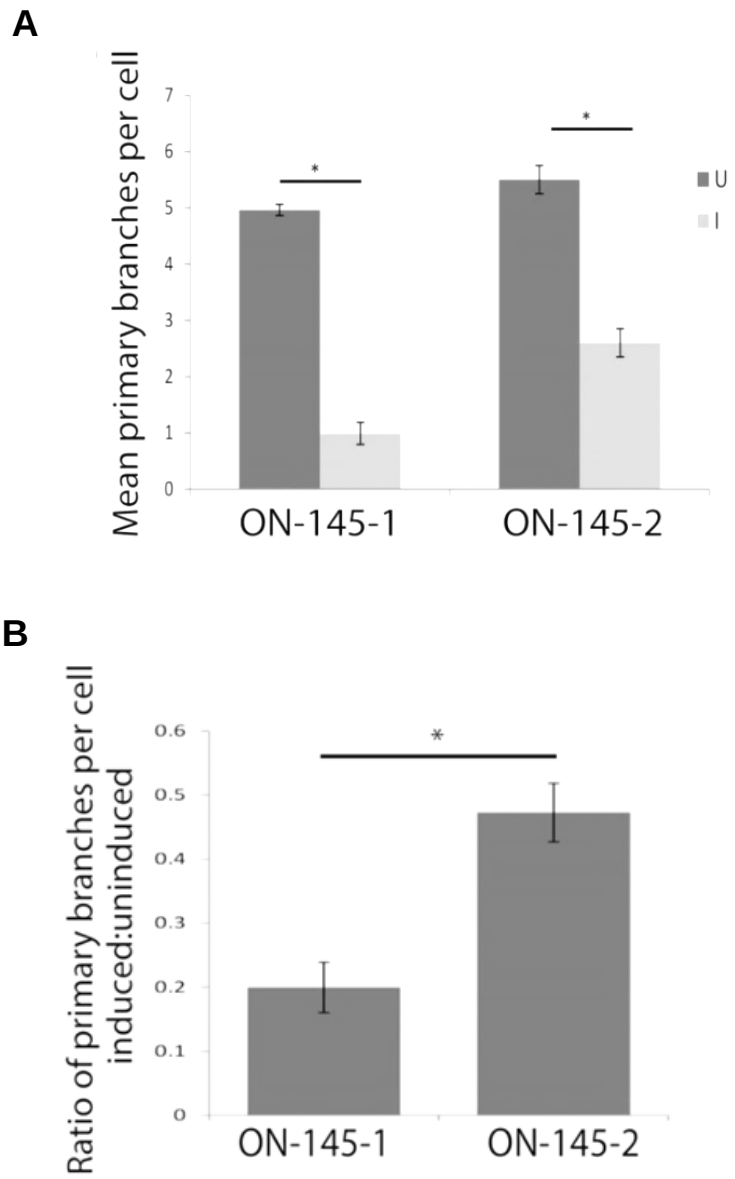

Figure 13. Global primary branching is reduced in miR-145 overexpressing cells early in differentiation. A. Quantification of mean primary branch number per cell ± SEM on DD3 for uninduced and induced cells from lines ON-145-1 and ON-145-2. B. Ratio of mean number of primary branches per cell ± SEM in induced cells to uninduced cells for ON-145-1 and ON-145-2 on DD3. * indicates $p<0.05$ (Student's two-tailed t-test), n=3. I indicates induced cells, U indicates uninduced cells.

On DD3, differences were also observed in secondary branching ability in induced cells of both cell lines (panels A - D, Figure 14). Secondary branching ability was quantified by measuring the average number of secondary branches extended per primary branch. Uninduced ON-145-1 cells were found to have a mean of between 3-4 secondary branches per primary branch, while induced cells showed a significant decrease at a mean of 0-1 ($p<0.05$, $n=3$; panel E, Figure 14). ON-145-2 cells showed a similar reduction, with ~4 secondary branches per primary branch in uninduced cells but significantly fewer in induced cells at ~1 ($p<0.05$, $n=3$; panel E, Figure 14). Interestingly, in contrast to primary branch numbers, when comparing the number of secondary branches per primary branch between cell lines, no significant difference was found between the ratios of induced to uninduced cells between ON-145-1 and ON-145-2 ($n=3$; panel F, Figure 14).

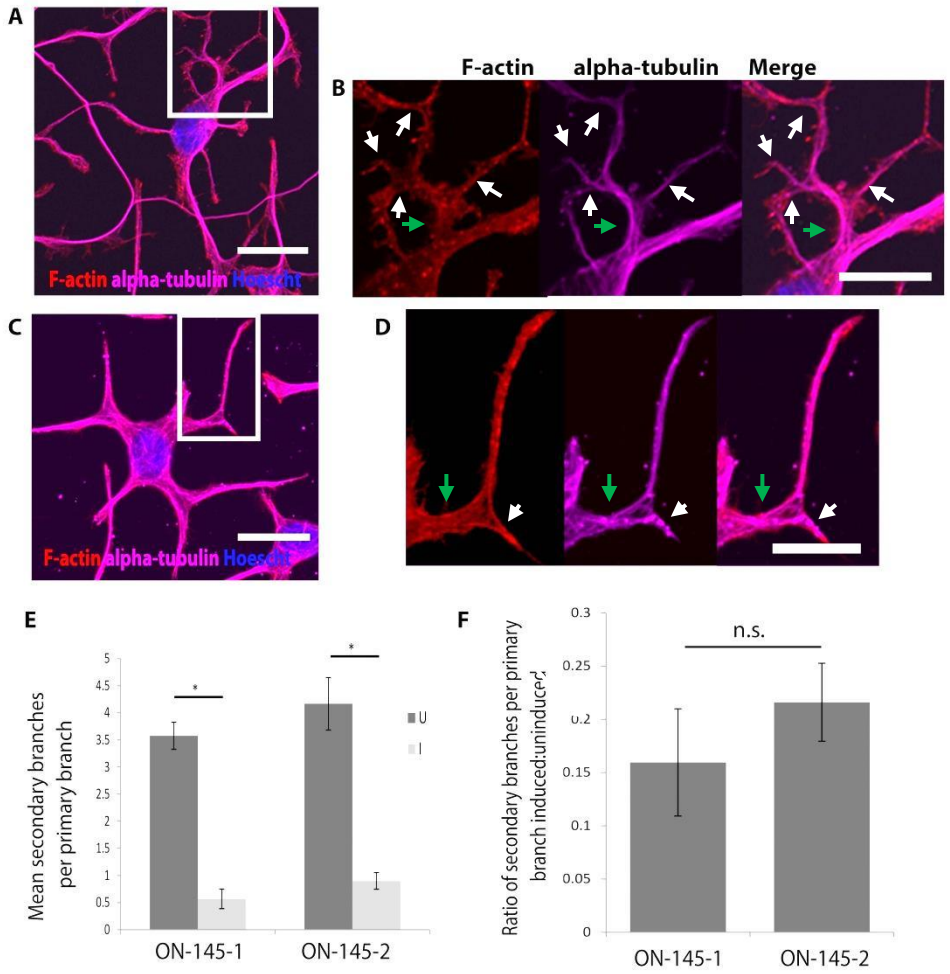

Figure 14. Early in differentiation, miR-145 overexpressing cells extend fewer secondary branches. A. Representative confocal micrograph of uninduced cell on DD3 (ON-145-2). B. Magnified branch area (white rectangle, panel A). C. Representative confocal micrograph of induced cell on DD3 (ON-145-2). D. Magnified branch area (white rectangle, panel C). Scale bars A/C = 10 µm; Scale bars B/D = 5 µm. Green arrows indicate a primary branch,hite arrows indicate secondary branches extending from that primary branch.. E. Quantification of the mean number of secondary branches (± SEM) per primary branch in inducedand uninducedON-145-1 and ON-145-2 cells. F. Ratio of induced:uninduced mean numbers of secondary branches per primary branch in ON-145-1 and ON-145-2 cells, n=3.

Primary and secondary branching defects persist late in differentiation in miR-145 overexpressing cells

On DD6, again a clear loss of branching complexity can be observed in induced cells compared to uninduced cells in both cell lines (Figure 15). As on DD3, cells did not exhibit a uniform number of primary branches, so cells were again binned to show branching profiles for each condition (Figure 16). Induced ON-145-1 cells showed a relatively large proportion of cells with no primary branches (24.6%), but in contrast to DD3 the majority of cells were able to extend 1 primary branch (28.0%). Further, the decrease in the proportion of these cells as branch numbers increased was less dramatic than on DD3; 15.8% extended 2, 14.0% extended 3, 12.3% extended 4, 1.8% extended 5 and 3.5% extended 6. While this suggests that branching ability was somewhat improved in this cell line by DD6, it still differed from the uninduced ON-145-1 branching profile, which showed no cells with 0 branches, 4.6% with 1 branch, 6.1% with 2 branches, 13.8% with 3 branches, 23.0% with 4 branches, 24.6% with 5 branches, 12.3% with 6 branches, 9.2% with 7 branches and 6.2% with 8 branches. Similar to what was observed on DD3, ON-145-2 cells had a branching profile which was different from both uninduced cells from the same line as well as ON-145-1 induced cells. The proportion of induced ON-145-2 cells with no primary branches was 6.7%, 11.3% had 1, 32.0% had 2, 20.7% had 3, 16.9% had 4, 5.8% had 5, 3.4% had 6 and 3.1% had 7. The frequency distribution of the branching profile for uninduced ON-145-2 cells was akin to that for uninduced ON-145-1; cells without primary branches were not

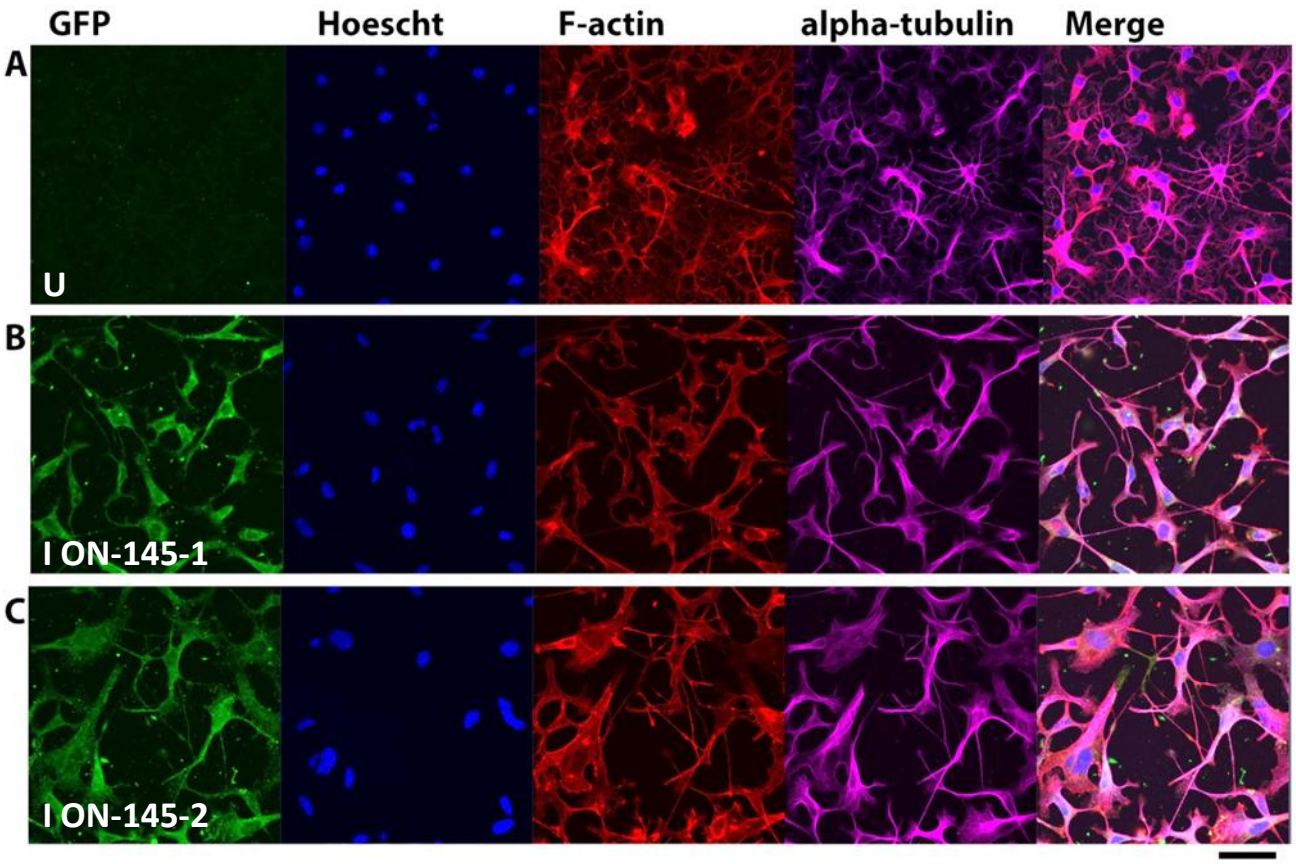

Figure 15.**On differentiation day 6 (DD6), cells overexpressing miR-145 display altered morphology.**Confocal micrographs of ON-145-1 and ON-145-2 cells on DD6.Uninduced cells were treated with 1mM dbcAMP every 24 hrs for 6 days. Induced cells were treated with 1 ng/mL tetracycline every 24 hrs for 3 days, followed by treatment with 1 ng/mL tetracycline + 1 mM dbcAMP for 6 days. A. Representative uninduced cells (ON-145-1) on DD6. B. Induced ON-145-1 cells on DD6. C. Induced ON-145-2 cells on DD6. Scale bar = 50 µm.

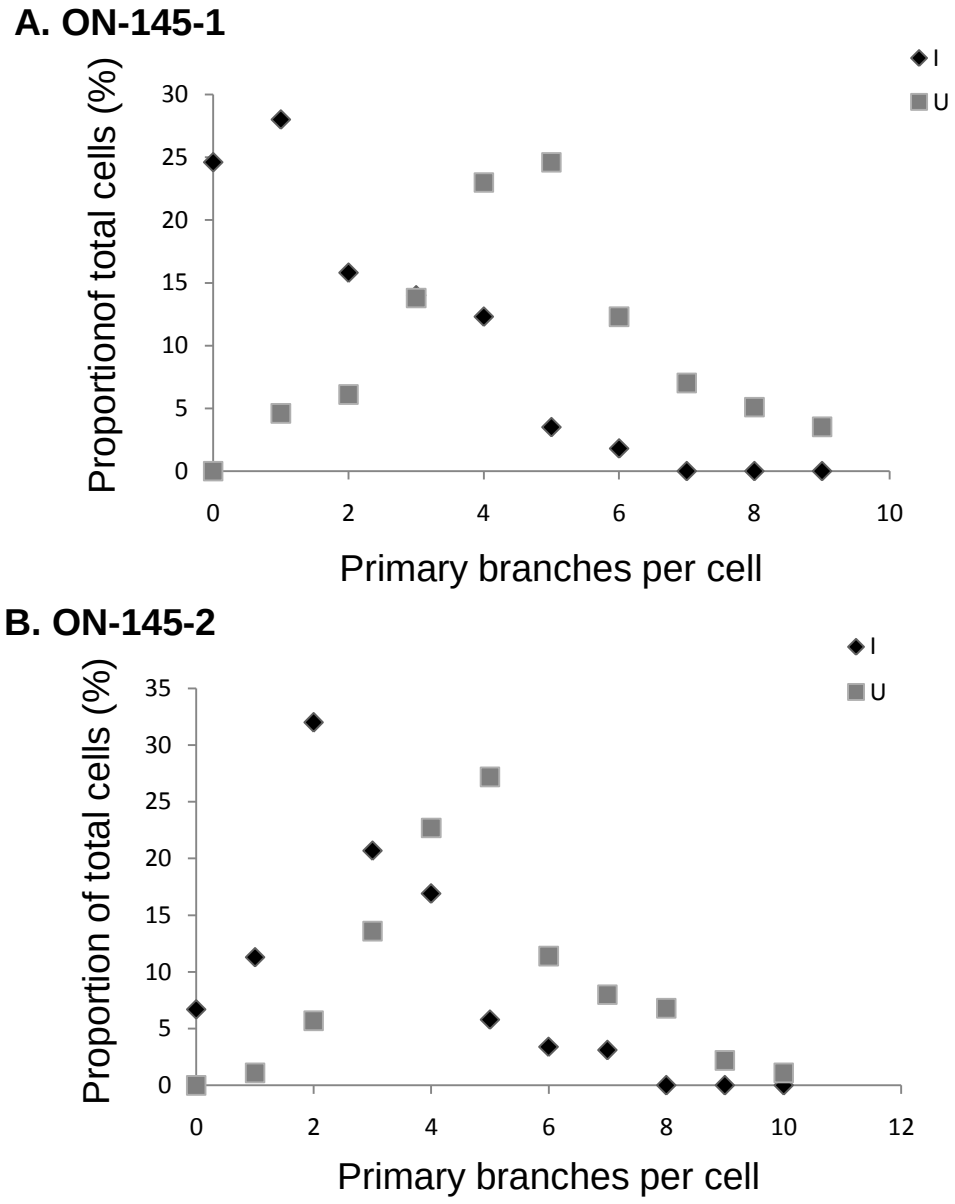

Figure 16. On differentiation day 6, the primary branching profile is altered between induced and uninduced cells. Uninduced cells were treated with 1mM dbcAMP every 24 hrs for 6 days. Induced cells were treated with 1 ng/mL tetracycline every 24 hrs for 3 days, followed by treatment with 1 ng/mL tetracycline + 1 mM dbcAMP for 6 days. A. ON-145-1 cells on DD6. B. ON-145-2 cells on DD6. Each condition shows pooled results for n=3. I indicates induced cells, U indicates uninduced cells.

observed, 1.1% of cells extended1 branch, 5.7% extended 2, 13.6% extended 3, 22.7% extended 4, 27.2% extended 5, 11.4% extended 6, 8.0% extended 7, 6.8% extended 8, 2.2% extended 9, and 1.1% extended 10.

In parallel with the analysis done for DD3, global primary branching was again compared between induced and uninduced cells for ON-145-1 and ON-145-2 by calculating the average primary branch number per cell on DD6. This number was significantly decreased for ON-145-1 from ~5 to ~2 in uninduced versus induced cells, respectively, and a decrease of ~6 to ~3 primary branches per cell was seen in uninduced versus induced ON-145-2 cells ($p<0.05$, $n=3$; panel A, Figure 17). As was detected on DD3, there was a significant difference between the ratio of induced to uninduced primary branch numbers per cell between cells lines, with ON-145-1 again showing a more severe reduction ($p<0.05$, $n=3$; panel B, Figure 17).

Differences were observed late in differentiation in secondary branching ability for induced cells of both cell lines (panels A - D, Figure 18). On DD6, both ON-145-1 and ON-145-2 cells were found to have significantly fewer secondary branches per primary branch in induced cells at ~1, while uninduced cells extended ~4 ($p<0.05$, $n=3$; panel E, Figure 18). When comparing the ratios of induced to uninduced secondary branch numbers between the two cell lines, no significant difference was observed ($n=3$; panel F, Figure 18).

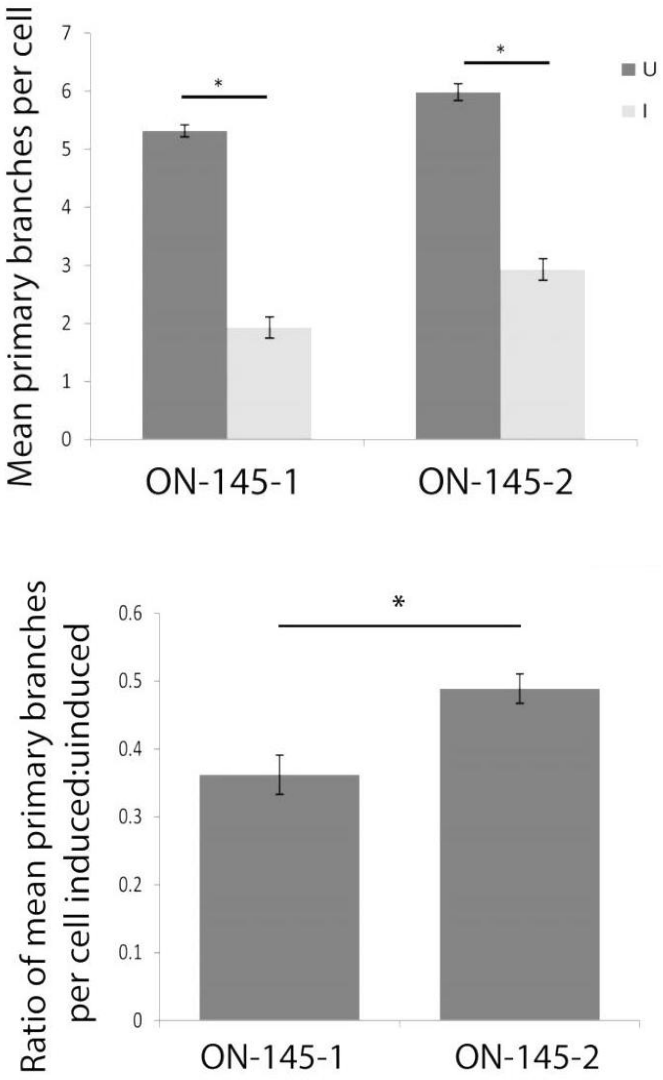

Figure 17.**Global primary branching is reduced late in miR-145 overexpressing cells late in differentiation.** A. Quantification of mean primary branch number per cell ± SEM on DD6 for uninduced and induced cells from lines ON-145-1 and ON-145-2. B. Ratio of mean number of primary branches per cell ± SEM in induced cells to uninduced cells for ON-145-1 and ON-145-2 on DD6. * indicates $p<0.05$ (Student's two-tailed t-test), n=3.

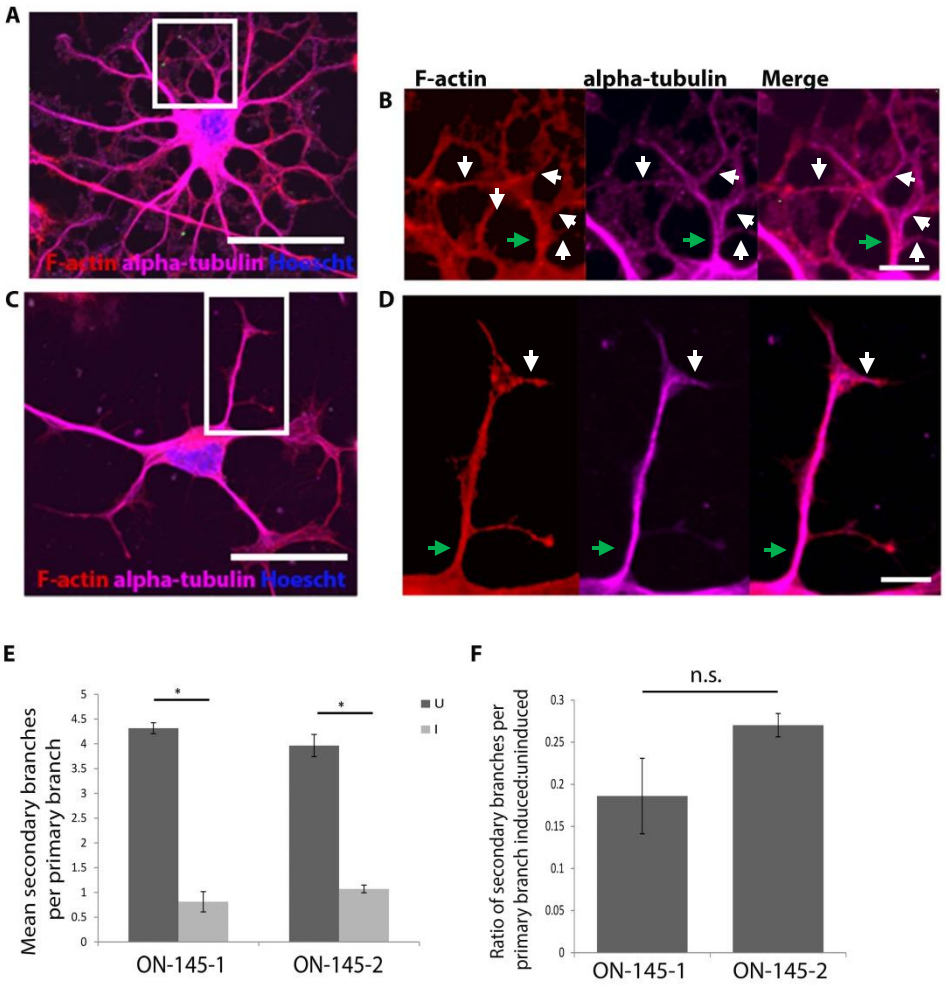

Figure 18. Late in differentiation, a reduction in secondary branching in miR-145 overexpressing cells persists. A. Representative confocal micrograph of uninduced cell on DD6 (ON-145-2). B. Magnified branched area, indicated by white rectangle in panel A. C. Representative confocal micrograph of induced cell on DD6 (ON-145-2). Scale bars A/C = 25 µm ; Scale bars B/D = 5 µm. D. Magnified branch area, indicated by white rectangle in panel C. White arrows indicate secondary branches. E. Quantification of the mean number of secondary branches per primary branch in induced and uninduced ON-145-1 and ON-145-2 cells. F. Ratio of induced to uninduced mean numbers of secondary branches per primary branch in ON-145-1 and ON-145-2 cells, n=3. I = induced, U = uninduced.

MAG expression is dramatically reduced early and late in differentiation when miR-145 is overexpressed

Since differentiation was shown to be significantly affected by miR-145 overexpression, we also wanted to assess whether or not myelin gene regulation was affected. It is known that *Oli-neu* cells express myelin associated glycoprotein (MAG) both early and late in differentiation in differing patterns of localization. On DD3, uninduced cells were found to have perinuclear MAG staining, while ON-145-1 and ON-145-2 induced cells showed almost no MAG expression (panels A, B, C, Figure 19). This was quantified as mean percent MAG+ (±SEM) cells per total cells. A significant decrease was observed from 82.2% in uninduced to 1.7% in induced ON-145-1 cells ($p<0.05$, $n=3$; panel D, Figure 19). A similar decrease was found in ON-145-2 cells from 76.5% MAG+ uninduced cells to only 1.3% MAG+ uninduced cells ($p<0.05$, $n=3$; panel E, Figure 19).

On DD6, uninduced cells were characterized by diffuse MAG expression but loss of MAG staining was again observed in induced ON-145-1 and ON-145-2 cells (panels A, B, C, Figure 20). Quantification was done to determine the percent of MAG+ cells (±SEM) per total cells. Significant reductions from 74.0% in uninduced cells to 3.2% in induced cells and from 77.1% in uninduced cells to 2.1% in induced cells were observed in ON-145-1 and ON-145-2 cells, respectively (panels D, E, Figure 20).

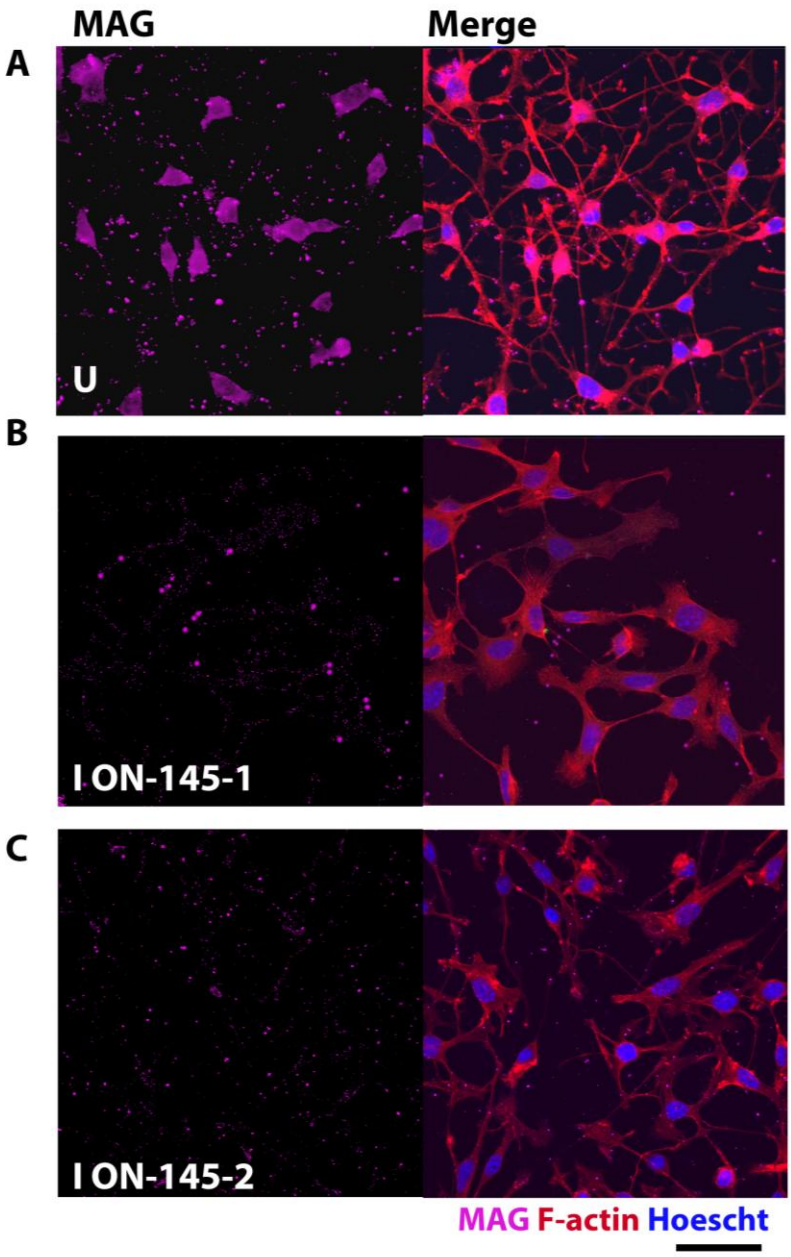
MAG
Merge
A
U
B
I ON-145-1
C
I ON-145-2
MAG F-actin Hoescht

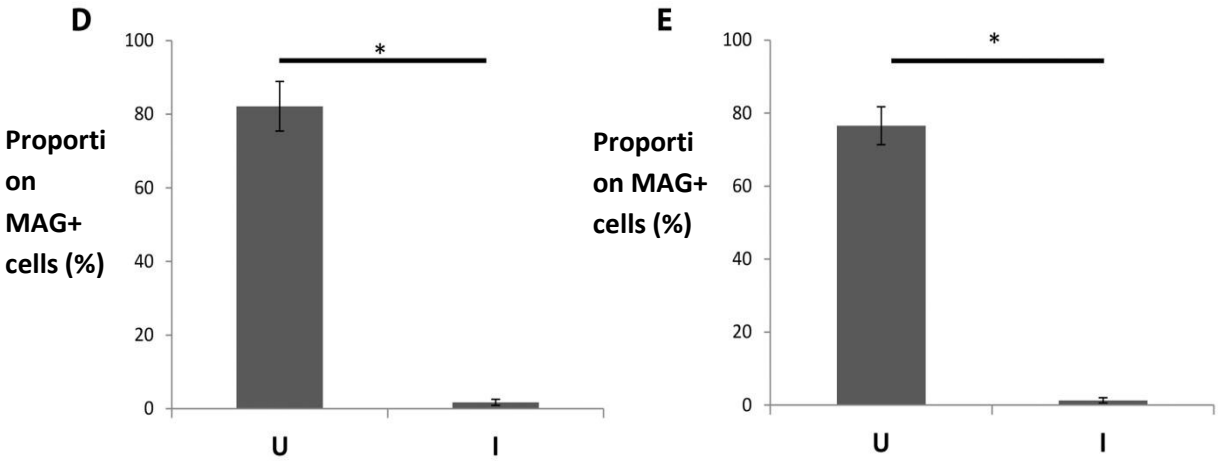

Figure 19.On differentiation day 3, MAG expression is severely reduced in miR-145 overexpressing cells. A. Representative confocal micrograph of uninduced cells (ON-145-1) showing early perinuclear MAG staining. B. Induced ON-145-1 cells. C. Induced ON-145-2 cells. Scale bar = 50 µm. D. Quantification of mean percent (± SEM) of MAG+ uninduced and induced ON-145-1 cells. E. Quantification of percent (± SEM) of MAG+ uninduced and induced ON-145-2 cells per field of view. * indicates $p<0.05$, n=3. U indicates ununinduced, I indicates induced.

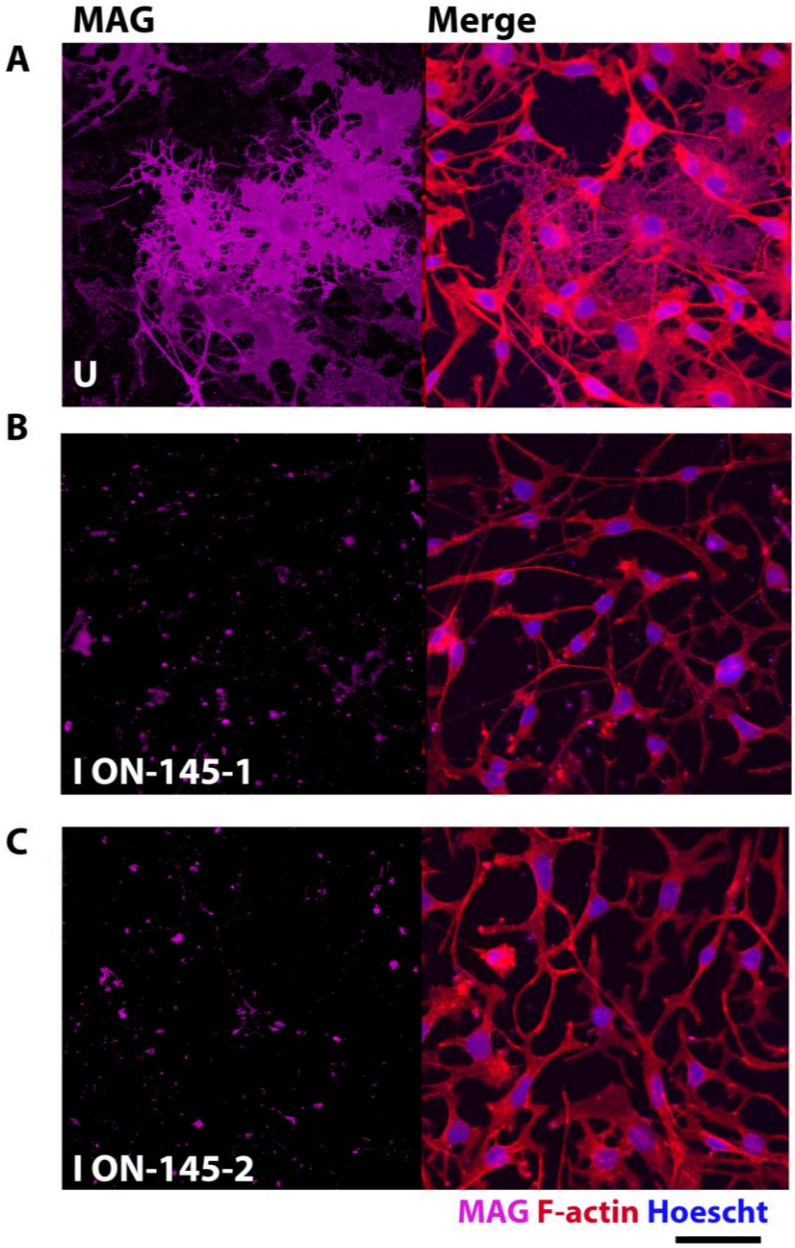
MAG
Merge
A
U
B
I ON-145-1
C
I ON-145-2
MAG F-actin Hoescht

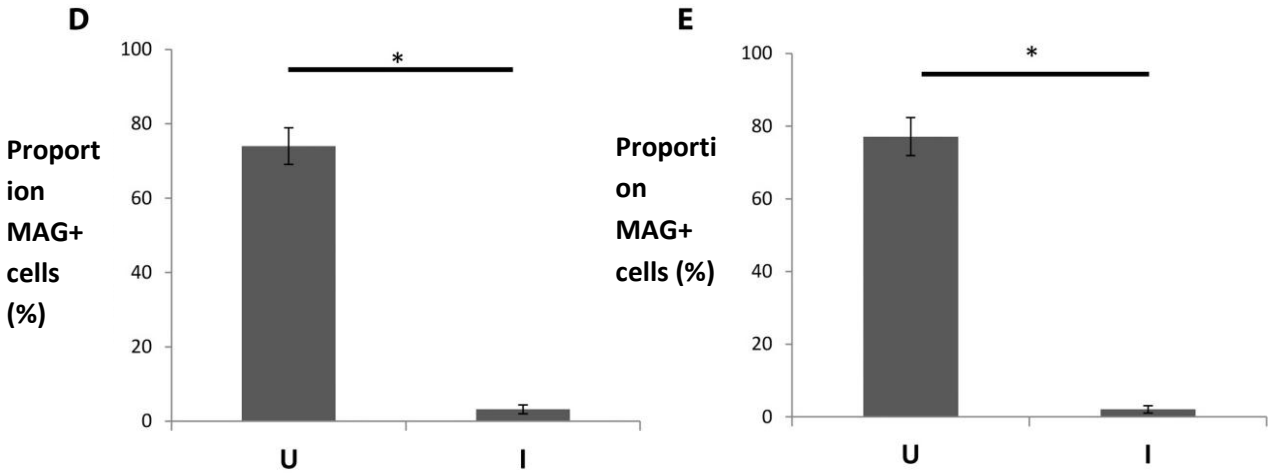

Figure 20. Loss of MAG expression continues in miR-145 overexpressing cells late in differentiation. A. Representative confocal micrograph of uninduced cells (ON-145-1) diffuse MAG staining. B. Induced ON-145-1 cells. C. Induced ON-145-2 cells. Scale bar = 50 µm. D. Quantification of mean percent (± SEM) of MAG+ uninduced and induced ON-145-1. E. Quantification of percent (± SEM) of MAG+ uninduced and induced ON-145-2 cells per field of view. * indicates $p<0.05$, n=3. U indicates uninduced, I indicates induced.

Actin- and myelin-related genes are downregulated when miR-145 is overexpressed during differentiation

In order to assess how miR-145 overexpression might be affecting normal gene expression, comparisons were made between induced and uninduced ON-145-1 cells using qRT-PCR arrays. These arrays were designed to include genes in the relevant clusters that were revealed to be significantly enriched in the bioinformatics analysis. The genes include putative miR-145 targets related to actin cytoskeleton organization, focal adhesions, adherens junctions and myelination, as well as two others which did not arise in the clustering analysis but are known to be important in OL differentiation and myelination (*Tppp3* and *MRF/GM98*). The full list of genes included in the array is listed in Table 1.

During proliferation, no significant differences >2-fold change could be detected between gene expression levels in induced and uninduced ON-145-1 cells (n=3; Figure 21). A significant but modest change in *Tppp3* expression was found; however this was an upregulation of ~1.3-fold and not a downregulation as would be expected if miR-145 was specifically targeting this gene at this time point.

In contrast, expression of several genes were found to be significantly altered >2-fold both early and late in differentiation (n=4; Figure 22). Of 42 genes assayed in the array, 14 were significantly downregulated on DD3 in induced versus uninduced ON-145-1 cells (Table 3), while none were found to be significantly upregulated. Expression level changes >2-fold were also observed late in differentiation (n=4; Figure 23). When comparing induced to uninduced ON-145-1 cells on DD6, 5 genes were found to be significantly downregulated >2-fold, and one gene was significantly upregulated >2-fold (Table 4).

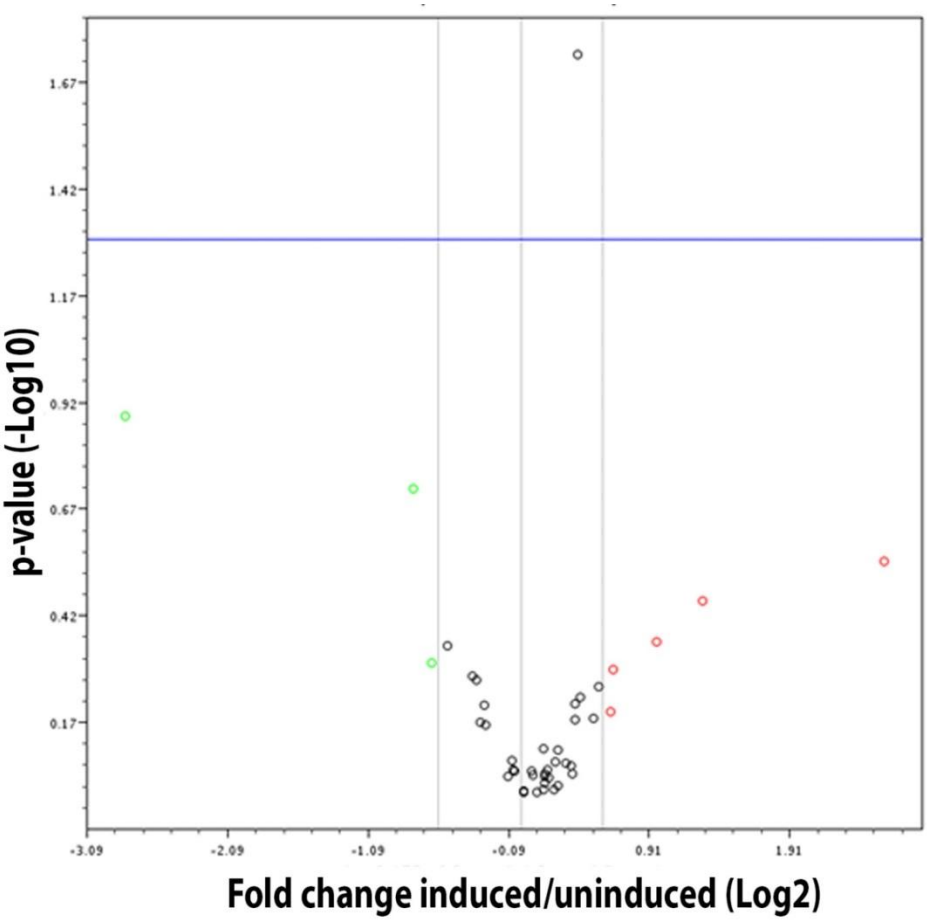

Figure 21. Gene expression was unaltered in miR-145 overexpressing cells while proliferating. Volcano plot representing fold change and significance for induced cells compared to uninduced cells for proliferating ON-145-1 cells.Fold change differences were calculated between induced and uninduced ON-145-1 cells using the ΔΔCt method. Each circle represents one gene; cut-off boundary was set at 2, black circles indicate fold change inside the boundary, green/red circles indicate fold change outside the boundary. The genes analysed in the array are listed in Table 1. Middle vertical line represents fold change of 1; vertical lines on either side show the cut-off boundary (2-fold change). The horizontal blue line indicates significance cut-off of $p<0.05$. n=3.

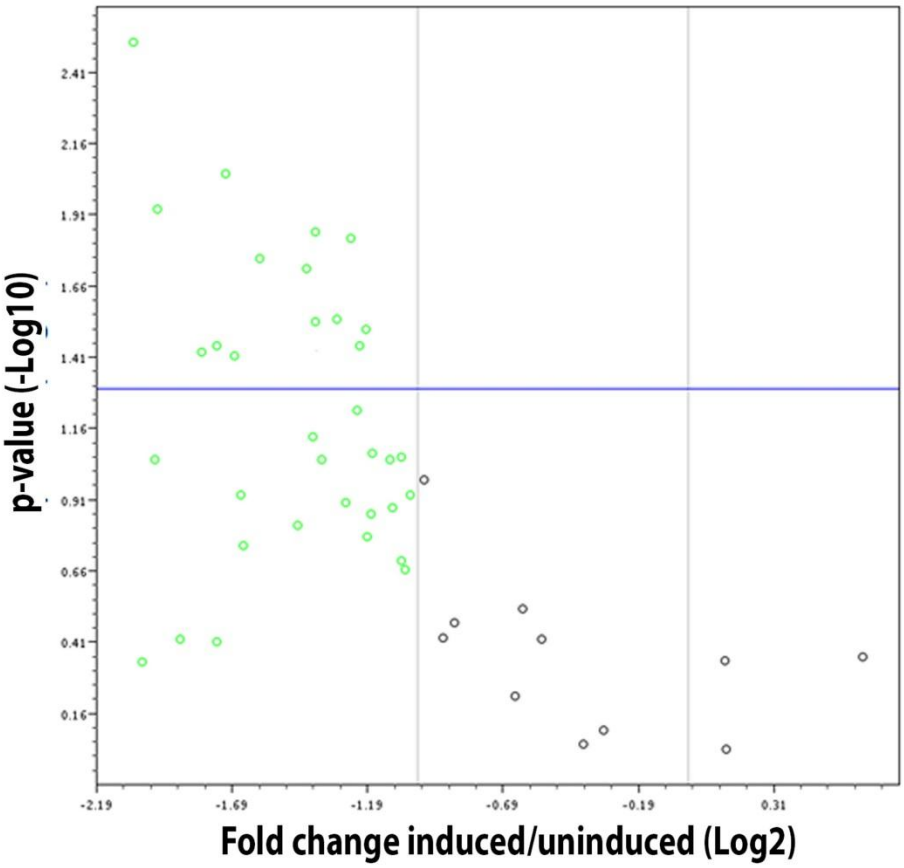

Figure 22. Gene expression levels are altered in miR-145 overexpressing cells early in differentiation. Volcano plot representing fold change and significance for induced cells compared to uninduced cells for ON-145-1 cells DD3.Fold change differences were calculated between induced and uninduced ON-145-1 cells using the ΔΔCt method. Each circle represents one gene; cut-off boundary was set at 2, black circles indicate fold change inside the boundary, green circles indicate fold change outside the boundary. The genes analysed in the array are listedin Table 1; genes with significant expression change >2 are listed in Table 3. Right vertical line represents fold change of 1; left vertical line shows the cut-off boundary (2-fold change). The horizontal blue line indicates significance cut-off of $p<0.05$. n=4.

Table 3. Early in differentiation,miR-145 overexpression cells show changes in expression of genes involved in actin cytoskeleton organization and myelination. On DD3,14 of 42 genes included in the qRT-PCR array showed a change in expression in induced ON-145-1 cells compared to uninduced ON-145-1 cells. Red indicates downregulation. n=4.

DD3		
Gene Symbol	Fold Change	p-value
Pak4	-4.1458	0.00304
Pmp22	-3.4849	0.037087
Ctnnd1	-3.3476	0.035277
Flnb	-3.2709	0.008797
Serinc5	-3.1991	0.038292
Tln2	-2.9942	0.017434
Crkl	-2.662	0.019015
Gmfb	-2.6085	0.037455
Igf1r	-2.6002	0.014135
Add3	-2.5992	0.029103
MRF/Gm98	-2.462	0.028508
Epb4.1l5	-2.3737	0.014836
Ssh2	-2.3208	0.035224
Coro2b	-2.2864	0.031037

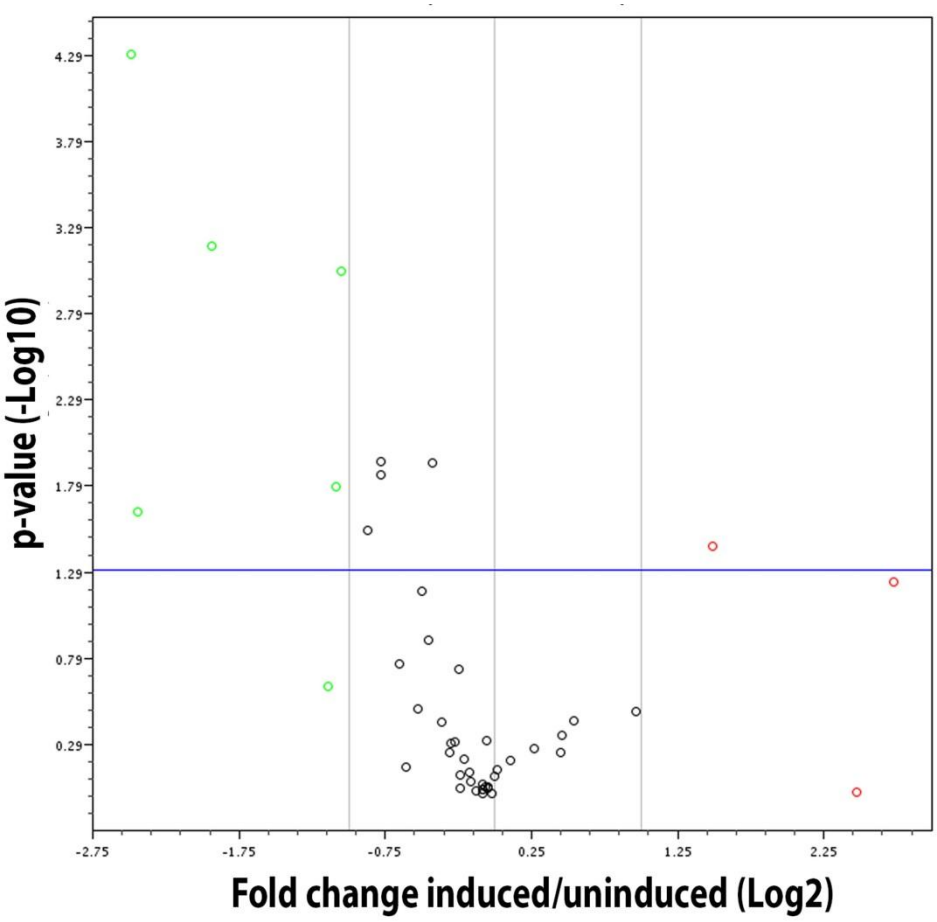

Figure 23. Gene expression is altered in miR-145 overexpressing cells latein differentiation. Volcano plot representing fold change and significance for induced cells compared to uninduced cells for ON-145-1 cells on DD6.Fold change differences were calculated between induced and uninduced ON-145-1 cells using the ΔΔCt method. Each circle represents one gene; cut-off boundary was set at 2, black circles indicate fold change inside the boundary, green/red circles indicate fold change outside the boundary. The genes analysed in the array are listedin Table 1. Middle vertical line represents fold change of 1; vertical lines on either side show the cut-off boundary (2-fold change). The horizontal blue line indicates significance cut-off of $p<0.05$. n=4.

Table 4. Late in differentiation,miR-145 overexpression cells show altered expression of genes involved in actin cytoskeleton organization and myelination. On DD6,6 of 42 genes included in the qRT-PCR array showed a change in expression in induced ON-145-1 cells compared to uninduced ON-145-1 cells. Red indicates downregulation, blue indicates upregulation. n=4.

DD6		
Gene Symbol	Fold Change	p-value
Add3	-5.4357	0.023009
MRF/Gm98	-2.0671	0.000926
Serinc5	-3.8179	0.000666
Tppp3	-5.6148	0.023009
Trim2	-2.1185	0.016427
Ctnnd1	2.7987	0.036293

Discussion

Previous work has clearly established that miRNAs are critical regulators of oligodendrocyte differentiation (Dugas *et al*., 2010; Zhao *et al*., 2010; Shin *et al*., 2009). Microarray experiments have revealed differential expression patterns of individual miRNA species as OPCs progress to mature OLs (Letzen *et al*., 2010), and while the roles of some of these species has been determined, much work remains to explore their functions on an individual basis. Additional work has revealed that lesion tissue taken from post-mortem MS patients shows an altered profile of miRNA expression compared to that of white matter from healthy patients (Junker *et al*., 2009). Mir-145 was found to be both differentially expressed as oligodendrocytes mature, and its abundance is also increased by ~4-fold in chronic MS lesions. Speculation has been made regarding its function based on a myelin-related putative target, *myelin gene regulatory factor* (*MRF/Gm98*), but without any supporting experimental evidence. With this study, we aimed to elucidate the part miR-145 plays in the OL differentiation process as well as how OL differentiation may be affected by the upregulation of miR-145 in MS lesions. To this end, two inducible miR-145 overexpressing cell lines were established, ON-145-1 and ON-145-2, which upregulate miR-145 ~33-fold and ~11-fold, respectively (Figure 7).

Bioinformatic analysis of miR-145 putative targets reveals enrichment of genes involved in critical differentiation and myelination pathways

Clustering by gene ontology and KEGG pathway analysis revealed that miR-145 was a good candidate for investigation in OL differentiation and myelination. Significant

clusters included putative targets involved in the organization of the actin cytoskeleton as well as in myelination (Table 1; Figure 4). KEGG pathway analysis further strengthened the cluster analysis results as three pathways showing significant enrichment paralleled the three clusters related to actin cytoskeletal organization (Figure 5).

The clusters and pathways showing significant enrichment related to actin cytoskeletal organization fit under the general headings of actin cytoskeleton, focal adhesions and adherens junctions. Focal adhesions are areas of tight contact between cells and the extracellular matrix (ECM), providing an association between the ECM and the intracellular actin cytoskeleton network. They include factors which appear to be specific to focal adhesions as well as ones which are also involved in other actin cytoskeleton organization pathways (Burridge & Chrzanovska-Wodnicka, 1996). General actin cytoskeletal organization and focal adhesion formation are known to be important for process extension as well as stabilization of actin microfilaments (Bauer *et al*., 2009; Lafrenaye & Fuss, 2010). Loss of factors involved in these pathways such as integrin-linked kinase, focal adhesion kinase, and fyn have elicited OL phenotypes which demonstrate reduced process length, reduced numbers of primary and secondary branches, or complete suppression of branch outgrowth (O'Meara *et al*., 2013; Hoshina *et al*., 2007). Adherens junctions are cell to cell interactions mediated by actin cytoskeletal organization that act to anchor cells to one another (Gotz & Huttner, 2005). In oligodendrocytes, adherens junctions are found in the paranodal regions of myelin sheaths; loss of proper formation of these axon-oligodendrocyte contacts leads to a loss

of compact myelin and expression of MBP typified by the *Shiverer* mouse model (Tait *et al*., 2000).

Because our miR-145 overexpressing model cells are not myelinating cells and are cultured with inert poly-L-lysine and not ECM factors, players involved exclusively in focal adhesion, adherens junction, or compact myelin formation are not likely to be causative in any defects observed in this system. However, any downregulation in the expression of these genes might point to potential clues to miR-145 regulation of these processes *in vivo*, as well as provide a potential connection to remyelination failure in the miR-145 enriched microenvironment of the MS lesion. To parse this out further, similar studies to the ones done here need to be undertaken in primary oligodendrocytes, which can be cultured on a variety of ECM substrates as well as induced to myelinate axons in co-culture.

miR-145 expression in Oli-neu cells parallels that of human OLs as they differentiate

Oli-neu cells are immortalized mouse OPCs which constitutively express the oncogene tyrosine kinase *t-neu* (Jung *et al*., 1995). They can be induced to differentiate by treatment with dbcAMP, and are able to differentiate into premyelinating but not myelinating OLs, gaining process complexity as they differentiate (panel A, Figure 6). As such, it was unknown whether or not these cells would express miRNAs in the same patterns as primary cells while differentiating. To determine this, we performed qRT-PCR for miR-145 in *Oli-neu* cells while they were proliferating, early in differentiation (DD3) and late in differentiation (DD6). While proliferating, miR-145 expression was

found to be relatively high, was significantly reduced on DD3 by ~80%, and this reduction was maintained on DD6 ($p<0.05$; panel B, Figure 6). This profile is very similar to what has been found in human embryonic stem cells induced to differentiate to mature OLs. Letzen *et al*. (2010) found that miR-145 was reduced by ~99% as OPCs progressed to pro-OLs, and expression levels were unchanged as pro-OLs progressed to myelinating OLs, indicating that generally miR-145 expression is high in OPCs and low in differentiating OLs. As *Oli-neu* cells exhibit this same trend in miR-145 expression, its functions in differentiation may be similar to that of primary cells.

Proliferating OPCs are largely unaffected by miR-145 overexpression

When proliferating ON-145-1 and ON-145-2 cells were induced to overexpress miR-145, no apparent morphological differences could be observed compared to uninduced cells (Figure 8). Cells maintained a mostly bipolar or round morphology, which is typical in proliferating *Oli-neu* cells (panel A, Figure 6). Considering the enrichment in miR-145 targets for cytoskeletal factors, this apparent lack of change was somewhat counterintuitive, as cytoskeletal organization is critical to both cell growth and division. Lack of alteration in actin and tubulin organization suggest that the factors required to promote proper cytoskeletal function at this timepoint are not under regulatory control of miR-145, or compensatory mechanisms exist which overcome the effects of miR-145. Support for the former explanation was found when qRT-PCR arrays were performed to compare expression of putative cytoskeleton- and myelin-related targets of miR-145, which showed no significant downregulation of any of the genes assayed (Figure 21). Without miR-145 overexpression, the endogenous

expression level of miR-145 is already relatively high in proliferating cells. Given that this is the case, increased expression of miR-145 during proliferation may not result in obvious biological relevance in an environment where expression is already high.

Recent studies have illustrated that miR-145 has a well-established role in proliferation via targeting of non-cytoskeleton-related genes (Sachdeva & Mo, 2010). This has been best characterized by its role as a tumour suppressor. Loss of miR-145 in lung adenocarcinoma, ovarian cancer, prostate cancer, renal cell carcinoma and neuroglioma has been linked to hyperplasia and migration of cancer cells, and restoration of miR-145 levels has proven to halt promiscuous proliferation (Fuse *et al*., 2011; Rani *et al*., 2013; Yoshino *et al*., 2013; Zhang *et al*., 2013; Cho *et al*., 2009). If miR-145 functions in a similar manner in OPCs, its overexpression might limit proliferation. To determine whether or not miR-145 was acting in this role in our overexpressing cells, proliferating cells were incubated with EdU to measure DNA replication *in vitro*. ON-145-1 cells demonstrated a significant decrease in proliferation of ~10% in miR-overexpressing cells compared to uninduced cells, but no difference was observed in ON-145-2 cells (Figure 9). Interestingly, this suggests a dose-dependent response to miR-145 overexpression, as ON-145-1 cells showed a much higher rate of miR-145 overexpression than ON-145-2 cells (panel C, Figure 7). These results indicate that while miR-145 may be working in some manner to control proliferation rates in OPCs, only a very large upregulation elicited a fairly subtle effect. Further, expression profiling in oligodendrogliomas has not identified a loss of miR-145 expression as a cause of hyperplasia as has been observed in other cancerous cells (Lages *et al*., 2011; Kim *et al.*, 2011).

Apoptosis is positively regulated by endogenous application of miR-145 in some cancer cells, through both caspase-dependent and caspase-independent mechanisms (Zhang *et al*., 2010; Ostenfeld *et al*., 2010). However, it also has a protective role against apoptosis in cardiomyocytes (Li *et* al., 2012), making its role in this process somewhat unclear and likely to be cell-type specific. In order to investigate this in OPCs, proliferating cells were stained for cleaved caspase-3 and the percentage of apoptotic cells was quantified (Figure 10). No significant difference could be detected between induced and uninduced cells of either cell line, indicating that at least at this timepoint overexpression of miR-145 at the reported levels did not promote caspase-mediated cell death in OLs.

Primary and secondary branching is negatively affected by miR-145 overexpression in differentiation OLs

In contrast to the mild effects observed in proliferating OPCs, the transition to differentiating OLs was dramatically influenced by miR-145 overexpression. Both early and late in differentiation, obvious morphological differences were present in induced cells compared to uninduced cells (Figures 11 & 15). Staining of cytoskeletal components F-actin and α-tubulin revealed a clear reduction in branching ability. In both induced cell lines, quantification of primary branch numbers per cell revealed a change in both branching profile (Figures 12 & 16) and mean branch numbers per cell (panel A, Figures 13 & 17). The non-uniformity of primary branch number between cells represented by the branching profile suggests that the ability to extend processes may be determined on a cell by cell basis. In induced cells, this may be due to the fact that

cells that survived selection subsequent to lentiviral infection represented a pool of infected OPCs, and not a single clone; thus the population may represent cells with different copy numbers of the lentiviral vector. However, differentiated *Oli-neu* cells in culture also display highly variable process extension (panel A, Figure 6). Further, it is well established that OLs exhibit highly variable morphology *in vivo* even in relatively homogeneous environments (Butt & Ransom, 1993), indicating that these cells are inherently plastic.

As was observed in proliferating cells, a dose-dependent response to miR-145 overexpression was found between the two cell lines during differentiation. Primary branching of ON-145-1 cells was more severely affected by miR-145 overexpression than cells of ON-145-2 (Figures 11 & 15). This was indicated by the differing branching profiles of induced cells of ON-145-1 and ON-145-2 and confirmed by a significant difference in the ratio of induced:uninduced mean primary branch numbers between cell lines (panel B, Figure 13).

Secondary branching was also severely affected early and late in differentiation in both cells lines (panels A-D, Figures 14 & 18). Individual branches of induced cells were found to extend significantly fewer secondary branches than uninduced cells (panel E, Figures 14 & 18). Curiously, no dose dependent difference in secondary branching ability was observed between the cell lines (panel F, Figures 14 & 18). It must be noted that this would not be the case had secondary branches been quantified on a cell by cell basis instead of by primary branch, as most ON-145-1 cells extended zero or 1 primary branches while most ON-145-2 cells extended 2, 3 or 4 branches (Figures 12 & 16).

While this work represents the first example indicating a role for miR-145 in oligodendrocyte process extension, it has been found previously that exogenous application of miR-145 to dorsal root ganglia (DRGs) *in vitro* results in a drastic reduction in neurite outgrowth through targeting of the gene *Roundabout 2* (*Robo2)*, a promoter of actin polymerization (Zhang *et al*., 2011). While there is no known role for Robo2 in oligodendrocytes, a zebrafish model encoding a functional null mutation of *Robo2* bears evidence of normal oligodendrocyte development indicating it is unlikely to be essential to their differentiation (Wyatt *et al*., 2010); however, Zhang *et al*. (2011) did not investigate any other putative targets of miR-145 in their study, and thus *Robo2* may not be the only factor implicated in the defect in neurite formation. Multiple genes involved in cytoskeletal regulation were found to be downregulated >2-fold in miR-145 overexpressing cells both early and late in differentiation ($p<0.05$; Tables 3 & 4). The extension of neurites from the neuron cell body initiates as what is termed a “growth cone,” a well- characterized progression of filopodia to lamellipodia which involves coordination of cytoskeleton organizing factors, many of which are shared in common with those required for OL process formation such as FAK, Fyn, and N-WASP (Dent *et al*., 2011; Rajasekharan & Kennedy, 2009). Based on the similar importance of these well-studied cytoskeleton-related proteins in both neurite and OL branch outgrowth, they likely rely on additional factors which they have in common. Taken together, these findings suggest that miR-145 may be acting to suppress OL branching and neurite outgrowth in a similar manner.

MiR-145 may lead to deficits in MAG expression through downregulation of MRF/Gm98

In addition to the reduction in primary and secondary branching ability, miR-145 overexpressing cells exhibited a significant reduction in MAG expression in both ON-145-1 and ON-145-2 induced cells ($p<0.05$; Figures 20 & 21). Very few appeared to express MAG at all, or at levels too low to be detectable by our antibody. One of the putative targets of miR-145 is *MRF/Gm98,* homolog to human gene *C11orf9*. Recently, Emery *et al.* (2009) discovered that this gene encodes for a transcription factor expressed exclusively in postmitotic OLs. To elucidate its role, siRNA knockdown experiments were done in cultured mouse OPCsthat resulted in myelin gene expression being severely reduced in *in vitro*. Conversely, forced expression of MRF was found to upregulate myelin genes both *in vitro* and *in vivo.* They next generated a conditional MRF knockout mouse model, which was characterized by a loss of mature OLs and suffered from severe tremors, ataxia and seizures before dying around postnatal day 21. OPCs cultured from these mice were deficient for myelin proteins and exhibited less mature morphology than found in wild-type littermates. Further study has indicated that MRF is also required for myelin maintenance in adult mice (Koenning *et al*., 2012). In both of these studies, severe deficits in MAG expression were observed subsequent to loss of MRF. In our miR-145 overexpressing cells, *MRF/Gm98* expression detected by qPCR was significantly reduced by ~2.5-fold in early differentiation and ~2-fold in late differentiation ($p<0.05$, Figures 22 & 23). Based on the known roles of MRF, these results suggest that the loss of MAG in our cells is due to miR-145 targeting of *MRF/Gm98*. It has been previously theorized that the relatively high expression of miR-

145 in OPCs may serve to inhibit the expression of MRF until cells are ready to differentiate (Letzen *et* al., 2010; Emery, 2010; Barca-Mayo & Lu, 2012). Our work represents the first evidence of a link between miR-145 and MRF expression.

miR-145 overexpression in MS lesions may negatively impact OPC differentiation

The microenvironment of the MS lesion is drastically different from healthy white matter; not only in its cellular makeup but also in the gene expression profile of those cells. OPCs arriving at the lesion for the purpose of regenerating lost myelin encounter a milieu that is clearly inhospitable for differentiation; this is evidenced by the fact that OPC density in lesions often approaches or is equal to that found in healthy white matter, suggesting that lack of remyelination is not due to scarcity of OPCs but rather a blockage of OPC differentiation (Wolswijk, 1997). Multiple factors that inhibit OPC differentiation are found to be upregulated in the lesion environment; however, the roles of miRNAs have not yet been considered in this context. It has been shown that miR-145 is upregulated selectively in chronic MS lesions (Junker *et al*., 2009), and we have shown that overexpression of this miRNA in immortalized OPCs causes a failure to differentiate normally *in vitro.*

While our model system does not progress so far along the OL lineage as to develop into mature, myelinating OLs, the severe loss of process extension as well as the severe reduction in the proportion of differentiated cells expressing MAG suggests that miR-145 overexpressing cells would be unable to myelinate axons. Our two miR-145 overexpressing cell lines also upregulate miR-145 to a greater extent than the ~4-fold increase observed in chronic MS lesions compared to healthy white matter. However, this does not preclude a more modest change in miR-145 abundance in

differentiating OLs from having a negative effect. The dose-dependent responses observed in our results suggest that a lower overexpression of miR-145 would likely lead to a milder phenotype *in vitro*. But several of the genes observed to be downregulated are thought to be involved in the organization of focal adhesions and adherens junctions, and these complexes are unlikely to contribute to the phenotype of miR-145 overexpressing *Oli-neu* cells due to their culture conditions. Thus, it is possible that a 4-fold change in miR-145 abundance might have an even greater effect *in vivo*, where the downregulation of genes involved in focal adhesions and adherens junctions would be expected to have greater biological relevance. Further study of miR-145 overexpression in primary cell culture and animal models will serve to clarify this question, and investigation of miR-145 expression in lesions from animal models of MS will serve to advance our understanding of how miR-145 may be affecting OPC differentiation in remyelination failure.

Conclusions

MicroRNAs are known to be vitally important to OL differentiation. It has been previously established that miR-145 is differentially regulated as OPCs progress to mature, myelinating OLs. This miRNA is abnormally abundant in chronic MS lesions. Bioinformatic analysis revealed that putative targets of miR-145 were enriched for both cytoskeleton- and myelin-related genes, warranting further investigation of the role of this miRNA in OL differentiation. Development of an inducible miR-145 overexpressing mouse OPC model revealed that the upregulation of miR-145 severely reduces both primary and secondary branching ability, and leads to deficits in the expression of

myelin protein MAG. Gene expression analyses in these cells showed that the expression of multiple genes related to cytoskeletal organization as well as myelination was significantly decreased with the overexpression of miR-145. These results indicate that proper expression of miR-145 is required for successful OL differentiation *in vitro*, and may lend insight into the importance of its differential regulation in differentiating OLs *in vivo*. Further, this study implicates miR-145 as a negative regulator of remyelination in MS lesions by inhibiting differentiation of incoming OPCs. Future study must address the role of this miRNA *in vivo* as well as in pathogenesis of an animal model of MS such as experimental autoimmune encephalitis (EAE). Finally, the results of this study emphasize the need to continue characterization of the roles of miRNAs in demyelinating disease in an effort to elucidate new therapeutic targets in the future.

References

Antel, J., S. Antel, Z. Caramanos, D. Arnol & T. Kuhlmann.2012. Primary progressive multiple sclerosis: part of the MS disease spectrum or separate disease entity? *Acta Neuropathol.***123:**627-638.

Bacon, C., V. Lakics, L. Machesky and M. Rumsby. 2007. N-WASP regulatesextension of filopodia and processes by oligodendrocyte progenitors, oligodendrocytes, and Scwann cells – implications for axon ensheathment at myelination. *Glia***55:**844-858.

Bakiri, Y., R. Karadottir, L. Cossell & D. Attwell. 2011. Morphological and electrical properties of oligodendrocytes in the white matter of the corpus callosum and cerebellum. *J. Physiol.* **589(3):**559-573.

Barres BA, Lazar MA, Raff MC. 1994. A novel role for thyroid hormone, glucocorticoids and retinoic acid in timing oligodendrocyte development. Development 120(5):1097-108.

Bartel, D. 2004. MicroRNAs: genomics, biogenesis, mechanism and function. *Cell***116:**281-297.

Bauer, N., C. Richter-Landsberg & C. Ffrench-Constant. 2009. Role of the oligodendroglial cytoskeleton in differentiation and myelination. *Glia***57:**1691-1705.

Baumann, N. & D. Pham-Dinh. 2001. Biology of oligodendrocyte and myelin in the mammalian central nervous system. *Physiological Reviews***81(2):**871-927.

Biggar, K., S. Kornfeld & K. Storey. 2011. Amplification and sequencing of mature microRNAs in uncharacterized animal models using stem-loop reverse transcription-polymerase reaction. *Anal Biochem* **416(2):**231-233.

Blakemore, W., & H. KEirstead. 1999. The origin of remyelinating cells in the central nervous system. *Journal of Immunology* **98:**69-76.

Boyd, A., H. Zhang & A. Williams. 2013. Insufficient OPC migration into demyelinated lesions is a cause of poor remyelination in MS and mouse models. *Acta Neuropathol.***125(6):**841-859.

Burrdige, K., & M. Chrzanowska-Wodnicka. 1996. Focal adhesions, contractility and signalling. *Annu. Rev. Cell Dev. Biol.* **12:**463-518.

Butt, A., & B. Ransom. 1993. Morphology of astrocytes and oligodendrocytes during development in the intact optic nerve. *Comp. Neur.* **338(1):**141-158.

Chan, J., A. Krichevsky & K. Kosik. 2005. MicroRNA-21 is an antiapoptotic factor in human glioblastoma cells. *Cancer Res.* **65(14):**6029-6033.

Cho, W., A. Chow & J. Au. 2009. Restoration of tumour suppressor has-miR-145 inhibits cancer cell growth in lung adenocarcinoma patients with epidermal growth factor receptor mutation. *Eur. J. Cancer* **45(12):**2197-21206.

Cui, Q., G. Fragoso, V. Miron, P. Darlington, W. Mushynski, J. Antel & G. Almazan. 2011. Response of human oligodendroctye progenitors to growth factors and axons signals. *J. Neuropathol. Exp. Neurol.* **69(9):**930-944.

De Angelis, F., A. Bernardo, V. Magnaghi, L. Minghetti & A. Tata. Muscarinic receptor subtypes as potential targets to modulate oligodendrocyte progenitor survival, proliferation and differentiation. *Dev. Neurobiol.* **72(5):**713-728.

Dent, E., S. Gupton, & F. Gertler. 2011. The growth cone cytoskeleton in axon outgrowth and guidance. *Cold Spring Harb.Perspect. Biol.* **3(3):**a001800.

D'hooghe, M., T. D'Hooghe & J. De Keyser. 2013. Female gender and reproductive factors affecting risk, relapses and progression in multiple sclerosis. *Gynecol Obstet. Invest.* **76(1):**73-84.

Dugas, J., T. Cuellar, A. Scholze, B. Ason, A. Ibrahim, B. Emery, J Zamanian, L. Foo, M. McManus & B. Barres. 2010. Dicer1 and miR-219 are required for normal oligodendrocyte differentiation and myelination. *Neuron* **65:**597-611.

Dugas, J., & L. Notterpek. 2010. MicroRNAs in oligodendrocyte and Schwann cell differentiation. *Dev Neuro.***33:**14-20.

Dugas, J., Y. Tai, T. Speed, J. Ngai & B. Barres. 2006. Functional genomic analysis of oligodendrocyte differentiation. *J. Neurosci.* **26(43):**10967-10983.

Emery, B. 2010.Regulation of oligodendrocyte differentiation and myelination.*Science* **330:**779-782.

Emery, B., D. Agalliu, J. Cahoy, T. Watkins, J. Dugas, S. Mulinyawe, A. Ibrahim, K. Ligon, D. Rowith & B. Barres. 2009. Myelin gene regulatory factor is a critical transctiptional regulator required for CNS myelination. *Cell* **138(1):**172-185.

Fancy, S., C. Zhao & R. Franklin. 2004. Increased expression of Nkx2.2 and Olig2 identifies reactive oligodendrocyte progenitor cells responding to demyelination in the adult CNS. *Mol Ce;ll Neurosci* **27:**247-254.

Forrest, A., H. Beggs, L. Reichardt, J. Dupree, R. Colello & B. Fuss. 2009. Focal adhesion kinase (FAK): a regulator of CNS myelination. *J. Neurosci. Res.* **87(15):**3456-3464.

Fortin, D., E. Rom, H. Sun, A. Yayon & R. Bansal. 2005. Distinct fibroblast growth factor (FGF)/FGF receptor signalling pairs initiate diverse cellular responses in the oligodendrocyte lineage. *The Journal of Neuroscience* **25(32):**7470-7479.

Franklin, R. 2002. Why does remyelination fail in multiple sclerosis? *Nat. Rev. Neurosci.***3:**705-714.

Franklin, R., & C. Ffrench-Constant. 2008. Remyelination in the CNS: from biology to therapy. *Nat. Rev. Neurosci.* **9:**839855.

Friedman, L. & K. Avraham. 2009a. MicroRNAs and epigenetic regulation in the mammalian inner ear: implications for deafness. *Mamm. Genome***20:**581-603.

Friedman, R., K. Farh, C. Burge & D. Bartel. 2009b. Most mammalian mRNAs are conserved targets of microRNAs. *Genome Res.***19:**92-105.

Fuse, M., N. Nohata, S. Kojima, S. Sakamoto, T. Chiyomaru, K. Kawakami, H. Enokida, M. Nakagawa, Y. Naya, T. Ichikawa & N. Seki. 2011. Restoration of miR-145 expression suppresses cell rpliferation, migration and invasion in protstate cancer by targeting *FSCN1*. *International Journal of Oncology* **38:**1093-1101.

Gao, F., B. Durand & M. Raff. 1997. Oligodendrocyte precursor cells count time but not cell divisions before differentiation. *Current biology***7:**152-155.

Goto, J., T. Tezuka, T. NAkazawa, N. Tsukamoto, T. Nakamura, R. Ajima, K. Yokoyama, T. Ohta, M. Ohki & T. Yamamoto. 2004. Altered gene expression in the adult brain of fyn-deficient mice. *Cell Mol. Neurobiol.* **24(1):**149-159.

Gotz, M., & W. Huttner.The cell biology of neurogenesis.*Nat. Rev. Mol. Cell Biol.* **6:**777788.

Grandberg, T., J. Martola, M. Kristoffersen-Wiberg, P. Aspelin & S. Fredrikson. 2013. Radiologically isolated syndrome – incidental magnetic resonance imagning findings suggestive of multiple sclerosis, a systematic review. *Mult.Scler.***19(3):**271-280.

Grimson, A., K. Farh, W. Johnston, P. Garrett-Engele & D. Bartel. 2007. MicroRNA targeting specificity in mammals: determinants beyond seed pairing. *Molecular Cell***27:**91-105.

Hausser, J., M. Landthaler, L. Jaskiewicz, D. Gaidatzis & M. Zavolan. 2009. Relative contribution of sequence and structure features to the mRNA binding of Argonaute/EIF2C-miRNA complexes and the degradation of miRNA tarets. *Genome Research* **19:**2009-2020.

Hernandez-Pedro, N., G. Espinosa-Ramirez, V. dela Cruz B. Pineda & J. Sotelo.2013. Initial immunopathogenesis of multiple sclerosis: innate immune response. *Clin. Dev. Immunol.* **2013:**413465.

Hoshina, N., T. Tezuka, K. Yokoyama, H. Kozuka-Hata, M. Oyama & T. Yamamoto. 2007. Focal adhesion kinase regulates lamini-induced oligodendroglial process outgrowth. *Genes Cells* **12(11):**1245-1254.

Hu, H., Z. Tan, Y. Xu, H. Hu, C. Menzel, Y. Zhou, W. Chen, P. Khaitovich. 2009. Sequence features associated with microRNA strand selection in humans and flies. *BMC Genomics* **10:**413-424.

Huang, D., B. Sherman, & R. Lempicki.2009a. Systematic and integrative analysis of large gene lists using DAVID Bioinformatics Resources.*Nature Protoc.***4(1):**44-57.

Huang, D., B. Sherman, & R. Lempicki. 2009b. Bioinformatics enrichment tools: paths toward the comprehensive functional analysis of large gene lists. *Nucleic Acids Res.* **37(1):**1-13.

Huang, H., X. Zhao, K. Zheng & M. Qiu. 2013. Regulation of the timing of oligodendrocyte differentiation mechanisms and perspectives. *Neurosci. Bull.***29(2):**155-164.

Ikeda, K., M. Satoh, K. Pauley, M. Fritzler, W. Reeves & E. Chan. 2006. Detection of the Argonaute protein Ago2 and microRNAs in the RNA induced silencing complex (RISC) using a monoclonal antibody. *J Immunol Methods***317(1-2):**38-44.

Ivey, K., & D. Srivastava. 2010. MicroRNAs as regulators of differentiation and cell fate decisions. *Cell Stem Cell.***7(1):**36-41.

Jackman, N., A. Ishii & R. Bansal. 2009. Myelin biogenesis and oligodendrocyte development: parsing out the roles of glycosphingolipids. *Physiology* **24:**290-297.

Jones, S., D. Jolson, K. Cuta, C. Mariash, & G. Anderson. 2003. Triiodothyronin is a survival factor for developing oligodendrocytes. *Mol. Cell Endocrinol.***199:**49-60.

Jung, M., E. Kramer, M. Grzenkowski, K. Tang, W. Blakemore, A. Aguzzi, K. Khazaie, K. Chlichlia, G. Von Banlkenfeld, H. Kettenman & J. Trotter. 1995. Lines of murine oligodendroglial precursor cells immortalized by an activated *neu* tyrosine kinse show distinct degrees of interaction with axons *in vitro* and *in vivo*. *European Journal of Neuroscience* **7:**1245-1265.

Junker, A., M. Krumbholz, S. Eisele, H. Mohan, F. Augstein, R. Bittner, H. Lassmann, H. Wekerle, R. Hohlfled & E. Meini. 2009. MicroRNA profiling of multiple sclerosis lesions identifies modulators of the regulatory protein CD47. *Brain* **132:**3342-3352.

Kawase-Koga, Y., G. Otaegi & T. Sun. 2009. Different timings of Dicer deletion affect neurogenesis and gliogenesis in the developing mouse central nervous system. *Dev Dyn.* **238(11):**2800-2812.

Keller, A., P. Leidinger, J. Lange, A. Borries, H. Schoers, M. Scheffler, H. Lenhof, E. Ruprecht & E. Meese. 2009. Multiple sclerosis: microrNA expression profiles accurately differentiate patients with relapsing-remitting disease from healthy controls. *PLoS ONE***4:**e7440.

Kim, G., E. Park, C. Ryu, S. Jeon, S. Kim, H. Jang, G. Kim & B. Choi. 2011. MicroRNA profiling in recurrent anaplastic oligodendroglioma treated with postoperative radiotherapy. *JAST***2(2):**97-104.

Kim, H., A. DiBernardo, J. Sloane, M. Rasband, D. Solomon, B. Kosaras, S. Kwak & T. Vartanian. 2006. WAVE1 is required for oligodendrocyte morphogenesis and normal CNS myelination. *J. Neurosci.* **26(21):**5849-5859.

Koenning, M., S. Jackson, C. Hay, C. Faux, T. Kilpatrick, M. Willingham & B. Emery. 2012. Myelin gene regulatory factor is required for maintenance of myelin and mature oligodendrocyte identity in the adult CNS. *J. Neurosci.* **32(36):**12528-12542.

Kotter, M., C. Stadelmann & H. Hartung. 2011. Enahncing remyelination in disease – can we wrap it up? *Brain* **134:**1882-1900.

Krol, J., I. Loedige & W. Filipowicz. 2010. The widespread regulation of microRNA biogenesis, function and decay. *Nature Reviews* **11:**597-610.

Krol, J., K. Sobczak, U. Wilczynska, M. Drath, A. Jasinska, D. Kaczynska & W. Krzyzosiak. 2004. Structural features of miRNA (miRNA) precursors and their relevance to miRNA biogenesis and small interfering RNA/short hairpin RNA design. *The Journal of Biological Chemistry***279(40):**42230-42239.

Lages, E., A. Guttin, M. Atifi, C. Ramus, H. Ipas, I. Dupres, D. Rolland, C. Salon, C. Godfraind, F. deFraipont, M. Dobb, L. Pelletier, D. Rion & J. Issartel. 2011. MicroRNA and target protein patterns reveal physiopathological features of glioma subtypes.

Lau, P., J. Verrier, J. Nielsen, K. Johnson, L. Notterpek & L. Hudson. 2008. Identification of dynamically regulation microRNA and mRNA networks in developing oligodendrocytes. *Journal of Neuroscience***28(45):**11720-11730.

Lee, Y., M. Kim, J. Han, K. Yeom, S. Lee, S. Baek & B. Kim. 2003. MicroRNA genes are transcribed by RNA polymerase II. *EMBO J.***23(20):**4051-4060.

Lehotzky, A., P. Lau, N. Tokesi, N. Muja, L. Hudson & J. Ovadi. 2010. Tubulin polymerization promoting protein (TPPP/p25) is critical for oligodendrocyte differentiation. *Glia***58(2):**157-168.

Letzen, B., C. Liu, N. Thakor, J. Gearhart, A.All & C. Kerr. 2010. MicroRNA expression profiling of oligodendrocyte differentiation from human embryonic stem cells. *PLOS One* **doi:10.1371/journal.pone.0010480**.

Leung, K., & P. Sharp. 2010. MicroRNA functions in stress responses. *Molecular Cell***40:**205-215.

Lewis, B., C. Burge & D. Bartel. 2005. Conserved seed pairing, often flanked by adenosines, indicates that thousands of human genes are microRNAs targets. *Cell***120(1):**15-20.

Lewis, B., I. Shih, M. Jones-Rhoades, D. Bartel & C. Burge. 2003. Prediction of mammalian microRNA targets. *Cell***115:**787-798.

Li, J-S., & Z-X. Yao. 2012. MicroRNAs: novel regulators of oligodendrocyte differentiation and potential therapeutic targets in demyelination-related diseases. *Mol. Neurobiol.* **45:**200-212.

Li, R., G. Yan, Q. Li, X. Sun, Y. Hu, J. Sun & B. Xu. 2012. MicroRNA-145 protects cardiomyocytes against hydrogen peroxide-induced apoptosis through targeting the mitochondria apoptotic pathway. *PLoS ONE***7(9):**e44907.

Lin, S., & Y. Fu. 2008. miR-23 regulation of lamin B1 is crucial for oligodendrocyte development and myelination. *Dis. Model Mech.* **2(3-4):**178-188.

Lin, S., Y Huang, L. Zhang, M. Heng, L. Ptacek & Y. Fu. 2013. MicroRNA-23a promotes myelination in the central nervous system. *PNAS***110(43):**17468-17473.

McFarland, R., & R. Martin. 2007. Multiple sclerosis: a complicated picture of autoimmunity. *Net. Immunol.***8:**913-919.

Miller, D., F. Barkhof, X. Montalban, A. Thompson & M. Filippi. 2005. Clinically isolated syndromes suggestive of multiple sclerosis, part I: natural history pathogenesis, diagnosis and prognosis. *Lancet. Neurol.* **4:**281-288.

Miron, V., T. Kuhlmann & J. Antel. 2011. Cells of the oligodendroglial lineage, myelination and remyelination. *Biochimica et Biophysica Acta* **1812:**184-193.

Nishihara, T., L. Zekri, J. Braun & E. Izaurralde. 2013. miRISC recruits decapping factors to miRNA targets to enhance their degradation. *Nucl. Acids Res.* **41(18):**8692-8705.

Noseworthy, J. C. Lucchinetti, M. Rodriguez & B. Weinshenker. 2000. Multiple Sclerosis. *N. Englang J. Med.* **343:**938-952.

O'Connell, R., D. Kahn, W. Gibson, J. Round, R. Scholz, A. Chauduri, M. Kahn, D. Rao & D. Baltimore. 2010. MicroRNA-155 promotes autoimmune inflammation by enhancing inflammatory T-cell development. *Immunity* **33(4):**607-619.

O'Meara, R., J. Michalski, C. Anderson, K. Bhanot, P. Rippstein & R. Kothary. 2013. Integrin-linked kinase regulates process extension in oligodendrocytes via control of actin cytoskeletal dynamics. *J. Neurosci.* **33(23):**9798-9793.

Ostenfeld, M., J. Bramsen, P. Lamy, S. Villadsen, N. Fristrup, K. Sorensen, B. Ulhoi, J. Kjems, L. Dyrskjot & T. Orntoft. 2010. miR-145 induces caspase-dependent and –independent cell death in urothelial cancer cell lines with targeting of an expression signature present in Ta bladder tumors. *Oncogene***29(7):**1073-1084.

Otaegui, D., S. Baranzini, R. Armananzas, B. Calvo, M. Munoz-Culla, P. Khankhanian, I. Inza, J. Lozano, T. Castillo-Trivino, A. Asensio, J. Olaskoaga & A. Lopez de Munain. 2009. Differential microRNA expression in PBMC from multiple sclerosis patients. *PLoS ONE***4:**e6309.

Pakpoor, J., G. Disanto, J. Gerber, R. Dobson, U. Meier, G. Giovannoni & S. Ramagopalan. 2013. The risk of developing multiple sclerosis in individuals seronegative for Epstein-Barr virus: a meta-analysis. *Mult.Scler.***19(2):**162-166.

Paraboschi, E., G. Solda, D. Gemmati, E. Orioli, G. Zeri, M. Benedetti, A. Salviati, N. Barizzone, M. Leone, S. Duga & R. Asselta. 2011. Genetic association and altered gene expression of miR-155 in multiple sclerosis patients. *Int. J. Mol. Sci.* **12:**8695-8712.

Pauley, K., T. Eystatioy, A. Jakymiw, J. Hamel, M. Fritzler & E. Chan. 2006 Formation of GW bodies is a consequence of microRNA genesis. *EMBO J.* **7:**904-910.

Perron, M., & P. Provost. 2008. Protein interactions and complexes in human microRNA biogenesis. *Front Biosci.* **13:**2537-2547.

Pfeiffer, S., A. Warrington & R. Bansal. 1993. The oligodendrocyte and its many processes. *Trends Cell Biol.* **3(6):**191-197.

Rajasekharan, S., & T. Kennedy. 2009. The netrin protein family. *Genome Biology* **10:**239.

Rani, S., S. Rathod, S. Karthik, N. Kaur, D. Muzumdar & A. Shiras. 2013. Mir-145 functions as a tumor-suppressive RNA by targeting Sox9 and adducing 3 in human glioma cells. *Neuro-Oncology* **15(10):**1302-1316.

Richardson, W., N. Kessaris & N. Pringle. 2006. Oligodendrocyte Wars. *Nature Reviews Neuroscience* **7:**11-18.

Sachdeva, M., & Y. Mo. 2010.miR-145-mediated suppression of cell growth, invasion and metastasis. *Am. J. Transl. Res.* **2(2):**170-180.

Schier, A., & A. Giraldez. 2006. MicroRNA function and mechanism: insights from zebrafish. *Cold Spring Harbour Symposia on Qunatitative Biology***121:**195-203.

Shabalina, S., & E. Koonin. 2009. Origins and evolution of eukaryotic RNA interference. *Trends Ecol Evol.***23(10):**578-587.

Shi, Y., & Y. Jin. 2010. MicroRNA in cell differentiation and development. *Sci China C Life Sci.* **52(3):**205-211.

Shin, D., J-Y Shin, M. McManus, L. Ptacek & Y-H Fu. 2009. *Dicer* ablationin oligodendrocytes provokes neuronal impairment in mice. *Ann Neurol.* **66(6):**843-857.

Sim, F., C. Zhao, J. Penderis & R. Franklin. 2002. The age-related decrease in CNS remyelination efficiency is attributable to an impairment of both oligodendrocyte progenitor recruitment and differentiation. *J. Neurosci.* **22:**2451-2459.

Simpson, S., L. Blizzard, P. Otahal, I. Van der Mei & B. Taylor. 2011. Latitude is significantly associated with the prevalence of Multiple Sclerosis. *J. Neurol. Neurosurg. Psychiatry* **82(10):**1132-1141.

Stolt, C., S. Rehberg, M. Ader, P. Lommes, D. Reithmacher, U. Bartsch & M. Wegner. 2002. Terminal differentiation of myelin-forming oligodendrocytes depends on the transctiption factor Sox10. *Genes Dev.***16(2):**165-170.

Tait, S. F. Gunn-Moore, J. Collinson, J. Huang, C. Lubetzki, L. Pedraza, D. Sherman, D. Colman & P. Brophy. 2000. An oligodendrocyte cell adhesion molecule at the site of assembly of the paranodal axo-glial junction. *J. Cell Biol.* **150(3):**657-666.

Temple, S. & M Raff. 1986. Clonal analysis of oligodendrocyte development in culture: evidence for a developmental clock that counts cell divisions. *Cell* **44(5):**773-779.

Tosic, M., S. Torch, V. Comte, M. Dolivo, P. Honegger & J. Matthieu. 1992. Triiodothyronin has diverse and multiple stimulating effects on expression of the major myelin protein genes. *J. Neurochem.* **59:**1770-1777.

Van't Veer, A., Y. Du, T. Fischer, D. Boetig, M. Wood & Cheryl Dreyfus. 2009. Brain-derived neurotrophic factor effects on oligodendrocyte progenitors of the basal forebrain are mediated through TrkB and the MAP kinase pathway. *J. Neurosci. Res.* **87:**69-78.

Watanabe, W., T. Hadzic & A. Nishiyana. 2004. Transient upregulation of Nkx2.2 expression in oligodendrocyte lineage cells during remyelination. *Glia* **46:**311-322.

Watkins, T., B. Emery, S. Mulinyawe & B. Barres. 2008. Distinct stages of myelination regulated by gamma-secretase and astrocytes in a rapidly myelinating CNS coculture system. *Neuron* **60:**555-569.

Weng, Q, Y. Chen, H. Wang, X. Xu, B. Yang, W. Shou, Y. Chen, Y. Higashi, V. van den Berghe, E. Seuntjens, S. KErnie, P. Bukshpun, E. Sherr, D. Huylebroeck & Q. Lu. 2012. Dual-mode modulation of Smad signalling by Smad-interacting protein Sip1 is required for myelination in the central nervous sstem. *Neuron* **73(4):**713-728.

Weston, M., M Pierce, S. Rocha-Sanchez, K. Beisel & G. Soukup. 2006. MicroRNA gene expression in the mouse inner ear. *Brain Research* **1111:**95-104.

Wolswijk G. 1997. Oligodendrocyte precursor cells in chronic multiple sclerosis lesions.*Mult.Scler.***3(2):**168-169.

Wyatt, C., A. Ebert, M. Reimer, K. Rasband, M. Hardy, C. Chien, T. Becker & C. Becker. 2010. Analysis of the *astray/robo2* zebrafish mutant reveals that degenerating tracts do not provide strong guidance cues for regenerating optic axons. *J. Neurosci.***30(41):**13838-13849.

Yang, J., & E. Lai. 2011. Alternative miRNA biogenesis pathways and the interpretation of core miRNA pathway mutants. *Mol Cell***43:**892-903.

Yang, J., T. Maurin & E. Lai. 2012. Functional parameters of Dicer-independent microRNA biogenesis. *RNA* **18:**doi:10.1261/rna.032938.112.

Yoshikawa, H. 2001 Myelin-associated oligodendrocytic basic protein modulates the arrangement of radial growth of the axon and the radial component of myelin. *Med Electron Microsc.***34(3):**160-164.

Yoshino, H., H. Enokia, T. Itesako, S. Kojima, T. Kinoshita, S. Tatarano, T. Chiomaru, M. Nakagawa & N. Seki. 2013. The tumor-suppressive microRNA-143-145 cluster targets hexokinase-2 in renal cell carcinoma. *Cancer Sci.* **doi:10.1111/cas.12280**.Epub ahead of print.

Young, K., K. Psachoulia, R. Tripathi, S. Dunn, L. Cossell, D. Attwell, K. Tohyama & W. Richardson. 2013. Oligodendrocyte dunamics in the healthy adult CNS: evidence for myelin remodelling. *Neuron* **77:**873-885.

Yu, W. E. Collarini, N. Pringle, & W. Richardson. 1994. Embryonic expression of myelin genes: evidence for a focal source of oligodendrocyte precursors in the ventricular zone of the neural tube. *Neuron* **12(6):**1353-1362.

Zeng, Y. & B. Cullen. 2005. Efficient processing of primary microRNA hairpins by Drosha requires flanking nonstructured RNA sequences. *The Journal of Biological Chemistry***280(30):**27595-27608.

Zhang, H., S. Zheng, J. Zhao, W. Zhao, L. Zheng, D. Zhao, J. Li, X. Zhang, Z. Chen & X. Yi. 2011. MicroRNAs 144, 145 and 214 are down-regulated in primary neurons responding to sciatic nerve transection. *Brain Research* **1383:**62-70.

Zhang, W., Q. Wang, M. Yu, N. Wu & H. Wang. 2013. MicroRNA-145 function as a cell growth repressor by directly targeting c-Myc in human ovarian cancer. *Technol. Cancer Res. Treat.***PMID 23919393** Epub ahead of print.

Appendix A – Optimization of lentiviral transduction, culture conditions and induction

Oli-neu cells and OLs in general are notoriously difficult to transfect or transduce. As such, careful optimization was undertaken at each step of transduction. This included assays to determine the ideal concentration of polybrene required for infection (Figure A1) as well as of puromycin required for selection (Figure A2). After successful transduction, induction conditions were optimized by assaying tetracycline dose and dose timing at 6 different concentrations over 4 days and observing induction efficiency (Figure A3). Finally, loss of induction without daily tetracycline treatment was confirmed by loss of the GFP signal 6 days after a single initial dose (Figure A4).

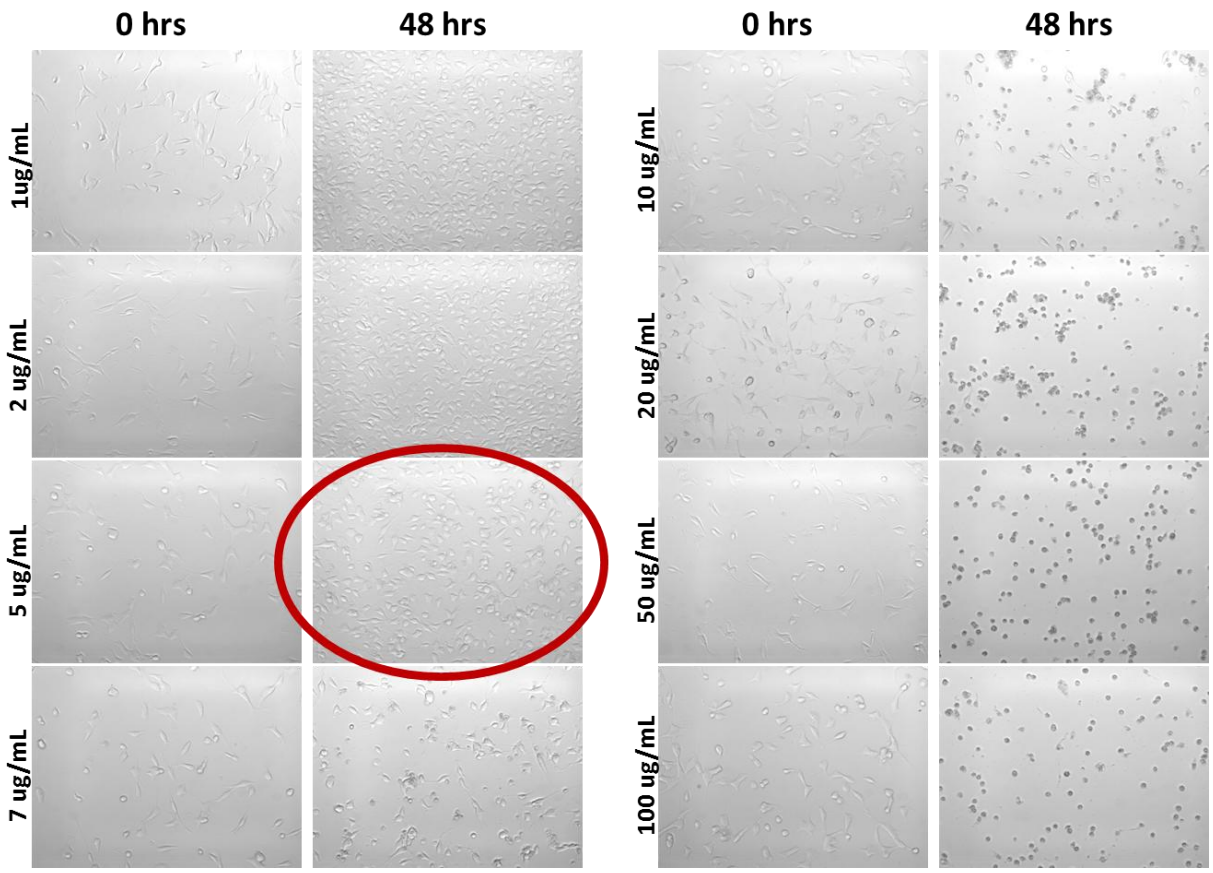

Figure A1. Optimization of polybrene concentration for lentiviral transduction of *Oli-neu* cells. Phase contrast images of proliferating *Oli-neu* cells just prior to incubation with varying concentrations of polybrene (0 hrs) and after incubation (48 hrs). The red circle indicates the optimal concentration.

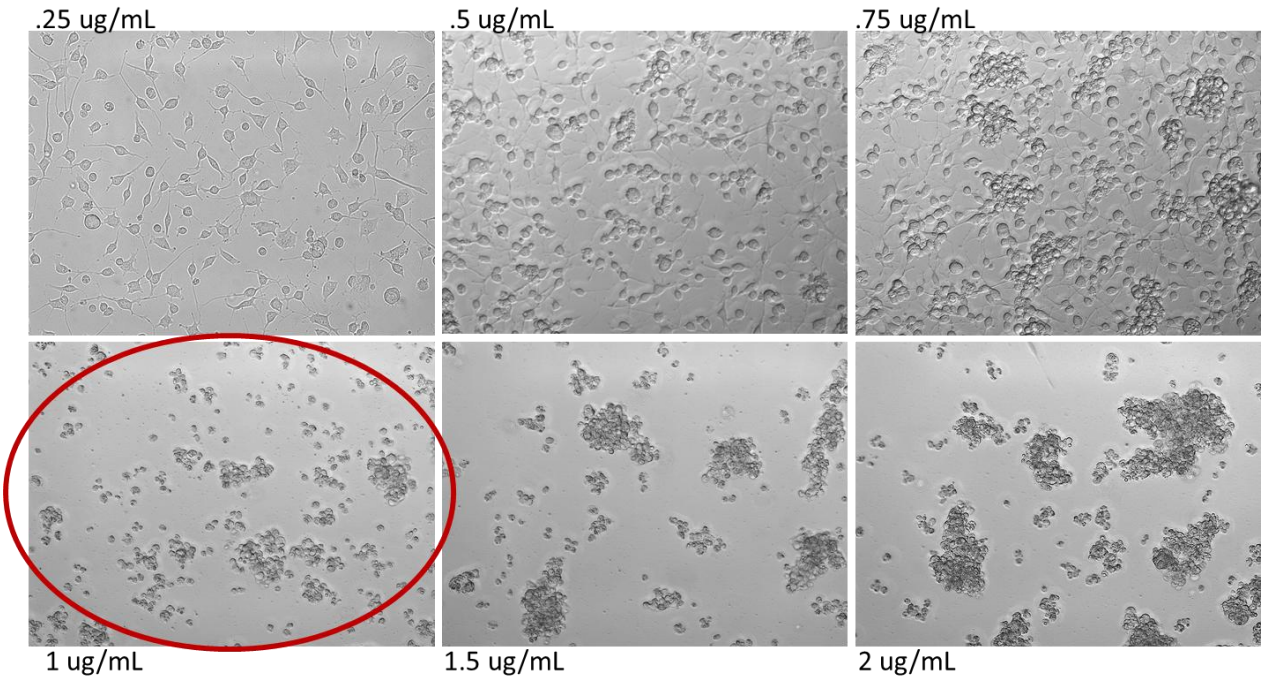

Figure A2. Optimization of puromycin concentration for selection of transduced *Oli-neu* cells after lentiviral infection. Phase contrast images of proliferating *Oli-neu* cells after 72 hrs incubation with varying concentrations of puromycin. The red circle indicates the optimal concentration.

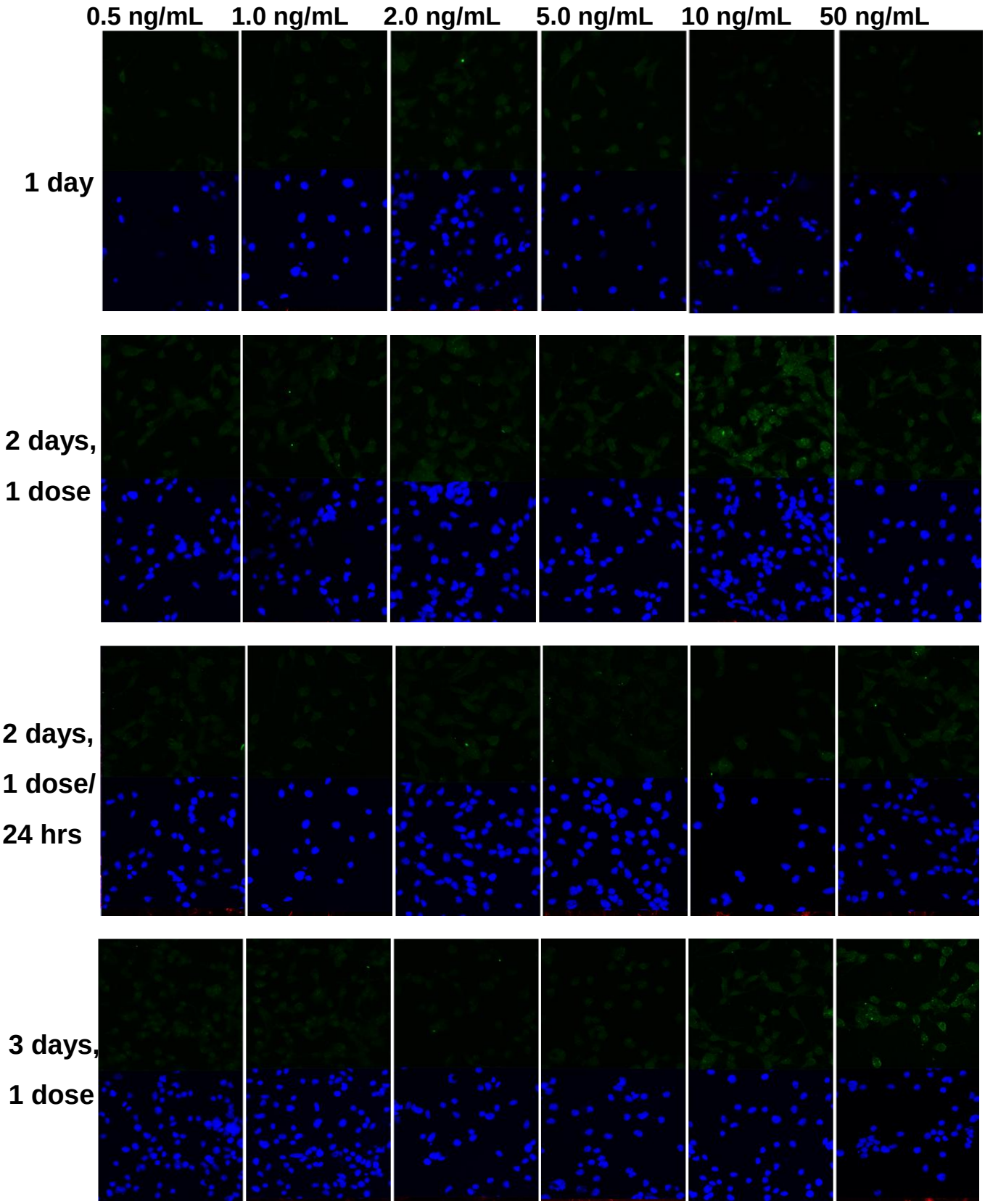
0.5 ng/mL
1.0 ng/mL
2.0 ng/mL
5.0 ng/mL
10 ng/mL
50 ng/mL
1 day
2 days,
1 dose
2 days,
1 dose/
24 hrs
3 days,
1 dose

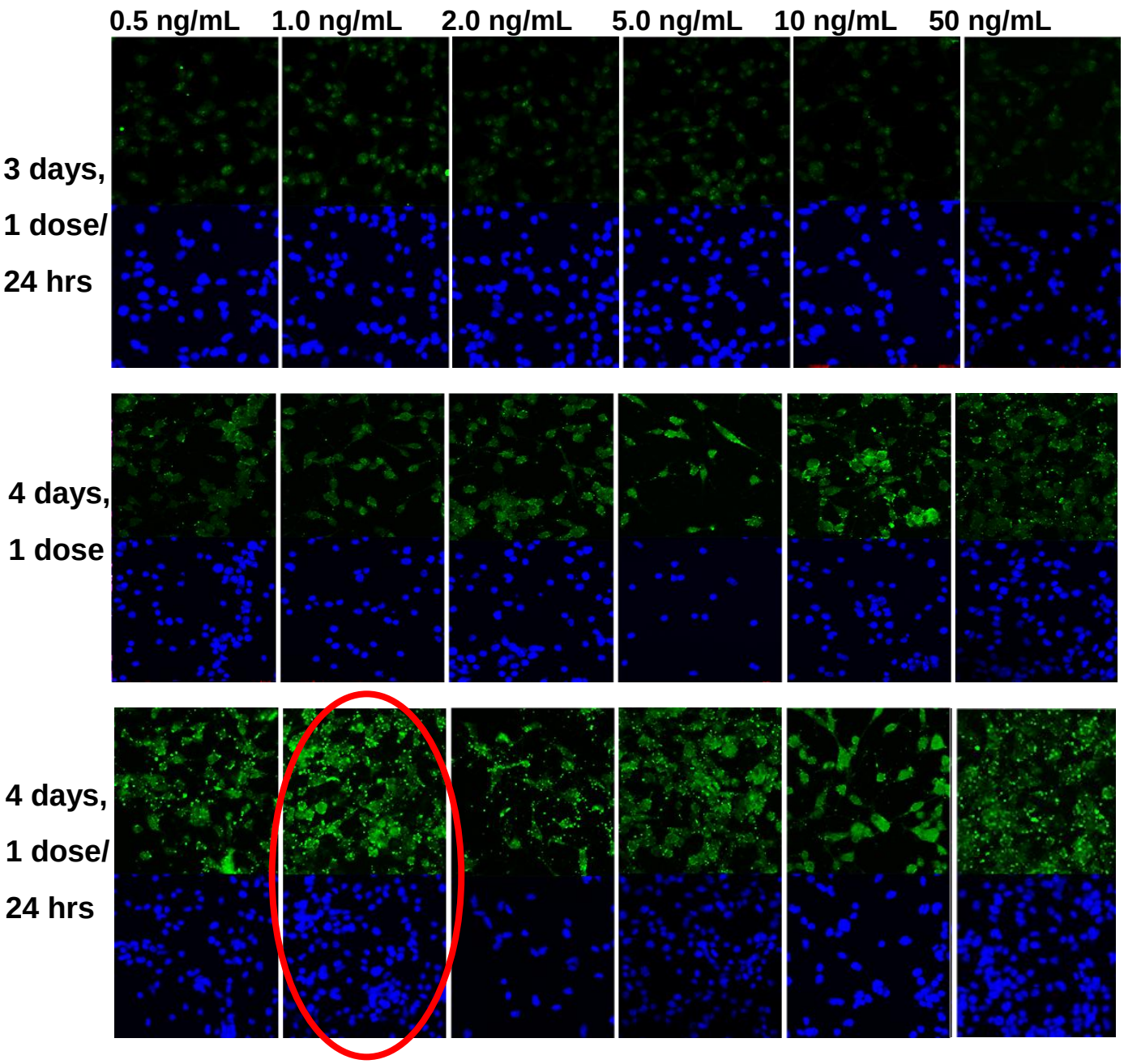

Figure A3. Optimization of tetracycline dosage and dose timing for induction of transduced *Oli-neu* cells. Using the cell line ON-145-1, induction (as evidence by the top panel of each test condition shows GFP expression, while the bottom panel shows Hoescht staining). The red circle indicates the dosing conditions selected for subsequent experiments.

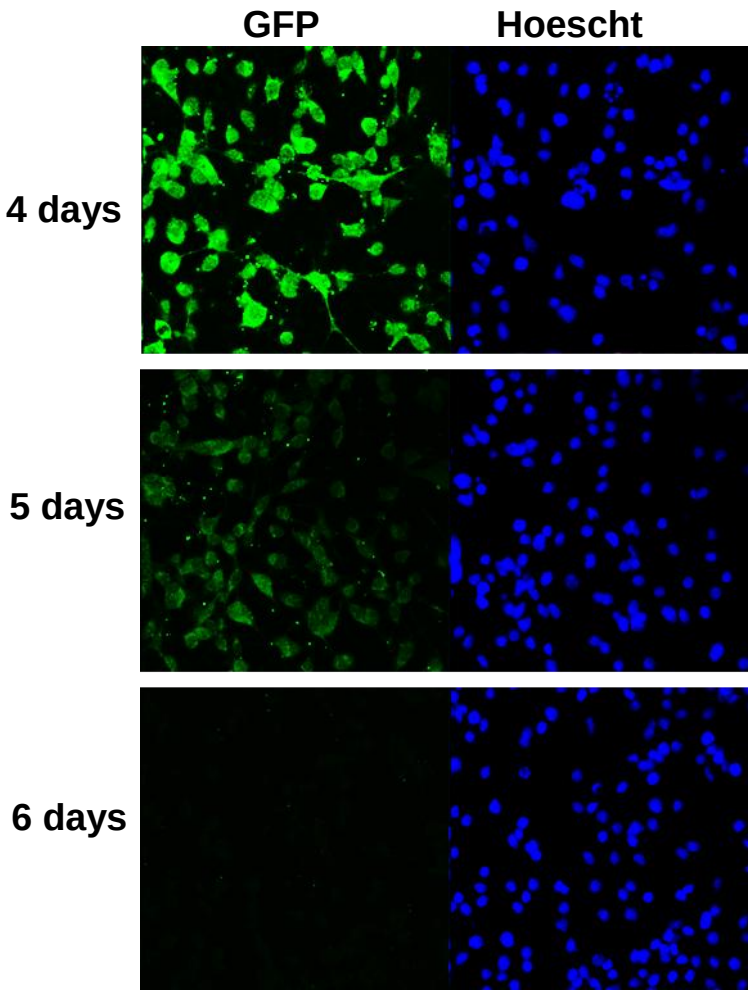

Figure A4. GFP expression is lost without continued tetracycline treatment. ProliferatingON-145-1 cells were treated with a single dose of 1 ng/mL tetracycline**.** After 4 days, robust GFP expression was observed. Expression was observable but diminished by day 5, and could not be observed by day 6.

Appendix B –*Oli-neu* differentiation is unaffected by tetracycline treatment

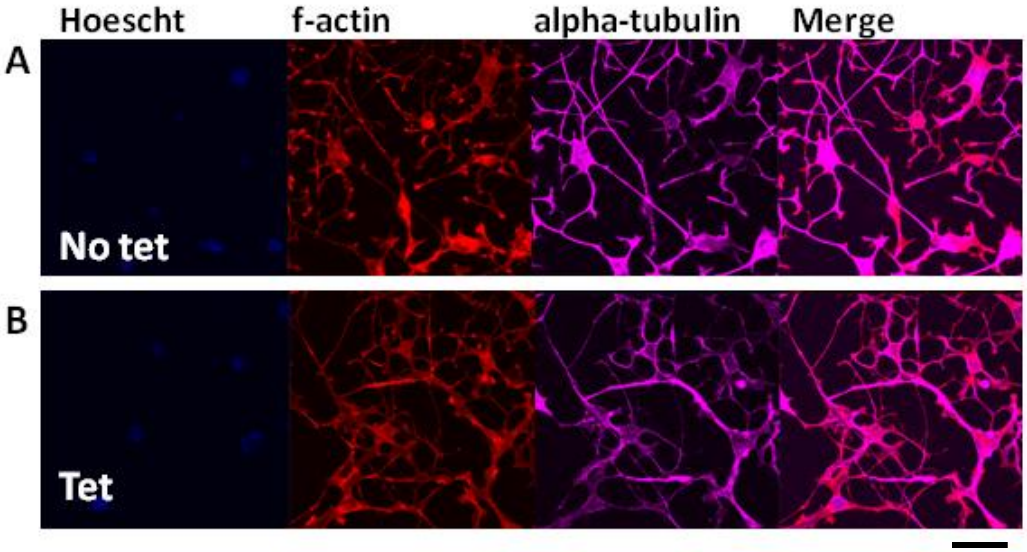

Figure B1. *Oli-neu* cells appear to differentiate normally in medium containing tetracycline. A. *Oli-neu* cells differentiated for 3 days in normal differentiation medium containing 1 mM dbcAMP. B. *Oli-neu* cells differentiated for 3 days in differentiation medium containing 1 mM dbcAMP + 1 ng/mL tetracycline. Scale bar = 50 µm.